12-2017

Aerodynamic Centers of Arbitrary Airfoils

Orrin Dean Pope
Utah State University

AERODYNAMIC CENTERS OF ARBITRARY AIRFOILS

by

Orrin Dean Pope

A thesis submitted in partial fulfillment
of the requirements of the degree

of

MASTER OF SCIENCE

in

Mechanical Engineering

Approved:

_____	_____
Douglas Hunsaker, Ph.D. Major Professor	Stephan A. Whitmore, Ph.D. Committee Member
_____	_____
Geordi Richards, Ph.D. Committee Member	Mark R. McLellan, Ph.D. Vice President for Research and Dean of the School of Graduate Studies

UTAH STATE UNIVERSITY
Logan, Utah

2017

ABSTRACT

Aerodynamic Centers of Arbitrary Airfoils

by

Orrin Dean Pope, Master of Science

Utah State University, 2017

Major Professor: Douglas Hunsaker, Ph.D.
Department: Mechanical and Aerospace Engineering

A method for accurately predicting the aerodynamic center of an airfoil is presented based on a general form for the nonlinear lift and pitching-moment of an airfoil as a function of angle of attack. This method does not suffer from small-angle, small-camber, and thin-airfoil approximations, and is shown to match inviscid results to much higher accuracy than the traditional methods. It is shown that the aerodynamic center of an airfoil with arbitrary amounts of thickness and camber in an inviscid flow does not, in general, lie at the quarter-chord. Rather, it is a single, deterministic point, independent of angle of attack, which lies at the quarter chord only in the limit as the airfoil thickness and camber approach zero. Furthermore, it is shown that once viscous effects are included, the aerodynamic center is not in general a single point as predicted by traditional thin airfoil theory, but is a function of angle of attack. Differences between nonlinear predictions and those based on thin airfoil theory are on the order of 1-5%, which can be significant when predicting aircraft stability.

(135 pages)

PUBLIC ABSTRACT

Aerodynamic Centers of Arbitrary Airfoils

Orrin Dean Pope

The study of designing stable aircraft has been widespread and ongoing since the early days of Orville and Wilbur Wright and their famous Wright Flyer airplane. All aircraft as they fly through the air are subject to minor changes in the forces acting on them. The field of aircraft stability seeks to understand and predict how aircraft will respond to these changes in forces and to design aircraft such that when these forces change the aircraft remains stable. The mathematical equations used to predict aircraft stability rely on knowledge of the location of the aerodynamic center, the point through which aerodynamic forces act on an aircraft. The aerodynamic center of an aircraft is a function of the aerodynamic centers of each individual wing, and the aerodynamic center of each wing is a function of the aerodynamic centers of the individual airfoils from which the wing is made. The ability to more accurately predict the location of the airfoil aerodynamic center corresponds directly to an increase in the accuracy of aircraft stability calculations.

The Aerolab at Utah State University has develop new analytic mathematical expressions to describe the location of the airfoil aerodynamic center. These new expressions do not suffer from any of the restrictions, or approximations found in traditional methods, and therefore result in more accurate predictions of airfoil aerodynamic centers and by extension, more accurate aircraft stability predictions.

ACKNOWLEDGMENTS

I would like to specifically thank Dr. Doug Hunsaker for his guidance, support, and unending passion for aircraft and aeronautics. I am also thankful to the Utah NASA Space Grant Consortium (award NNX15A124H) for funding this research.

I give special thanks to my colleagues, friends, and especially my family who have always supported me throughout my Master's program and through all of my engineering education.

Orrin Dean Pope

CONTENTS

Page

ABSTRACT iii

PUBLIC ABSTRACT iv

ACKNOWLEDGMENTS v

LIST OF TABLES viii

LIST OF FIGURES ix

NOTATION x

CHAPTER

1 INTRODUCTION 1

1.1 Research Motivation 1

1.2 Literature Review 2

1.2.1 Traditional Thin Airfoil Theory Relations for the Aerodynamic Center 2

1.2.2 General Relations for the Aerodynamic Center 5

2 ALTERNATIVE APPROACH TO FINDING THE LOCATION OF THE AERODYNAMIC CENTER 8

2.1 The Aerodynamic Center as a Function of Coefficient of Lift 8

2.2 The Aerodynamic Center as a Function of Normal-force Coefficient 12

2.2.1 Equivalence Proof 15

2.3 Sample Results 18

2.3.1 Vortex Panel Method 18

2.3.2 Finite Difference Method 20

3 THE AERODYNAMIC CENTER OF INVISCID AIRFOILS 24

3.1 Classical Thin Airfoil Theory 24

3.2 General Airfoil Theory 27

3.2.1 Theory Development 28

3.2.2 Comparison to Inviscid Computational Results 38

3.3 Least Squares Regression Fit Coefficients-Inviscid Flow....44
3.3.1 Fit to Thin Airfoil Theory Equations....44
3.3.2 Fit to General Airfoil Theory Equations....46
3.4 The Aerodynamic Center of Airfoils in Inviscid Flow....48
3.4.1 Thin Airfoil Theory with Trigonometric Nonlinearities....48
3.4.2 General Airfoil Theory....49

4 THE AERODYNAMIC CENTER OF VISCOUS AIRFOILS....54
4.1 The Aerodynamic Center of Airfoils in Viscous Flow....54
4.2 Third Order Approximation....58
4.3 Sample Results....60
4.4 Least Squares Regression Fit Coefficients-Viscous Flow....70

5 CONCLUSION....74

REFERENCES....77

APPENDICES....80
A Viscous Least Squares Regression Fit Coefficients....81
B Vortex Panel Method Code....86
C Analytical Symbolic Solver Code....93
D Inviscid Aerodynamic Center NACA Airfoil Camber/Thickness Code....117

LIST OF TABLES

Table Page

1 Vortex panel method data for NACA 8415 airfoil, $-7 \le \alpha \le 10$ 19

2 Vortex panel method data for NACA 8415 airfoil, $-10 \le \alpha \le 15$ 40

3 Least squares regression coefficients for NACA 8415 airfoil 41

4 Viscous least squares regression fit coefficient data for a series of NACA four digit airfoils.....61

5 RMS error of high order solution and third order approximation using XFOIL data.....63

6 RMS error of high order solution and third order approximation using XFOIL data.....66

LIST OF FIGURES

Figure		Page
1	Forces and pitching moment on an airfoil	3
2	The aerodynamic center of a NACA 8415 airfoil in inviscid flow as a function of angle of attack and the normal-force	21
3	Superposition of a uniform flow and a curved vortex sheet along the camber line of a thin airfoil section	26
4	Circular cylinder in the complex ζ - plane	31
5	RMS error for thin airfoil theory and general airfoil theory lift predictions for 250 NACA airfoils in inviscid flow	42
6	RMS error for thin airfoil theory and general airfoil theory pitching moment predictions for 250 NACA airfoils in inviscid flow	42
7	The aerodynamic center of a NACA 8415 airfoil in inviscid flow predicted by thin airfoil theory, general airfoil theory, and finite differencing	51
8	The pitching moment about the aerodynamic center of a NACA 8415 airfoil in inviscid flow predicted by thin airfoil theory, general airfoil theory, and finite differencing	51
9	The aerodynamic center of 250 NACA airfoils in inviscid flow as a function of airfoil thickness and camber	52
10	The aerodynamic center location of a selection of NACA airfoils in viscous flow comparing the high order solution and third order approximation using Abbott & Von Doenhoff data	62
11	The aerodynamic center location of a selection of NACA airfoils in viscous flow comparing the high order solution and third order approximation using XFOIL data	65
12	Aerodynamic center locations for a NACA 1408 airfoil in viscous flow data	68
13	Pitching moment about the aerodynamic center of a NACA 1408 airfoil in viscous flow	69

NOTATION

B_n = coefficients in the expansion given in Eq. (47)

$\widetilde{C}_A$ = section axial-force coefficient

$\widetilde{C}_{A,\alpha}$ = first derivative of $\widetilde{C}_A$ with respect to α

$\widetilde{C}_{A,\alpha,\alpha}$ = second derivative of $\widetilde{C}_A$ with respect to α

$\widetilde{C}_D$ = section drag coefficient

$\widetilde{C}_{D_0}$ = section drag coefficient at zero lift, Eq. (67)

$\widetilde{C}_{D_0,L}$ = coefficient of $\widetilde{C}_L$ in the parabolic relation for $\widetilde{C}_D$, Eq. (67)

$\widetilde{C}_{D_0,L^2}$ = coefficient of $\widetilde{C}_L^2$ in the parabolic relation for $\widetilde{C}_D$, Eq. (67)

$\widetilde{C}_L$ = section lift coefficient

$\widetilde{C}_{L,\alpha}$ = first derivative of $\widetilde{C}_L$ with respect to α

$\widetilde{C}_{L0,\alpha}$ = first derivative of $\widetilde{C}_L$ with respect to α, at α=0

$\widetilde{C}_m$ = section moment coefficient about the point (x, y)

$\widetilde{C}_{m_{ac}}$ = section moment coefficient about the aerodynamic center

$\widetilde{C}_{m_{c/4}}$ = section moment coefficient about the quarter-chord

$\widetilde{C}_{m_{le}}$ = section moment coefficient about the leading-edge

$\widetilde{C}_{m_O}$ = section moment coefficient about the origin

$\widetilde{C}_{m_O,\alpha}$ = first derivative of $\widetilde{C}_{m_O}$ with respect to α

$\widetilde{C}_{m_O,\alpha,\alpha}$ = second derivative of $\widetilde{C}_{m_O}$ with respect to α

$\widetilde{C}_{m,A}$ = constant coefficient used in Eqs. (55) and (68)

$\widetilde{C}_{m,N}$ = constant coefficient used in Eqs. (55) and (68)

$\widetilde{C}_{m0,\alpha}$ = constant coefficient used in Eqs. (55) and (68)

$\widetilde{C}_N$ = section normal-force coefficient

$\widetilde{C}_{N,\alpha}$ = first derivative of $\widetilde{C}_N$ with respect to α

$\widetilde{C}_{N,\alpha,\alpha}$ = second derivative of $\widetilde{C}_N$ with respect to α

C_n = complex constants in the Laurent series expansion

c = section chord length

F_1, F_2 = Laurent series expansions used in Eqs. (44) and (45)

K_1, K_2 = constants defined in Eq. (78)

$\widetilde{L}$ = section lift

$\widetilde{m}_0$ = pitching moment about the origin

n = term in the Laurent series expansion

R = radius of the circular cylinder used for the conformal transformation

V_∞ = freestream airspeed

w = complex velocity field

w_1 = complex velocity in the plane of the circular cylinder

w_2 = complex velocity in the plane of the airfoil

x, y = axial and upward-normal coordinates relative to the leading edge

x_0 = real coordinate of the center of the circular cylinder in the complex plane

x_{ac}, y_{ac} = x and y coordinates of the aerodynamic center

y_c = y coordinate of the camber line

y_0 = imaginary coordinate of the center of the circular cylinder in the complex plane

z = coordinate in the complex plane

z_l = leading edge of the airfoil in the z-plane

z_t = trailing edge of the airfoil in the z-plane

z_0 = center of the circular cylinder in the complex plane, $z_0 = x_0 + iy_0$

α = angle of attack

α_{L0} = zero-lift angle of attack

Γ = circulation strength

ζ = analytic transformation function

ζ_l = point in the complex plane that maps to the airfoil leading edge

ζ_{surface} = coordinates of the cylinder surface

ζ_t = point in the complex plane that maps to the airfoil trailing edge

Θ = change of variables for the axial coordinate of an airfoil

θ = angle relative to the horizontal axis in the complex plane

θ_t = value of θ at the airfoil trailing edge

ρ = fluid density

Φ_1 = complex potential in the plane of the circular cylinder

Φ_2 = complex potential in the plane of the airfoil

ϕ = local camber angle

CHAPTER 1
INTRODUCTION

1.1 Research Motivation

Correctly identifying the location of the aerodynamic center of a lifting surface is extremely important in aircraft design and analysis. For example, the location of the aerodynamic center of a complete aircraft relative to the center of gravity is an important measure of longitudinal pitch stability [1-2]. This location, often referred to as the neutral point, is a function of the aerodynamic center of each lifting surface or wing. In addition to longitudinal pitch stability, accurate knowledge of the location of the aerodynamic center of a lifting surface or wing has been shown to be a fundamental parameter in aeroelastic analysis as well as flutter and divergence speed calculations [3]. The importance of correctly identifying the location of the aerodynamic center of a lifting surface is also apparent in supersonic aircraft design. Efforts to minimize trim drag, maximize load factor capability, and to provide acceptable handling qualities, rely on accurate knowledge of the location of the aerodynamic center of a supersonic lifting surface [4]. The aerodynamic center of a wing is a function of the aerodynamic center of the individual airfoils from which the wing is made, as well as wing sweep, dihedral, and planform. Thus, correctly predicting the aerodynamic center or neutral point of a complete airframe during preliminary design depends on the accuracy to which we can predict the aerodynamic centers of airfoils and finite wings.

1.2 Literature Review

1.2.1 Traditional Thin Airfoil Theory Relations for the Aerodynamic Center

The aerodynamic center is traditionally defined to be the point about which the pitching moment is invariant to small changes in angle of attack, i.e.

$$\frac{\partial \widetilde{C}_{m\,ac}}{\partial \alpha} \equiv 0 \tag{1.1}$$

The pitching moment about any point in the airfoil plane can be found from a simple transformation of forces and moments about the origin to the point of interest, i.e.,

$$\widetilde{C}_m = \widetilde{C}_{m_O} + \frac{x}{c}\widetilde{C}_N - \frac{y}{c}\widetilde{C}_A \tag{1.2}$$

where $\widetilde{C}_{m_O}$ is the pitching moment about the origin, $\widetilde{C}_A$ is the axial force coefficient, and $\widetilde{C}_N$ is the normal force coefficient. The axial and normal force coefficients are related to the lift and drag coefficients through a transformation in angle of attack, as shown in Fig. 1

$$\widetilde{C}_A = \widetilde{C}_D \cos\alpha - \widetilde{C}_L \sin\alpha \tag{1.3}$$

$$\widetilde{C}_N = \widetilde{C}_L \cos\alpha + \widetilde{C}_D \sin\alpha \tag{1.4}$$

Using Eqs. (1.3) and (1.4) in Eq. (1.2), the pitching moment about the aerodynamic center is

$$\widetilde{C}_{m_{ac}} = \widetilde{C}_{m_O} + \frac{x_{ac}}{c}(\widetilde{C}_L \cos\alpha + \widetilde{C}_D \sin\alpha) - \frac{y_{ac}}{c}(\widetilde{C}_D \cos\alpha - \widetilde{C}_L \sin\alpha) \tag{1.5}$$

For a typical airfoil, the vertical offset of the aerodynamic center from the airfoil chord line is small, and the drag is much less than the lift. Additionally, the angle of attack is small for normal flight conditions. Therefore, applying the traditional approximations, $\widetilde{C}_L \cos\alpha >> \widetilde{C}_D \sin\alpha$, $y_{ac} \sin\alpha \cong 0$, $y_{ac}\widetilde{C}_D \cong 0$, $\cos\alpha \cong 1$, gives

$$\widetilde{C}_{m_{ac}} = \widetilde{C}_{m_O} + \frac{x_{ac}}{c}\widetilde{C}_L \tag{1.6}$$

Taking the derivative of Eq. (1.6) with respect to angle of attack, applying the constraint given by Eq. (1.1), and rearranging gives the traditional approximation for the aerodynamic center

$$\frac{x_{ac}}{c} = -\frac{\widetilde{C}_{m_O,\alpha}}{\widetilde{C}_{L,\alpha}}, \quad \frac{y_{ac}}{c} = 0 \tag{1.7}$$

Note that the *y*-coordinate is traditionally assumed to be zero due to the approximations applied in the development of Eq. (1.6).

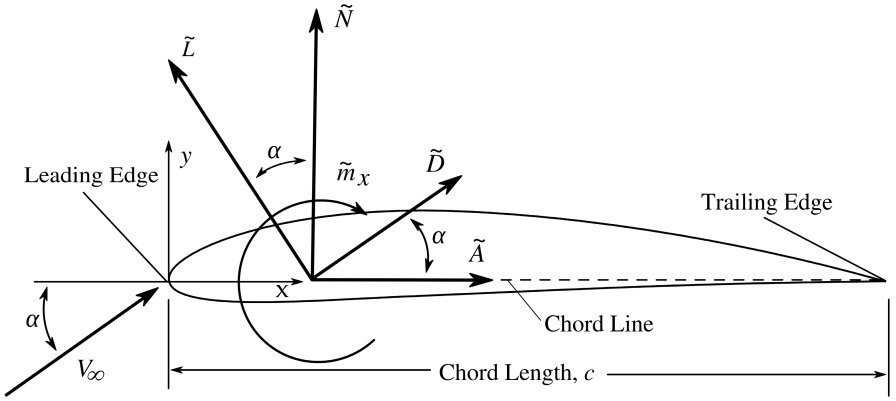

Figure 1. Forces and pitching moment on an airfoil.

Equation (1.7) gives the traditional approximation for the location of the aerodynamic center of an airfoil. These relations require knowledge of the lift and pitching moment slopes of a given airfoil. This prediction for the location of the aerodynamic center of an airfoil is widely used today across the aerospace industry and academia. Furthermore, these relations are traditionally used to approximate the location of the neutral point of an aircraft, and are used to evaluate aircraft static stability. The traditional thin airfoil theory approach as developed by Max Munk [5-9] predicts solutions to Eq. (1.7) as lying at the airfoil quarter chord, or 25% aft of the airfoil leading edge, and directly on the chord line. However, solutions to Eq. (1.7) suffer from small-angle, small-camber, and thin-airfoil approximations. What's more, the assumptions leading to the result given by Eq. (1.7) include a linear lift slope and a moment slope below stall, and therefore neglect nonlinearities in lift, pitching moment, and drag. Furthermore, this traditional approach reduces the nonlinear trigonometric relations in Eq. (1.5) to linear functions of angle of attack. These linearizing approximations significantly hinder our understanding of the effects of nonlinearities associated with pitch stability of airfoils and aircraft. Attempts have been made to develop less restrictive definitions for the location of the airfoil aerodynamic center, however do not account for all of the trigonometric and aerodynamic nonlinearities, nor remove all small-angle, small-camber, and thin-airfoil approximations [10-11].

In order to provide a more accurate solution for the location of the aerodynamic center, we shall now relax the linearizing assumptions in a more general development of the aerodynamic center.

1.2.2 General Relations for the Aerodynamic Center

Phillips, Alley, and Niewoehner [12] presented general relations for the aerodynamic center, which do not include the linearizing approximations used in the traditional approach. From Eq. (1.2) or (1.5), the pitching moment about the aerodynamic center can be written

$$\widetilde{C}_{m_{ac}} = \widetilde{C}_{m_O} + \frac{x_{ac}}{c}\widetilde{C}_N - \frac{y_{ac}}{c}\widetilde{C}_A \tag{1.8}$$

Taking the derivative of Eq. (1.8) with respect to angle of attack and applying the traditional constraints given in Eq. (1.1) gives

$$\frac{x_{ac}}{c}\widetilde{C}_{N,\alpha} - \frac{y_{ac}}{c}\widetilde{C}_{A,\alpha} = -\widetilde{C}_{m_O,\alpha} \tag{1.9}$$

Note that application of the constraint given in Eq. (1.1) produces an equation for a line, not a point. The line given in Eq. (1.9) is the neutral axis of the airfoil [12]. All points along this line satisfy the constraint given in Eq. (1.1). Therefore, the single constraint given in Eq. (1.1) is not sufficient to specify a single point as the aerodynamic center. Phillips, Alley, and Niewoehner [12] suggest a second constraint to isolate the location of the aerodynamic center, namely, that the location of the aerodynamic center must be invariant to small changes in angle of attack, i.e.,

$$\frac{\partial x_{ac}}{\partial \alpha} \equiv 0\,, \quad \frac{\partial y_{ac}}{\partial \alpha} \equiv 0 \tag{1.10}$$

Differentiating Eq. (1.9) with respect to angle of attack, and applying Eq. (1.10) gives

$$\frac{x_{ac}}{c}\widetilde{C}_{N,\alpha,\alpha} - \frac{y_{ac}}{c}\widetilde{C}_{A,\alpha,\alpha} = -\widetilde{C}_{m_O,\alpha,\alpha} \tag{1.11}$$

The intersection of the two lines specified by Eqs. (1.9) and (1.11) defines a unique point where both of the constraints are simultaneously satisfied, and therefore defines the location of the aerodynamic center. Solving Eqs. (1.9) and (1.11) for x_{ac} and y_{ac}, and using the result in Eq. (1.8) gives the location of the aerodynamic center and the pitching moment coefficient about the aerodynamic center

$$\frac{x_{ac}}{c} = \frac{\widetilde{C}_{A,\alpha}\widetilde{C}_{m_O,\alpha,\alpha} - \widetilde{C}_{m_O,\alpha}\widetilde{C}_{A,\alpha,\alpha}}{\widetilde{C}_{N,\alpha}\widetilde{C}_{A,\alpha,\alpha} - \widetilde{C}_{A,\alpha}\widetilde{C}_{N,\alpha,\alpha}} \tag{1.12}$$

$$\frac{y_{ac}}{c} = \frac{\widetilde{C}_{N,\alpha}\widetilde{C}_{m_O,\alpha,\alpha} - \widetilde{C}_{m_O,\alpha}\widetilde{C}_{N,\alpha,\alpha}}{\widetilde{C}_{N,\alpha}\widetilde{C}_{A,\alpha,\alpha} - \widetilde{C}_{A,\alpha}\widetilde{C}_{N,\alpha,\alpha}} \tag{1.13}$$

$$\widetilde{C}_{m_{ac}} = \widetilde{C}_{m_O} + \frac{x_{ac}}{c}\widetilde{C}_N - \frac{y_{ac}}{c}\widetilde{C}_A \tag{1.14}$$

Equations (1.12) and (1.13) offer a more accurate description of the location of the aerodynamic center for any lifting surface. They allow both the x and y coordinates of the aerodynamic center to be evaluated, unlike the traditional approximations given in Eq. (1.7), which always predicts a y-coordinate for the aerodynamic center that lies on the chord line. Furthermore, Eqs. (1.12) and (1.13) correctly include the effects of vertical offsets as well as trigonometric nonlinearities and aerodynamic nonlinearities such as drag.

Note that Eqs. (1.12) and (1.13) are dependent on first and second aerodynamic derivatives with respect to angle of attack, while the traditional approximation given in

Eq. (1.7) depends only on first derivatives of aerodynamic properties. Therefore, this general solution for the aerodynamic center depends on accurately predicting any second-order aerodynamic nonlinearities, even below stall. To estimate the aerodynamic center of airfoils, thin airfoil theory is often applied, which, as will be shown in Chapter 3, neglects these second-order nonlinearities.

Two unique alternative forms of Eqs. (1.12) and (1.13) can be developed which do not rely on first and second aerodynamic derivatives with respect to angle of attack, but rather rely on first and second derivatives with respect to coefficient of lift and the normal-force coefficient respectively. These alternative forms may be useful when comparing the aerodynamic centers of two different lifting surfaces where one desires to fix the design for a given value of lift or normal-force while allowing variation in angle of attack.

CHAPTER 2

ALTERNATIVE APPROACH TO FINDING THE LOCATION OF THE AERODYNAMIC CENTER

2.1 The Aerodynamic Center as a Function of Coefficient of Lift

The relations developed for the location of the aerodynamic center using traditional thin airfoil theory and the more general approach as developed by Phillips [12] both are functions of angle of attack as can be seen in Eq. (1.7) and Eqs. (1.12-1.13) respectively. The value of these relations depend largely on wing and airfoil geometry. Consider two wings with different geometry, both at the same angle of attack. Each of these wings will have a unique coefficient of lift and therefore unique locations of their respective aerodynamic centers. This is due to the fact that the lift distribution generated over a range of angles of attack varies from wing to wing based on section and span geometry. It is advantageous therefore to be able to describe the location of the aerodynamic center independent of wing or airfoil geometry.

In order to accomplish this, we modify the method presented by Phillips [12] whereby we redefine the change in pitching moment coefficient and the location of the aerodynamic center to depend not on small changes in angle of attack, but rather on small changes in coefficient of lift. We redefine the original two constraints given by Eq. (1.1) and Eq. (1.10) as follows

1. *The pitching moment about the aerodynamic center must be invariant to small changes in coefficient of lift*

$$\frac{\partial \widetilde{C}_{mac}}{\partial \widetilde{C}_L} \equiv 0 \tag{2.1}$$

2. *The location of the aerodynamic center must be invariant to small changes in coefficient of lift*

$$\frac{\partial x_{ac}}{\partial \widetilde{C}_L} \equiv 0, \quad \frac{\partial y_{ac}}{\partial \widetilde{C}_L} \equiv 0 \tag{2.2}$$

Using these two new definitions, the location of the aerodynamic center as a function of coefficient of lift will be developed. Consider the definition of the pitching moment and force components normalized by span and divided by dynamic pressure

$$\frac{m_0}{\frac{1}{2}\rho V_\infty{}^2} = \int_{z=-b/2}^{z=b/2} \widetilde{C}_{m_{ac}} c^2 dz - \int_{z=-b/2}^{z=b/2} (\widetilde{C}_L \cos\alpha + \widetilde{C}_D \sin\alpha) c\, \widetilde{x}_{ac} dz - \int_{z=-b/2}^{z=b/2} (\widetilde{C}_L \sin\alpha - \widetilde{C}_D \cos\alpha) c\, \widetilde{y}_{ac} dz \tag{2.3}$$

Applying the definition for the mean moment coefficient and the mean aerodynamic chord length and dividing by the planform area S, we arrive at the modified definition for the pitching moment about the origin of an arbitrary wing.

$$\widetilde{C}_{m_O} c_{ref} = \frac{m_O}{\frac{1}{2}\rho V_\infty{}^2 S} \overline{\widetilde{C}}_{m_{ac}} c_{ref} - \widetilde{C}_L \bar{x}_L \cos\alpha - \widetilde{C}_D \bar{x}_D \sin\alpha - \widetilde{C}_L \bar{y}_L \sin + \widetilde{C}_D \bar{y}_D \cos\alpha \tag{2.4}$$

where $\overline{\widetilde{C}}_{m_{ac}} \equiv \frac{2}{S\bar{c}_{m_{ac}}} \int_{z=0}^{b/2} \widetilde{C}_{mac} c^2 dz$ and $\bar{c}_{mac} \equiv \frac{2}{S} \int_{z=0}^{b/2} c^2 dz$

Using the definition of the pitching moment about the aerodynamic center and dividing it by dynamic pressure and the planform area S gives

$$C_{m_O} c_{ref} = C_{m_{ac}} c_{ref} - \bar{x}_{ac}(C_L \cos\alpha - C_D \sin\alpha) - \bar{y}_{ac}(C_L \sin - C_D \cos\alpha) \tag{2.5}$$

Combining Eq. (2.4) and Eq. (2.5), we obtain

$$\begin{aligned} \bar{x}_{ac}(\widetilde{C}_L \cos\alpha - \widetilde{C}_D \sin\alpha) + \bar{y}_{ac}(\widetilde{C}_L \sin - \widetilde{C}_D \cos\alpha) - \widetilde{C}_{m_{ac}} c_{ref} = \\ \widetilde{C}_L(\bar{x}_L \cos\widetilde{C}_L + \bar{y}_L \sin\widetilde{C}_L) + \widetilde{C}_D(\bar{x}_D \sin\widetilde{C}_L - \bar{y}_D \cos\widetilde{C}_L) \\ - \widetilde{C}_{m_{ac}} \bar{c}_{m_{ac}} \end{aligned} \tag{2.6}$$

Modifying the definition of the section change in pitching moment about the aerodynamic center defined by Eq. (2.1) to be with respect to coefficient of lift is given as

$$\frac{\partial \widetilde{\widetilde{C}}_{m_{ac}}}{\partial \widetilde{C}_L} \equiv 0 \tag{2.7}$$

Using Eqs. (2.1), (2.2) and (2.7), in the first derivatives of Eqs. (2.4) and (2.6) with respect to coefficient of lift we obtain

$$\begin{aligned} \bar{x}_{ac} \frac{\partial}{\partial \widetilde{C}_L}(\widetilde{C}_L \cos\alpha + \widetilde{C}_D \sin\alpha) + \bar{y}_{ac} \frac{\partial}{\partial C_L}(\widetilde{C}_L \sin - \widetilde{C}_D \cos\alpha) = \\ \frac{\partial}{\partial \widetilde{C}_L}[\widetilde{C}_L(\bar{x}_L \cos\widetilde{C}_L + \bar{y}_L \sin\widetilde{C}_L) + \widetilde{C}_D(\bar{x}_D \sin\widetilde{C}_L - \bar{y}_D \cos\widetilde{C}_L)] \\ = -c_{ref} \frac{\partial \widetilde{C}_{m_O}}{\partial \widetilde{C}_L} \end{aligned} \tag{2.8}$$

As previously stated, the location of the aerodynamic center is not defined by a single point but rather by the intersection of two lines. The first line is defined by Eq.

(2.8). This equation describes a line in the plane of symmetry along which every point satisfies the first constraint on the location of the aerodynamic center (Eq. (2.1)). To uniquely define a point along this line a second equation is need that satisfies the second constraint given by Eq. (2.2). To obtain this additional equation we first rewrite Eqs. (2.5) and (2.8) in terms of axial and normal coefficients

$$\widetilde{C}_A = \widetilde{C}_D \cos\alpha - \widetilde{C}_L \sin\alpha \tag{2.9}$$

$$\widetilde{C}_N = \widetilde{C}_L \cos\alpha - \widetilde{C}_D \sin\alpha \tag{2.10}$$

which yields

$$\widetilde{C}_{m_O}\, c_{ref} = \widetilde{C}_{m_{ac}}\, c_{ref} - \overline{x}_{ac}\widetilde{C}_N + \overline{y}_{ac}\widetilde{C}_A \tag{2.11}$$

$$\overline{x}_{ac}\widetilde{C}_{N,\widetilde{C}_L} - \overline{y}_{ac}\widetilde{C}_{A,\widetilde{C}_L} = -\widetilde{C}_{m_O,\widetilde{C}_L}\, c_{ref} \tag{2.12}$$

Equation. (2.12) is equivalent to Eq. (2.8) and defines a line which satisfies the first constraint for given coefficients of lift. To obtain the second line, which is necessary to define the location of the aerodynamic center, we differentiate Eq. (2.12) with respect to coefficient of lift and apply the second constraint. This gives

$$\overline{x}_{ac}\widetilde{C}_{N,\widetilde{C}_L,\widetilde{C}_L} - \overline{y}_{ac}\widetilde{C}_{A,\widetilde{C}_L,\widetilde{C}_L} = -\widetilde{C}_{m_O,\widetilde{C}_L,\widetilde{C}_L}\, c_{ref} \tag{2.13}$$

As is the case for the line defined by Eq. (2.12), where every point along the line satisfies the first constraint, every point along the line defined by Eq. (2.13) satisfies the second constraint on the location of the aerodynamic center. The intersection of these two lines uniquely defines a point where both of the constraints are simultaneously satisfied,

and therefore defines the location of the aerodynamic center. Solving Eqs. (2.12) and (2.13) for x_{ac}/c and y_{ac}/c, and using the results in Eq. (2.11) we obtain

$$\frac{x_{ac}}{c} = \frac{\widetilde{C}_{A,\widetilde{C}_L}\widetilde{C}_{m_O,\widetilde{C}_L,\widetilde{C}_L} - \widetilde{C}_{m_O,\widetilde{C}_L}\widetilde{C}_{A,\widetilde{C}_L,\widetilde{C}_L}}{\widetilde{C}_{N,\widetilde{C}_L}\widetilde{C}_{A,\widetilde{C}_L,\widetilde{C}_L} - \widetilde{C}_{A,\widetilde{C}_L}\widetilde{C}_{N,\widetilde{C}_L,\widetilde{C}_L}} \tag{2.14}$$

$$\frac{y_{ac}}{c} = \frac{\widetilde{C}_{N,\widetilde{C}_L}\widetilde{C}_{m_O,\widetilde{C}_L,\widetilde{C}_L} - \widetilde{C}_{m_O,\widetilde{C}_L}\widetilde{C}_{N,\widetilde{C}_L,\widetilde{C}_L}}{\widetilde{C}_{N,\widetilde{C}_L}\widetilde{C}_{A,\widetilde{C}_L,\widetilde{C}_L} - \widetilde{C}_{A,\widetilde{C}_L}\widetilde{C}_{N,\widetilde{C}_L,\widetilde{C}_L}} \tag{2.15}$$

$$\widetilde{C}_{m_{ac}} = \widetilde{C}_{m_O} + \frac{x_{ac}}{c}\widetilde{C}_N - \frac{y_{ac}}{c}\widetilde{C}_A \tag{2.16}$$

Thus we see that the location of the aerodynamic center can be written as a function of coefficient of lift. Eqs. (2.14-2.16) are functions of coefficient of lift and are analogous to Eqs. (1.12-1.14), which as previously stated define the location of the aerodynamic center as a function of angle of attack.

2.2 The Aerodynamic Center as a Function of Normal-force Coefficient

Another alternative approach to finding the location of the aerodynamic center involves calculating its location as a function of the normal-force coefficient instead of the traditional approach, which depends on changes in angle of attack (Eq. (1.7) and Eqs. (1.12-1.13) respectively). As stated previously in Section 2.1, the traditional relations depend largely on wing and airfoil geometry and are therefore limited when attempting to compare multiple airfoils or wings at a given angle of attack.

In order to determine the location of the aerodynamic center and the associated pitching moment independent of wing or airfoil geometry, we modify the method presented by Phillips [12]. We redefine the original two constraints for the change in pitching moment coefficient and the location of the aerodynamic center given by Eqs. (1.1) and (1.10) to depend not on small changes in angle of attack but rather on small changes in the normal-force coefficient as follows.

1. *The pitching moment about the aerodynamic center must be invariant to small changes in coefficient of lift*

$$\frac{\partial \widetilde{C}_{mac}}{\partial \widetilde{C}_N} \equiv 0 \tag{2.17}$$

2. *The location of the aerodynamic center must be invariant to small changes in coefficient of lift*

$$\frac{\partial x_{ac}}{\partial \widetilde{C}_N} \equiv 0\,, \quad \frac{\partial y_{ac}}{\partial \widetilde{C}_N} \equiv 0 \tag{2.18}$$

Using these two new definitions, the location of the aerodynamic center as a function of normal-force coefficient is developed. Consider the following equation which describes the pitching moment coefficient about the aerodynamic center given in terms of the axial and normal-force coefficients $\widetilde{C}_A$ and $\widetilde{C}_N$.

$$\widetilde{C}_{m_{ac}}\, c_{ref} = \widetilde{C}_{m0}\, c_{ref} + \bar{x}_{ac}\widetilde{C}_N - \bar{y}_{ac}\widetilde{C}_A \tag{2.19}$$

Differentiating Eq. (2.19) with respect to $\widetilde{C}_N$ and applying the constraints given by Eqs. (2.17) and (2.18) yields

$$0 = \widetilde{C}_{m_O,\widetilde{C}_N}\, c_{ref} + \overline{x}_{ac} - \overline{y}_{ac}\widetilde{C}_{A,\widetilde{C}_N} \tag{2.20}$$

Equation (2.20) describes the neutral axis of the wing along which every point satisfies the first constraint as given by Eq. (2.17). To be able to apply the second constraint required to describe the location of the aerodynamic center we differentiate Eq. (2.20) again with respect to $\widetilde{C}_N$ and apply the constraints given by Eq. (2.18). This gives

$$0 = \widetilde{C}_{m_O,\widetilde{C}_N,\widetilde{C}_N}\, c_{ref} - \overline{y}_{ac}\widetilde{C}_{A,\widetilde{C}_N,\widetilde{C}_N} \tag{2.21}$$

Rearranging to solve for $\overline{y}_{ac}$ we obtain

$$\frac{y_{ac}}{c_{ref}} = \frac{\widetilde{C}_{m_O,\widetilde{C}_N,\widetilde{C}_N}}{\widetilde{C}_{A,\widetilde{C}_N,\widetilde{C}_N}} \tag{2.22}$$

Applying the result obtained in Eq. (2.22) to Eq. (2.20) and solving for $\overline{x}_{ac}$ we obtain

$$\frac{x_{ac}}{c_{ref}} = \frac{\widetilde{C}_{m_O,\widetilde{C}_N,\widetilde{C}_N}}{\widetilde{C}_{A,\widetilde{C}_N,\widetilde{C}_N}}\widetilde{C}_{A,\widetilde{C}_N} - \widetilde{C}_{m_O,\widetilde{C}_N} \tag{2.23}$$

Here we have obtained the location of the aerodynamic center as a function of the normal-force coefficient as given by Eqs. (2.22) and (2.23). Using the results of these two equations in Eq. (2.19) we obtain the pitching moment about the aerodynamic center

$$\widetilde{C}_{mac} = \widetilde{C}_{m_O} + \left(\frac{\widetilde{C}_{m_O,\widetilde{C}_N,\widetilde{C}_N}}{\widetilde{C}_{A,\widetilde{C}_N,\widetilde{C}_N}}\widetilde{C}_{A,\widetilde{C}_N} - \widetilde{C}_{m0,\widetilde{C}_N}\right)\widetilde{C}_N - \left(\frac{\widetilde{C}_{m0,\widetilde{C}_N,\widetilde{C}_N}}{\widetilde{C}_{A,\widetilde{C}_N,\widetilde{C}_N}}\right)\widetilde{C}_A \tag{2.24}$$

While Eqs. (2.23) and (2.22) are analogous to Eqs.(1.12) and (1.13) they appear to be of a different form. In order to verify the correctness of Eqs. (2.23) and (2.22), an equivalence proof is given here to show that the location of the aerodynamic center as a function of the normal-force coefficient is equivalent to the location of the aerodynamic center as a function of angle attack. This is important as sample results comparing these two methods will be presented in Section 2.3.

2.2.1 Equivalence Proof

In the alternative approach presented in Section 2.2 the location of the aerodynamic center was derived using constraints which enforce invariance of the pitching moment about the aerodynamic center and the location (x, y) of the aerodynamic center with respect to the normal force coefficient.

$$\frac{x_{ac}}{c_{ref}} = \frac{\widetilde{C}_{m_O,\widetilde{C}_N,\widetilde{C}_N}}{\widetilde{C}_{A,\widetilde{C}_N,\widetilde{C}_N}} \widetilde{C}_{A,\widetilde{C}_N} - \widetilde{C}_{m_O,\widetilde{C}_N} \tag{2.25}$$

$$\frac{y_{ac}}{c_{ref}} = \frac{\widetilde{C}_{m_O,\widetilde{C}_N,\widetilde{C}_N}}{\widetilde{C}_{A,\widetilde{C}_N,\widetilde{C}_N}} \tag{2.26}$$

These equations appear to be of a significantly different form compared to the analogous relations given by Eqs. (1.12) and (1.13) which are functions of angle of attack. Here an equivalence proof is given to show that the location of the aerodynamic center as a function of normal-force coefficient is indeed equivalent to the location of the aerodynamic center as a function of angle attack.

First, we define the numerator of the fraction in the first term of Eq. (2.25) as "$*$" and its denominator as "$**$." Notice that the numerator and denominator of this term are the same as in the case of Eq. (2.26). Starting with $*$ and expanding its partial derivatives with respect to angle of attack, α gives

$$\frac{\partial}{\partial \widetilde{C}_N}\frac{\partial \widetilde{C}_{m_O}}{\partial \widetilde{C}_N} = \frac{\partial}{\partial \widetilde{C}_N}\left(\frac{\partial \widetilde{C}_{m_O}}{\partial \alpha}\frac{\partial \alpha}{\partial \widetilde{C}_N}\right) = \frac{\partial \widetilde{C}_{m0,\alpha}}{\partial \widetilde{C}_N}\frac{\partial \alpha}{\partial \widetilde{C}_N} + \frac{\partial \widetilde{C}_{m0}}{\partial \alpha}\frac{\partial^2 \alpha}{\partial \widetilde{C}_N{}^2} \tag{2.27}$$

By expanding the partial derivate on the right hand side of Eq. (2.27) again with respect to angle of attack, α we obtain

$$\begin{aligned} &= \frac{\partial \widetilde{C}_{m_{O,\alpha}}}{\partial \widetilde{C}_\alpha}\frac{\partial \alpha}{\partial \widetilde{C}_N}\frac{1}{\left(\frac{\partial \widetilde{C}_N}{\partial \alpha}\right)} + \widetilde{C}_{m_{O,\alpha}}\left(\frac{\partial}{\partial \widetilde{C}_N}\frac{\partial \alpha}{\partial \widetilde{C}_N}\right) \\ &= \frac{\widetilde{C}_{m_{O,\alpha,\alpha}}}{\left(\widetilde{C}_{N,\alpha}\right)^2} + \widetilde{C}_{m_O,\alpha}\left(\frac{\partial}{\partial \widetilde{C}_N}\frac{1}{\left(\frac{\partial \widetilde{C}_N}{\partial \alpha}\right)}\right) \\ &= \frac{\widetilde{C}_{m_{O,\alpha,\alpha}}}{\left(\widetilde{C}_{N,\alpha}\right)^2} - \frac{\widetilde{C}_{m_{O,\alpha}}\widetilde{C}_{N,\alpha,\alpha}}{\left(\widetilde{C}_{N,\alpha}\right)^3} = * \end{aligned} \tag{2.28}$$

Applying the same procedure to ** yields

$$** = \frac{\widetilde{C}_{A,\alpha,\alpha}}{\left(\widetilde{C}_{N,\alpha}\right)^2} - \frac{\widetilde{C}_{A,\alpha}\widetilde{C}_{N,\alpha,\alpha}}{\left(\widetilde{C}_{N,\alpha}\right)^3} \tag{2.29}$$

Dividing $*$ by $**$ results in the following relation

$$\frac{*}{**} = \frac{\widetilde{C}_{N,\alpha}\widetilde{C}_{m_O,\alpha,\alpha} - \widetilde{C}_{m_O,\alpha}\widetilde{C}_{N,\alpha,\alpha}}{\widetilde{C}_{N,\alpha}\widetilde{C}_{A,\alpha,\alpha} - \widetilde{C}_{A,\alpha}\widetilde{C}_{N,\alpha,\alpha}} \tag{2.30}$$

Notice that the relation given by Eq. (2.30) is equal to Eq. (1.13) which is the vertical component of the aerodynamic center as obtained by Phillips. Therefore, we see that Eq. (2.26) which describes the vertical location of the aerodynamic center as a function of the normal-force coefficient is indeed equivalent to Eq. (1.13). We can use the result obtained in Eq. (2.30) in Eq. (2.25) to obtain

$$\frac{x_{ac}}{c_{ref}} = \left(\frac{\widetilde{C}_{N,\alpha}\widetilde{C}_{m_O,\alpha,\alpha} - \widetilde{C}_{m_O,\alpha}\widetilde{C}_{N,\alpha,\alpha}}{\widetilde{C}_{N,\alpha}\widetilde{C}_{A,\alpha,\alpha} - \widetilde{C}_{A,\alpha}\widetilde{C}_{N,\alpha,\alpha}} \right) \widetilde{C}_{A,C_N} - \widetilde{C}_{m_{O,C_N}} \tag{2.31}$$

Expanding the remaining partial derivatives with respect to angle of attack yields

$$\frac{x_{ac}}{c_{ref}} = \left(\frac{\widetilde{C}_{N,\alpha}\widetilde{C}_{m_O,\alpha,\alpha} - \widetilde{C}_{m_O,\alpha}\widetilde{C}_{N,\alpha,\alpha}}{\widetilde{C}_{N,\alpha}\widetilde{C}_{A,\alpha,\alpha} - \widetilde{C}_{A,\alpha}\widetilde{C}_{N,\alpha,\alpha}} \right) \frac{\widetilde{C}_{A,\alpha}}{\widetilde{C}_{N,\alpha}} - \frac{\widetilde{C}_{m_{O,\alpha}}}{\widetilde{C}_{N,\alpha}} \tag{2.32}$$

We manipulate this relation further by performing all multiplicative distributions, combining each term by the lowest common denominator, and cancelling common factors to obtain

$$\frac{x_{ac}}{c_{ref}} = \frac{\widetilde{C}_{A,\alpha}\widetilde{C}_{m_O,\alpha,\alpha} - \widetilde{C}_{m_O,\alpha}\widetilde{C}_{A,\alpha,\alpha}}{\widetilde{C}_{N,\alpha}\widetilde{C}_{A,\alpha,\alpha} - \widetilde{C}_{A,\alpha}\widetilde{C}_{N,\alpha,\alpha}} \tag{2.33}$$

Notice that we have recovered exactly Eq. (1.12) as derived by Phillips. Therefore, we see that Eq. (2.25) is equivalent to Eq. (1.12). We see furthermore that the location of the aerodynamic center can indeed be described as purely a function of the normal-force coefficient. This equivalence can further be shown by calculating values for x_{ac} and y_{ac}

using Eqs. (1.12) and (1.13) as functions of angle of attack and Eqs. (2.25) and (2.26) as functions of the normal-force coefficient.

2.3 Sample Results

Using the relations describing the location of the aerodynamic center as a function of angle of attack and those which describe it as a function of the normal-force coefficient respectively, values can be obtained which show the equivalence of the two methods. In both cases neither of these sets of relations make restrictions about the type of flow, whether inviscid or viscous, for which they calculate the location of the aerodynamic center. The sample results presented here reflect purely inviscid flow for which the effects of drag are ignored. Inviscid flow data can be obtained by a number of different methods, both analytical and numerical. One such numerical method, the Vortex Panel Method [Appendix B] provides accurate and fast results for inviscid flow over airfoils.

2.3.1 Vortex Panel Method

The vortex panel method uses a synthesis of straight-line segments and control points along the top and bottom surface of an airfoil. By using a sufficiently high number of straight line segments and control points this method can accurately predict the coefficient of lift and the pitching moment of a given airfoil as functions of angle of attack. Values for coefficient of lift can be related to the axial and normal force coefficients via the inviscid transformations

$$\widetilde{C}_A = -\widetilde{C}_L \sin\alpha \tag{2.34}$$

$$\widetilde{C}_N = \widetilde{C}_L \cos\alpha \tag{2.35}$$

The following data was generated for a NACA 8415 airfoil using a vortex panel method with 400 nodes, cosine clustering, and a non-closed trailing edge.

Table 1 Vortex Panel Method data for a NACA 8415 airfoil

Angle of Attack (degrees)	$\widetilde{C}_L$	$\widetilde{C}_N$	$\widetilde{C}_A$	$\widetilde{C}_m$
10	2.2845	2.2498	-0.39607	0.81502
9	2.1655	2.1388	-0.33875	0.78408
8	2.0457	2.0258	-0.28471	0.75269
7	1.9254	1.9110	-0.23464	0.72091
6	1.8044	1.7945	-0.18861	0.68876
5	1.6830	1.6765	-0.14668	0.65629
4	1.5609	1.5571	-0.10888	0.62353
3	1.4384	1.4364	-0.07528	0.59052
2	1.3155	1.3147	-0.04591	0.55731
1	1.1922	1.1920	-0.02081	0.52393
0	1.0685	1.0685	0.000000	0.49043
-1	0.94447	0.94433	0.01648	0.45684
-2	0.82017	0.81967	0.02862	0.42321
-3	0.69562	0.69467	0.03641	0.38958
-4	0.57086	0.56947	0.03982	0.35599
-5	0.44592	0.44423	0.03887	0.32248
-6	0.32085	0.31909	0.03354	0.28909
-7	0.19568	0.19423	0.02385	0.25586

Using this data, the first and second derivatives in Eqs. (1.12) and (1.13) and Eqs. (2.25) and (2.26) can be approximated numerically in order to find solutions to the location of the aerodynamic center. This numerical approximation can be achieved by means of a second order finite differencing method.

2.3.2 Finite Difference Method

In order to approximate the first and second derivatives required to compute values of the location of the aerodynamic center in Eqs. (1.12) and (1.13) and Eqs. (2.25) and (2.26) discrete approximations using the Taylor series expansion about a point may be employed. The Taylor series expansion of a function $\phi(y)$ about a point y for the value $y+\Delta y$ can be written as

$$\phi(y+\Delta y)=\phi(y)+\left(\frac{\partial\phi}{\partial y}\right)_y\Delta y+\left(\frac{\partial^2\phi}{\partial y^2}\right)_y\frac{\Delta y^2}{2}+\left(\frac{\partial^3\phi}{\partial y^3}\right)_y\frac{\Delta y^3}{6}+O(\Delta y^4)+\cdots \tag{2.36}$$

The second order approximation of the first derivative of $\phi(y)$ at a point j is given by

$$\left(\frac{\partial\phi}{\partial y}\right)_j=\frac{\phi_a\Delta y_b^2-\phi_b\Delta y_a^2-\phi_j(\Delta y_b^2-\Delta y_a^2)}{(\Delta y_b^2\Delta y_a-\Delta y_a^2\Delta y_b)} \tag{2.37}$$

Where a and b represent the points before and after j respectively.

The second order approximation of the second derivative of $\phi(y)$ at a point j is given by

$$\left(\frac{\partial\phi}{\partial y}\right)_j=\frac{2(\Delta y_a+\Delta y_b+\Delta y_c)}{\Delta y_a\Delta y_b\Delta y_c}\phi_j+\frac{2(\Delta y_b+\Delta y_c)}{\Delta y_a(\Delta y_a-\Delta y_b)(\Delta y_c-\Delta y_a)}\phi_a+\frac{2(\Delta y_c+\Delta y_a)}{\Delta y_b(\Delta y_b-\Delta y_c)(\Delta y_a-\Delta y_b)}\phi_b+\frac{2(\Delta y_a+\Delta y_b)}{\Delta y_c(\Delta y_b-\Delta y_c)(\Delta y_c-\Delta y_a)}\phi_c+O(\Delta y^2) \tag{2.38}$$

Where a represents the point before j and b and c represent the first and second point after j respectively.

Using the data from Table 1 in Eq. (2.37) and Eq. (2.38) we can generate approximations of the first and second derivatives of $\widetilde{C}_m, \widetilde{C}_A$, and $\widetilde{C}_N$ as functions of the traditionally used angle of attack, as well as the normal-force coefficient as discussed in Section 2.2. Using these derivatives in their corresponding equations for the location of the aerodynamic center results in Fig 2.

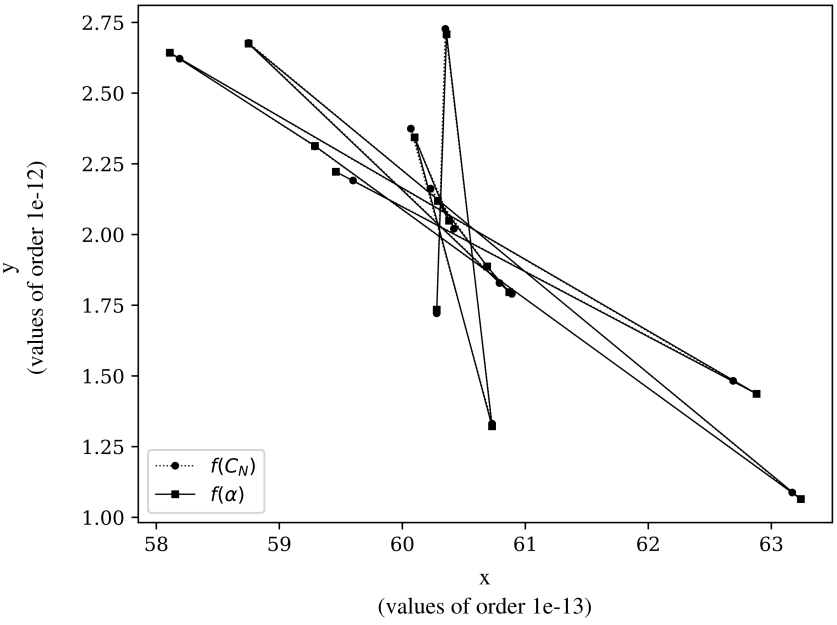

Figure 2. The (x, y) location of the aerodynamic center of a NACA 8415 airfoil using the traditional method as a function of angle of attack, Eqs. (1.12) and (1.13) and the modified method as a function of the normal-force coefficient, Eqs. (2.25) and (2.26).

From the figure we see that both methods give identical results to machine precision. Noting the scale on the axes, for all practical usages the x and y coordinates of

the aerodynamic center given in this figure describe a single point. The scatter in the data can be attributed to the numerical method used. The results of this figure further verify the conclusion given in Section 2.2.1, that the location of the aerodynamic center as a function of angle of attack can be equivalently described as a function of the normal-force coefficient. **However, the true significance of this figure is not that the two methods are equivalent. The true significance of this figure is that the aerodynamic center of an airfoil in an inviscid flow is described by a single point.**

Recall that both the general method for finding the location of the aerodynamic center, given by Eqs. (1.12) and (1.13), and the modified method, given by Eqs. (2.25) and (2.26), allow for evaluation of both the x and y coordinates and include the effects of vertical offsets as well as trigonometric and aerodynamic nonlinearities. Therefore, the fact that in the case of an airfoil in a purely inviscid flow the location of the aerodynamic center collapse to a single point is rather remarkable. This cannot readily be seen by examining Eqs. (1.12) and (1.13) or Eqs. (2.25) and (2.26) as in both cases the relations appear to be highly dependent on changes in angle of attack. However, as has been shown in Fig. 2 **the location of the aerodynamic center in purely inviscid flow is in fact a single point, independent of angle of attack.**

We desire to be able to describe the location of this point for any inviscid airfoil analytically with new, more simple relations, without the need for numerical approximations such as the finite differencing method in order to determine values of unknown derivatives. Additionally, we desire that these new relations analytically demonstrate the angle of attack independence observed in the sample results, while still

including the effects of vertical offsets as well as any trigonometric and or aerodynamic nonlinearities.

CHAPTER 3
THE AERODYNAMIC CENTER OF INVISCID AIRFOILS

As shown in Section 1.2.2, Eqs. (1.12) and (1.13) offer a more accurate description of the location of the aerodynamic center for any lifting surface. They allow for evaluation of both the x and y coordinates of the aerodynamic center, unlike the traditional approximations given in Eq. (1.7), which always predicts a y-coordinate for the aerodynamic center that lies on the chord line. Furthermore, Eqs. (1.12) and (1.13) correctly include the effects of vertical offsets as well as trigonometric and aerodynamic nonlinearities such as drag. These two equations are dependent on first and second aerodynamic derivatives with respect to angle of attack, while the traditional approximation given in Eq. (1.7) depends only on first derivatives of aerodynamic properties. Therefore, the general solution for the aerodynamic center depends on accurately predicting any second-order aerodynamic nonlinearities, even below stall. To estimate the aerodynamic center of airfoils, thin airfoil theory is often applied, which neglects these second-order nonlinearities.

3.1 Classical Thin Airfoil Theory

Thin airfoil theory was developed by Max Munk during the period between 1914 and 1922 [5–9]. In this classical theory, an airfoil is synthesized as the superposition of a uniform flow and a vortex sheet placed along the camber line of the airfoil as shown in Fig. 3. Small camber and small angle-of-attack approximations are applied such that

higher-order terms can be neglected. This results in the classical thin-airfoil lift and pitching-moment relations

$$\widetilde{C}_L = \widetilde{C}_{L,\alpha}(\alpha - \alpha_{L0}) \tag{3.1}$$

$$\widetilde{C}_{m_O} = \widetilde{C}_{m_{c/4}} - \frac{\widetilde{C}_L}{4} \tag{3.2}$$

where $\widetilde{C}_{L,\alpha}$ is the lift slope, α_{L0} is the zero-lift angle of attack, and $\widetilde{C}_{m_{c/4}}$ is the pitching moment about the quarter chord. The coefficients α_{L0} and $\widetilde{C}_{m_{c/4}}$ are constants that can be obtained from the camber line distribution,

$$\alpha_{L0} = \frac{1}{\pi}\int_{\theta=0}^{\pi} \frac{dy_c}{dx}(1-\cos\theta)\,d\theta \tag{3.3}$$

$$\widetilde{C}_{m_{c/4}} = \frac{1}{2}\int_{\theta=0}^{\pi} \frac{dy_c}{dx}[\cos(2\theta)-\cos\theta]\,d\theta \tag{3.4}$$

where θ represents the change of variables for the axial coordinate given by $x(\theta) \equiv (c/2)(1-\cos\theta)$. The coefficient $\widetilde{C}_{L,\alpha}$ is a constant, which from thin-airfoil theory is predicted to be

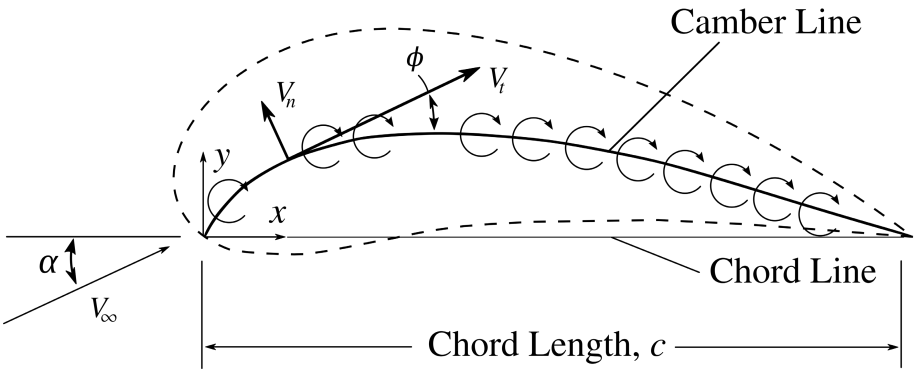

Figure 3. Synthesis of a thin airfoil section from superposition of a uniform flow and a curved vortex sheet distributed along the camber line.

$$\widetilde{C}_{L,\alpha} = 2\pi \tag{3.5}$$

The development of thin airfoil theory can be found in most engineering text books on aerodynamics [13-18]. Using Eq. (3.1) in Eq. (3.2) and applying the result to the traditional relation for the aerodynamic center given in Eq. (1.7) gives the aerodynamic center as predicted by thin airfoil theory,

$$\frac{x_{ac}}{c} = \frac{1}{4}, \quad \frac{y_{ac}}{c} = 0 \tag{3.6}$$

Notice from Eqs. (3.1) and (3.2) that the lift and pitching moment are predicted by this theory to be linear functions of angle of attack. All higher-order nonlinearities in angle of attack were neglected in the development of this theory. Strictly speaking, Eqs. (3.1)–(3.5) are only accurate in the limit as the airfoil geometry and operating conditions approach those of the approximations applied in the development of classical thin airfoil theory. These assumptions include an infinitely thin airfoil, small camber, and small

angles of attack. However, it is commonly assumed that the form of Eqs. (3.1) and (3.2) are correct for arbitrary airfoils at angles of attack below stall. Therefore, $\widetilde{C}_{L,\alpha}$, α_{L0}, and $\widetilde{C}_{m_{c/4}}$ are often used as coefficients to fit Eqs. (3.1) and (3.2) to airfoil data obtained from experimental measurements or numerical simulations. This results in predictions for lift and pitching moment that are linear functions of angle of attack, and do not contain any higher-order dependence on angle of attack below stall. However, as was discussed above, the location of the aerodynamic center is dependent on second-order aerodynamic effects with respect to angle of attack. Thus, in order to better understand the influence of nonlinear aerodynamics on the location of the aerodynamic center, we now consider a more general airfoil theory that does not include any approximations for thickness, camber, or angle of attack.

3.2 General Airfoil Theory

A general airfoil theory that does not include the approximations of small camber, small thickness, and small angles of attack can be developed from the method of conformal mapping [19, 20]. The theory presented here can be used to map flow about a circular cylinder to flow about any arbitrary two-dimensional surface. Pressure distributions can then be integrated to evaluate the resulting lift and pitching moment, as shown in the following development.

3.2.1 Theory Development

Flow about a circular cylinder of radius R centered at the point z_0,including the effects of angle of attack, α, and finite circulation, Γ, can be described by

$$w_1(z) = \frac{d\Phi_1}{dz} = V_\infty \left[e^{-i\alpha} + i\frac{\Gamma}{2\pi V_\infty}\frac{1}{(z - z_0)} - R^2 e^{i\alpha}\frac{1}{(z - z_0)^2} \right] \tag{3.7}$$

where Φ_1 is the complex potential and w_1 is the complex velocity in the plane of the circular cylinder. Using the method of conformal mapping, we can apply an arbitrary transformation of this flow from the plane of the cylinder to the plane of an airfoil of the form

$$\Phi_2(z) = \Phi_1[\zeta(z)] \tag{3.8}$$

where $\zeta(z)$ is an analytic transformation function. The complex velocity in the airfoil plane corresponding to this complex potential is

$$w_2(z) = \frac{d\Phi_2}{dz} = \frac{d}{d\zeta}\Phi_1[\zeta(z)]\frac{d\zeta}{dz} = w_1[\zeta(z)]\frac{d\zeta}{dz} = w_1[\zeta(z)] \Big/ \frac{dz}{d\zeta} \tag{3.9}$$

Thus, the complex velocity for the transformed flow field can be expressed as

$$w_2(z) = \frac{d\Phi_2}{dz} = V_\infty \left[e^{-i\alpha} + i\frac{\Gamma}{2\pi V_\infty}\frac{1}{(\zeta - z_0)} - R^2 e^{i\alpha}\frac{1}{(\zeta - z_0)^2} \right] \Big/ \frac{dz}{d\zeta} \tag{3.10}$$

The potential-flow solution about a circular cylinder can be transformed to obtain the potential-flow solution about a cylinder with any arbitrary cross section. In general, an

arbitrary transformation requires an infinite number of degrees of freedom, and can be expressed in terms of the Laurent series expansion [20],

$$z(\zeta) = \zeta + \sum_{n=1}^{\infty} \frac{C_n}{\zeta^n} \tag{3.11}$$

where the coefficients, C_n, are complex constants. The first derivative of this general transformation is

$$\frac{dz}{d\zeta} = 1 - \sum_{n=1}^{\infty} \frac{nC_n}{\zeta^{n+1}} \tag{3.12}$$

The equation for the surface of the circular cylinder in the ζ-plane can be written as

$$\zeta_{surface} = R\, e^{i\theta} + z_0 \tag{3.13}$$

Using Eq. (3.13) in Eq. (3.11), the transformed surface of the cylinder in the z-plane is given by the relation

$$z(\zeta_{surface}) = R\, e^{i\theta} + z_0 + \sum_{n=1}^{\infty} \frac{C_n}{(R\, e^{i\theta} + z_0)^n} \tag{3.14}$$

The derivative of the conformal transformation given in Eq. (3.12) can be zero at multiple points, depending on the values of the complex coefficients, C_n. These values of ζ are often referred to as the *critical points* of the transformation, at which the transformed velocity field given by Eq. (3.10) is singular. In order to map the flow of a circular cylinder to that over an airfoil, one of the critical points must lie on the circular cylinder in the ζ-plane at the point that maps to the airfoil's trailing edge in the ζ-plane.

All remaining critical points must lie inside the circular cylinder in the ζ -plane in order for the flow external to the cylinder to remain conformal. Here we denote the critical point in the ζ -plane that maps to the airfoil's trailing edge in the ζ -plane as ζ_t. It is convenient to choose ζ_t to be on the positive real axis, as shown in Fig. 4. This requires

$$\zeta_t = \sqrt{R^2 - {y_0}^2} + x_0 = R\, e^{i\theta_t} + z_0 \tag{3.15}$$

where θ_t is the value of θ at $\zeta = \zeta_t$, i.e.,

$$\theta_t = \sin^{-1}(-y_0/R) = -\tan^{-1}\left(y_0 \Big/ \sqrt{R^2 - {y_0}^2}\right) \tag{3.16}$$

Similarly, the left-hand real-axis intercept of the parent circular cylinder is

$$\zeta_l = -\sqrt{R^2 - {y_0}^2} + x_0 \tag{3.17}$$

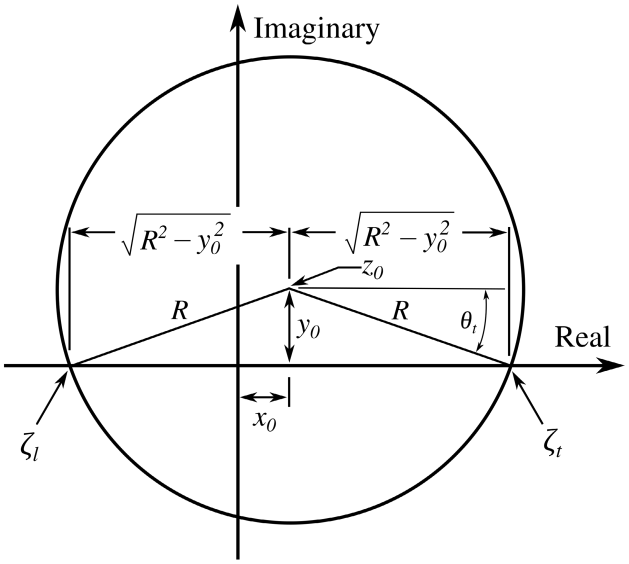

Figure 4. Circular cylinder in the complex ζ -plane, centered at $\zeta = z_0 = x_0 + iy_0$.

Note that for a symmetric airfoil, $y_0 = 0$. The Kutta condition must be satisfied at the trailing edge of the airfoil, and requires that ζ_t be a stagnation point for the flow in the ζ -plane. The complex velocity field is given in Eq. (3.10) and will have a stagnation point at the point on the parent circular cylinder that maps to the airfoil trailing edge if

$$e^{-i\alpha} + i\frac{\Gamma}{2\pi V_\infty}\frac{1}{(\zeta_t - z_0)} - R^2 e^{i\alpha}\frac{1}{(\zeta_t - z_0)^2} = 0 \qquad (3.18)$$

Solving this relation for Γ gives the circulation that will satisfy the Kutta condition at the trailing edge,

$$\Gamma = \frac{2\pi V_\infty}{i}\left[R^2 e^{i\alpha} \frac{1}{(\zeta_t - z_0)} - (\zeta_t - z_0) e^{-i\alpha} \right] \tag{3.19}$$

Using Eq. (3.15) we can evaluate

$$\zeta_t - z_0 = \sqrt{R^2 - y_0^{\,2}} + x_0 - (x_0 + iy_0) = \sqrt{R^2 - y_0^{\,2}} - iy_0 \tag{3.20}$$

Using Eq. (3.20) in Eq. (3.19) gives an alternate form for the circulation

$$\Gamma = 4\pi V_\infty \left(\sqrt{R^2 - y_0^{\,2}} \sin\alpha + y_0 \cos\alpha \right) \tag{3.21}$$

From the Kutta-Joukowski law [21,22], the section lift can be computed from the section circulation, i.e.,

$$\widetilde{L} = \rho V_\infty \Gamma \tag{3.22}$$

Using the circulation from Eq. (3.21) in Eq. (3.22) gives

$$\widetilde{L} = 4\pi\rho V_\infty^{\,2} \left(\sqrt{R^2 - y_0^{\,2}} \sin\alpha + y_0 \cos\alpha \right) \tag{3.23}$$

Notice that the predicted section lift given in Eq. (3.23) is independent of any particular transformation, and is a function only of the radius and vertical offset of the circular cylinder. On the other hand, the leading and trailing edges of the airfoil in the *z*-plane are dependent on the transformation, and are needed in order to compute the chord length and lift coefficient. For any given transformation, the section lift coefficient can be obtained from Eq. (3.23)

$$\widetilde{C}_L \equiv \frac{\widetilde{L}}{\frac{1}{2}\rho V_\infty{}^2 (z_t - z_l)} = \frac{8\pi\sqrt{R^2 - y_0{}^2}}{(z_t - z_l)}\left(\sin\alpha + \frac{y_0}{\sqrt{R^2 - y_0{}^2}}\cos\alpha\right) \tag{3.24}$$

where $c = z_t - z_l$ is the airfoil chord length. Thus, regardless of the transformation, the lift coefficient will be of the form

$$\widetilde{C}_L = \widetilde{C}_{L0,\alpha}(\sin\alpha - \tan\alpha_{L0}\cos\alpha) \tag{3.25}$$

where $\widetilde{C}_{L0,\alpha}$ is the lift slope at zero angle of attack and α_{L0} is the zero-lift angle of attack. From Eq. (3.24),

$$\widetilde{C}_{L0,\alpha} = \frac{8\pi\sqrt{R^2 - y_0{}^2}}{(z_t - z_l)}, \qquad \alpha_{L0} = \theta_t = -\tan^{-1}\left(y_0 \Big/ \sqrt{R^2 - y_0{}^2}\right) \tag{3.26}$$

Notice that from Eqs. (3.23) and (3.26) that the lift and zero-lift angle of attack do not depend on either the transformation or the real part of the cylinder offset, x_0. On the other hand, the lift coefficient and lift slope at zero angle of attack depend on the transformation, which in turn depends on x_0. In any case, Eq. (3.25) is a general form for the lift coefficient of an arbitrary airfoil. No assumptions of camber, thickness, or small angle of attack were made in the development of Eq. (3.25). Therefore, we would expect this form of equation to fit the inviscid lift properties of any airfoil at arbitrary angles of attack.

From the Blasius relations [23-24], the pitching moment about the origin for an arbitrary geometry is

$$\tilde{m}_O = \tfrac{1}{2}\rho \,\mathrm{real}\left\{\oint_C [w(z)]^2 z\, dz\right\} \tag{3.27}$$

Using Eq. (3.12) in Eq. (3.10), the square of the complex velocity of the transformed flow field is

$$[w(z)]^2 = V_\infty^2\left[e^{-i\alpha} + i\frac{\Gamma}{2\pi V_\infty}\frac{1}{(\zeta - z_0)} - R^2 e^{i\alpha}\frac{1}{(\zeta - z_0)^2}\right]^2 \Bigg/ \left(1 - \sum_{n=1}^{\infty}\frac{nC_n}{\zeta^{n+1}}\right)^2 \tag{3.28}$$

Using Eq. (3.28) in Eq. (3.27) and expanding in a Laurent series of $1/\zeta$ gives

$$\tilde{m}_O = \tfrac{1}{2}\rho V_\infty^2 \,\mathrm{real}\left\{\oint_C [F_1(\zeta)]^2 F_2(\zeta)\, d\zeta\right\} \tag{3.29}$$

where

$$[F_1(\zeta)]^2 = e^{-i2\alpha} + i\frac{\Gamma e^{-i\alpha}}{\pi V_\infty}\frac{1}{\zeta} + \left(i\frac{\Gamma z_0 e^{-i\alpha}}{\pi V_\infty} - \frac{\Gamma^2}{4\pi^2 V_\infty^2} - 2R^2\right)\frac{1}{\zeta^2} + \cdots \tag{3.30}$$

$$F_2(\zeta) = \left(\zeta + \sum_{n=1}^{\infty}\frac{C_n}{\zeta^n}\right)\Bigg/\left(1 - \sum_{n=1}^{\infty}\frac{nC_n}{\zeta^{n+1}}\right) = \zeta + \frac{2C_1}{\zeta} + \frac{3C_2}{\zeta^2} + \frac{4C_3 + 2C_1^{\,2}}{\zeta^3} + \cdots \tag{3.31}$$

and

$$[F_1(\zeta)]^2 F_2(\zeta) = e^{-i2\alpha}\zeta + i\frac{\Gamma e^{-i\alpha}}{\pi V_\infty} + \left(i\frac{\Gamma z_0 e^{-i\alpha}}{\pi V_\infty} - \frac{\Gamma^2}{4\pi^2 V_\infty^2} - 2R^2 + 2C_1 e^{-i2\alpha}\right)\frac{1}{\zeta} + \cdots$$

(3.32)

Therefore, the pitching moment about the origin can be written in terms of the series

$$\widetilde{m}_O = \tfrac{1}{2}\rho V_\infty^2 \,\mathrm{real}\left\{\oint_C \sum_{n=0}^{\infty} \frac{B_n}{\zeta^{n-1}} d\zeta\right\}, \tag{3.33}$$

where

$$B_0 = e^{-i2\alpha}, \quad B_1 = i\frac{\Gamma e^{-i\alpha}}{\pi V_\infty}, \quad B_2 = i\frac{\Gamma z_0 e^{-i\alpha}}{\pi V_\infty} - \frac{\Gamma^2}{4\pi^2 V_\infty^2} - 2R^2 + 2C_1 e^{-i2\alpha}, \cdots$$

(3.34)

Using Eq. (3.34) in Eq. (3.33) and integrating shows that the pitching moment is only a function of the first constant in the Laurent series,

$$\widetilde{m}_O = \mathrm{real}\left(i2\pi\rho V_\infty^2 C_1 e^{-i2\alpha} - \rho V_\infty \Gamma z_0 e^{-i\alpha}\right) \tag{3.35}$$

After applying the Kutta-Joukowski law given in Eq. (3.22), the pitching moment about the origin can be written as

$$\widetilde{m}_O = \mathrm{real}\left(i2\pi\rho V_\infty^2 C_1 e^{-i2\alpha} - \widetilde{L} z_0 e^{-i\alpha}\right) \tag{3.36}$$

Using the identity $e^{i\alpha} = \cos\alpha + i\sin\alpha$ as well as the definition $z_0 = x_0 + iy_0$ in Eq. (3.36) gives

$$\widetilde{m}_O = 2\pi\rho V_\infty^2 C_1 \sin(2\alpha) - \widetilde{L}\left(x_0 \cos\alpha + y_0 \sin\alpha\right) \tag{3.37}$$

Because the constant C_1 depends on the transformation, we see that unlike the section lift, the section pitching moment does depend on the transformation. Dividing Eq. (3.37) by

the dynamic pressure and chord length squared, the section pitching moment coefficient relative to the origin used in the transformation can be expressed as

$$\widetilde{C}_{m_O} \equiv \frac{\widetilde{m}_0}{\frac{1}{2}\rho V_\infty^2 (z_t - z_l)^2} = \frac{4\pi C_1}{(z_t - z_l)^2}\sin(2\alpha) - \widetilde{C}_L \frac{x_0 \cos\alpha + y_0 \sin\alpha}{z_t - z_l} \tag{3.38}$$

The moment coefficient about an arbitrary point in the z-plane can be found from the moment coefficient relative to the origin and the lift coefficient,

$$\widetilde{C}_m = \widetilde{C}_{m_O} + \widetilde{C}_L \frac{x\cos\alpha + y\sin\alpha}{z_t - z_l} \tag{3.39}$$

Using Eq. (3.38) in Eq. (3.39) gives

$$\widetilde{C}_m = \frac{4\pi C_1}{(z_t - z_l)^2}\sin(2\alpha) + \widetilde{C}_L \frac{(x - x_0)\cos\alpha + (y - y_0)\sin\alpha}{z_t - z_l} \tag{3.40}$$

In order to compute the pitching-moment coefficient, we need to know C_1, z_t, and z_l, which must be found from the transformation. However, regardless of the transformation, the pitching-moment coefficient for an airfoil in inviscid flow about any point in the domain is a function of angle of attack of the form

$$\widetilde{C}_m = \widetilde{C}_{m0,\alpha}\sin(2\alpha) + \widetilde{C}_{m,N}\widetilde{C}_L\cos\alpha - \widetilde{C}_{m,A}\widetilde{C}_L\sin\alpha \tag{3.41}$$

where $\widetilde{C}_{m0,\alpha}$, $\widetilde{C}_{m,N}$, and $\widetilde{C}_{m,A}$ are constant coefficients. As can be seen from Eq. (3.40), the values for the coefficients $\widetilde{C}_{m,N}$, and $\widetilde{C}_{m,A}$ are a function of the x, and y location of the pitching moment relative to the origin used in the transformation. Since the origin of the

transformation has little physical meaning in the traditional airfoil coordinate system, we will define $\widetilde{C}_{m,N}$, and $\widetilde{C}_{m,A}$ to be the coefficients with the pitching moment evaluated at the airfoil leading edge, i.e. $x = z_l$, and $y = 0$, which is the origin of the traditional airfoil coordinate system. For any given transformation, the pitching moment of an airfoil in an inviscid flowfield about the airfoil leading edge can be evaluated from Eq. (3.41) with the coefficients

$$\widetilde{C}_{m0,\alpha} = \frac{4\pi C_1}{(z_t - z_l)^2}, \quad \widetilde{C}_{m,N} = \frac{z_l - x_0}{z_t - z_l}, \quad \widetilde{C}_{m,A} = \frac{y_0}{z_t - z_l} \tag{3.42}$$

The form of Eqs. (3.25) and (3.41) hold for any airfoil transformation, and therefore, for any arbitrary airfoil shape. These relations were developed without any approximations for airfoil thickness, camber, or angle of attack, and are therefore not constrained under the same limitations that were used in the development of the traditional small-camber and small-angle relations given in Eqs. (3.1) and (3.2).

The coefficients $\widetilde{C}_{L0,\alpha}$, α_{L0}, $\widetilde{C}_{m0,\alpha}$, $\widetilde{C}_{m,N}$, and $\widetilde{C}_{m,A}$ required in Eqs. (3.25) and (3.41) can be evaluated analytically from a known parent cylinder offset and transformation by using Eqs. (3.26) and (3.42). For example, the Joukowski transformation is defined as a special case of Eq. (3.11) where

$$z(\zeta) = \zeta + \frac{\left(\sqrt{R^2 - y_0^2} + x_0\right)^2}{\zeta} \tag{3.43}$$

Using Eq. (3.43) as well as a given parent circular cylinder offset of z_0, the method described above gives the coefficients for a Joukowski airfoil

$$C_1 = \left(\sqrt{R^2 - y_0^2} + x_0\right)^2, \quad z_t = 2\left(\sqrt{R^2 - y_0^2} + x_0\right), \quad z_l = -2\frac{R^2 - y_0^2 + x_0^2}{\sqrt{R^2 - y_0^2} - x_0}$$

$$\widetilde{C}_{L0,\alpha} = \frac{2\pi}{1 + x_0 \Big/ \left(\sqrt{R^2 - y_0^2} - x_0\right)}, \quad \alpha_{L0} = -\tan^{-1}\left(y_0 \Big/ \sqrt{R^2 - y_0^2}\right)$$

$$\widetilde{C}_{m0,\alpha} = \frac{\pi}{4}\left(\frac{R^2 - y_0^2 - x_0^2}{R^2 - y_0^2}\right)^2, \tag{3.44}$$

$$\widetilde{C}_{m,N} = \frac{(x - x_0)\left(\sqrt{R^2 - y_0^2} - x_0\right)}{4(R^2 - y_0^2)}, \quad \widetilde{C}_{m,A} = -\frac{(y - y_0)\left(\sqrt{R^2 - y_0^2} - x_0\right)}{4(R^2 - y_0^2)}$$

The analytical solution for the coefficients given in Eq. (3.44) for a Joukowski airfoil sheds significant insight on an important aspect of the coefficients required in Eqs. (3.25) and (3.41). Note that for a Joukowski airfoil, the entire airfoil and transformation can be defined by only three variables, R, x_0, and y_0. All coefficients in Eq. (3.44) are functions of these three variables. Hence, the aerodynamic coefficients are not entirely independent. For example, after some algebraic manipulation, $\widetilde{C}_{m,N}$ can alternatively be expressed as $\widetilde{C}_{m,N} = \widetilde{C}_{L0,\alpha} \Big/ (8\pi) + (\widetilde{C}_{m0,\alpha} \Big/ \pi)^{1/2} \Big/ 2 - 1$. Although the number of variables required to define an airfoil may vary depending on the transformation, the aerodynamic coefficients of Eqs (3.25) and (3.41) will in general not be entirely independent.

3.2.2 Comparison to Inviscid Computational Results

For airfoil geometries that were not generated from conformal mapping techniques, the coefficients $\widetilde{C}_{L0,\alpha}$, α_{L0}, $\widetilde{C}_{m0,\alpha}$, $\widetilde{C}_{m,N}$, and $\widetilde{C}_{m,A}$ required for Eqs. (3.25) and (3.41) can be evaluated numerically. This can be accomplished by fitting Eqs. (3.25) and (3.41) to a set of airfoil data obtained from experimental or numerical results. A vertical

least squares regression method for fitting these coefficients to a set of data is outlined in Section 3.3. This method can be used to evaluate appropriate coefficients for Eqs. (3.1) and (3.2) or Eqs. (3.25) and (3.41) for cambered airfoils. Because the general airfoil theory relations given in Eqs. (3.25) and (3.41) were developed without any assumptions for airfoil geometry other than that of a single trailing edge, we should expect the form of these equations to match inviscid airfoil aerodynamic data more accurately than Eqs. (3.1) and (3.2), which were obtained from thin airfoil theory. Here we consider the accuracy of each of these equations for the NACA 4-digit series over a range of camber and thickness magnitudes.

Inviscid incompressible aerodynamic lift and pitching moment coefficient data for 250 NACA 4-digit series airfoils were generated over a wide range of camber and thickness using a numerical vortex panel method [Appendix B] employing linear vortex sheets along the airfoil surface [25]. The airfoil surfaces were discretized using 400 panels, which produced grid-resolved solutions. The panels were clustered near the leading and trailing edges of the airfoil using standard cosine clustering. Results were computed for each airfoil at angles of attack ranging from -10 to +15 degrees in increments of 1 degree. At each angle of attack, the lift and pitching moment coefficient about the airfoil leading edge were recorded. Table 2 shows a sample data set for the NACA 8415 airfoil.

Table 2. Inviscid lift and pitching-moment data generated from a vortex panel method for a NACA 8415 airfoil.

Angle of Attack (degrees)	$\widetilde{C}_L$	$\widetilde{C}_m$
15	2.86876	-0.96179
14	2.75352	-0.93361
13	2.63744	-0.90481
12	2.52056	-0.87542
11	2.40291	-0.84548
10	2.28453	-0.81502
9	2.16545	-0.78408
8	2.04571	-0.75269
7	1.92535	-0.72091
6	1.80441	-0.68876
5	1.68291	-0.65629
4	1.56090	-0.62353
3	1.43842	-0.59052
2	1.31549	-0.55731
1	1.19217	-0.52393
0	1.06848	-0.49043
-1	0.94447	-0.45684
-2	0.82017	-0.42321
-3	0.69562	-0.38958
-4	0.57086	-0.35599
-5	0.44592	-0.32248
-6	0.32085	-0.28909
-7	0.19568	-0.25586
-8	0.07045	-0.22284
-9	-0.05480	-0.19005
-10	-0.18003	-0.15755

The least-squares regression method was used to fit the aerodynamic data for each airfoil to the thin-airfoil equations given in Eqs. (3.1) and (3.2), and the RMS value for each case was recorded. Similarly, the least-squares regression method was used to fit the aerodynamic data for each airfoil to the general airfoil theory equations given in Eqs. (3.25) and (3.41), and the RMS value for each case was recorded. Table 3 shows sample resulting coefficients for the NACA 8415 airfoil, along with the associated RMS error from both thin airfoil theory and general airfoil theory. Figures 5 and 6 show the RMS

values for all 250 airfoils as a function of airfoil thickness and varying camber. It should be noted that Eq (3.55) which can be used for fitting data from symmetric airfoils to Eq. (3.41) produces a system of equations that has an infinite number of solutions. The anomaly for symmetric airfoils will be investigated in future work.

Table 3. Least-squares regression coefficients for a NACA 8415 airfoil using relations from thin and general airfoil theory respectively. Root-mean-square error values are also given for each theory compared against results from the vortex panel method.

Coefficient	Thin Airfoil Theory	Coefficient	General Airfoil Theory
$\widetilde{C}_{L,\alpha}$	7.00698	$\widetilde{C}_{L0,\alpha}$	7.09641
α_{L0}	-0.15121	α_{L0}	-0.14944
$\widetilde{C}_{m_{c/4}}$	-0.22746	$\widetilde{C}_{m0,\alpha}$	0.69403
		$\widetilde{C}_{m,N}$	-0.45900
		$\widetilde{C}_{m,A}$	0.04973

Room Mean Squared Error	Thin Airfoil Theory	General Airfoil Theory
$\widetilde{C}_L$	0.01069	machine zero
$\widetilde{C}_m$	0.01495	machine zero

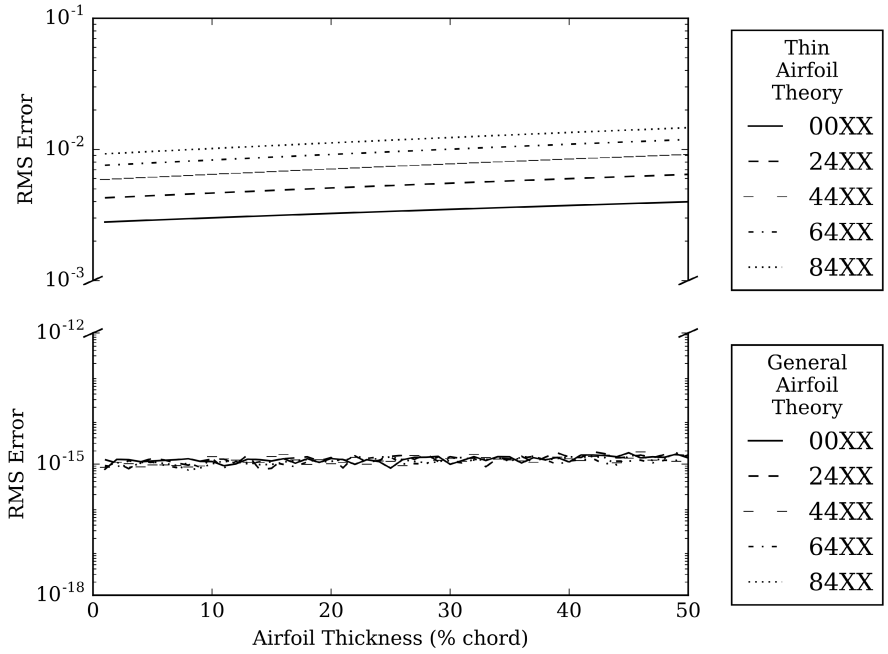

Figure 5. RMS error for lift predictions from thin airfoil theory and general airfoil theory for 250 NACA 4-digit airfoils.

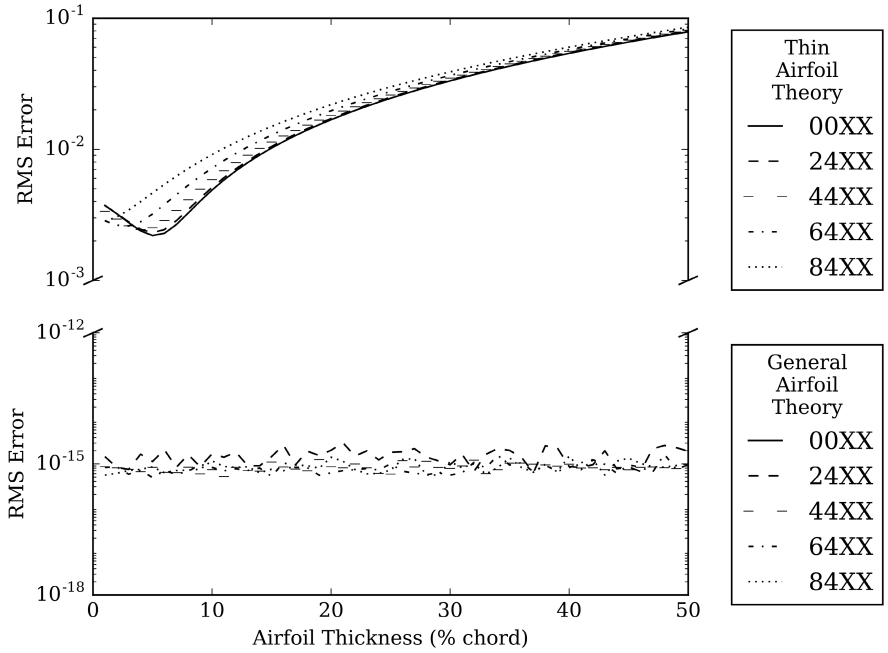

Figure 6. RMS error for pitching-moment predictions from thin airfoil theory and general airfoil theory for 250 NACA 4-digit airfoils.

Note that the RMS error from the general airfoil theory is several orders of magnitude smaller than that of the traditional relations based on thin airfoil theory. In fact, the RMS error from the general airfoil theory is on the order of machine precision. This indicates that the general airfoil theory equations can be fit exactly to the inviscid solutions, and therefore, are of the correct form. The error associated with the least-squares regression fits to the thin airfoil theory equations indicate that the form of the thin airfoil theory equations are not exactly correct. With current measurement technology for experimental setups, the accuracy gained from the general airfoil theory equations for lift and pitching moment predictions is clearly unwarranted. Experimental data is generally only known to 2 or 3 significant figures, which is the same order of accuracy as that obtained from thin airfoil theory. **Therefore, the significance of the general airfoil theory is not that it can more accurately fit experimental data or CFD simulations.** Indeed, the error in experimental data or CFD simulations often falls outside the range of accuracy to be found in either the general airfoil theory or thin airfoil theory. **Thus, using one theory over the other will not give significantly improved results if we wish only to predict lift or pitching moment over a range of angles of attack below stall. Rather, the significance of the general airfoil theory becomes apparent when second derivatives for lift or pitching moment as a function of angle of attack are needed.** Such is the case in the estimation of the location of the aerodynamic center.

3.3 Least-Squares Regression Fit Coefficients – Inviscid Flow

The method of least-squares regression was used to fit the aerodynamic data for each airfoil to the thin-airfoil equations given in Eqs. (3.1) and (3.2), and the general airfoil theory equations given in Eqs. (3.25) and (3.41). The least-squares regression method is commonly used in regression analysis, most importantly in data fitting. In general, the sum of the squares, *S*, of the vertical deviations between the best-fit equation and a set of *n* data points is given by

$$S \equiv \sum_{i=1}^{n} [y_i - f(x_i, \mathbf{a})]^2 \tag{3.45}$$

where (x_i, y_i) are discrete data points, $\mathbf{a}$ is a vector of the unknown coefficients to be determined, and $f(x_i, \mathbf{a})$ is the analytical expression to which the data is to be fitted. The vertical least-squares method seeks to minimize *S* for a given data set and expression $f(x_i, \mathbf{a})$. The RMS error for a given solution can be computed from

$$\text{RMS} \equiv \sqrt{\frac{S}{n}} \tag{3.46}$$

3.3.1 Fit to Thin Airfoil Theory Equations

Applying the traditional lift relation given in Eq. (3.1) to Eq. (3.45) yields

$$S_{\widetilde{C}_L} = \sum_{i=1}^{n} \left[\widetilde{C}_{L_i} - \widetilde{C}_{L,\alpha} (\alpha_i - \alpha_{L0}) \right]^2 \tag{3.47}$$

Best-fit values for $\widetilde{C}_{L,\alpha}$ and α_{L0} can be determined by setting the partial derivatives of Eq. (3.47) with respect to $\widetilde{C}_{L,\alpha}$ and α_{L0} equal to zero. Expressions for the partial derivatives are

$$\frac{\partial S_{\widetilde{C}_L}}{\partial \widetilde{C}_{L,\alpha}} = -2\sum_{i=1}^{n}\left\{\left[\widetilde{C}_{L_i} - \widetilde{C}_{L,\alpha}(\alpha_i - \alpha_{L0})\right](\alpha_i - \alpha_{L0})\right\} = 0 \tag{3.48}$$

$$\frac{\partial S_{\widetilde{C}_L}}{\partial \alpha_{L0}} = 2\sum_{i=1}^{n}\left\{\left[\widetilde{C}_{Li} - \widetilde{C}_{L,\alpha}(\alpha_i - \alpha_{L0})\right]\widetilde{C}_{L,\alpha}\right\} = 0 \tag{3.49}$$

Solving Eqs. (3.48) and (3.49) simultaneously for $\widetilde{C}_{L,\alpha}$ and α_{L0} yield the best-fit values for these two coefficients for the traditional lift equation given in Eq. (3.1),

$$\widetilde{C}_{L,\alpha} = \frac{\sum_{i=1}^{n}(\widetilde{C}_{L_i}\alpha_i) - \alpha_{L0}\sum_{i=1}^{n}\widetilde{C}_{L_i}}{\sum_{i=1}^{n}\alpha_i^{\,2} - 2\alpha_{L0}\sum_{i=1}^{n}\alpha_i + n\alpha_{L0}^{\,2}} \tag{3.50}$$

$$\alpha_{L0} = \frac{\sum_{i=1}^{n}\widetilde{C}_{L_i}\cdot\sum_{i=1}^{n}\alpha_i^2 - \sum_{i=1}^{n}\alpha_i\cdot\sum_{i=1}^{n}(\widetilde{C}_{L_i}\alpha_i)}{\sum_{i=1}^{n}\widetilde{C}_{L_i}\cdot\sum_{i=1}^{n}\alpha_i - n\cdot\sum_{i=1}^{n}(\widetilde{C}_{L_i}\alpha_i)} \tag{3.51}$$

Using the results from Eqs. (3.50) and (3.51) in Eq. (3.1), an estimate for the lift coefficient as a function of angle of attack can be obtained. This vertical least-squares fitting process can also be used to evaluate the best-fit quarter-chord pitching moment for the traditional equation given in Eq. (3.2), i.e.,

$$\widetilde{C}_{m_{c/4}} = \sum_{i=1}^{n}\left(\widetilde{C}_{m_{Oi}} + \frac{\widetilde{C}_{L_i}}{4}\right)\Big/ n \tag{3.52}$$

3.3.2 Fit to General Airfoil Theory Equations

The best-fit coefficients required to fit Eq. (3.25) to a data set can be solved using the process described above, which yields the following expressions for $\widetilde{C}_{L0,\alpha}$ and α_{L0}

$$\alpha_{L0} = \tan^{-1}\left[\frac{\sum_{i=1}^{n}(\widetilde{C}_{L_i}\cos\alpha_i)\cdot\sum_{i=1}^{n}\sin^2\alpha_i - \sum_{i=1}^{n}(\widetilde{C}_{L_i}\sin\alpha_i)\cdot\sum_{i=1}^{n}(\sin\alpha_i\cos\alpha_i)}{\sum_{i=1}^{n}(\widetilde{C}_{L_i}\cos\alpha_i)\cdot\sum_{i=1}^{n}(\sin\alpha_i\cos\alpha_i) - \sum_{i=1}^{n}(\widetilde{C}_{L_i}\sin\alpha_i)\cdot\sum_{i=1}^{n}\cos^2\alpha_i}\right] \tag{3.53}$$

$$\widetilde{C}_{L0,\alpha} = \frac{\sum_{i=1}^{n}\widetilde{C}_{L_i}(\sin\alpha_i - \tan\alpha_{L0}\cos\alpha_i)}{\sum_{i=1}^{n}(\sin\alpha_i - \tan\alpha_{L0}\cos\alpha_i)^2} \tag{3.54}$$

Using the results from Eqs. (3.53) and (3.54) in Eq. (3.25) an estimate for the lift coefficient as a function of angle of attack can be obtained. The least-squares process can then be repeated to evaluate the best-fit coefficients for Eq. (3.41) as a function of angle of attack and lift coefficient. After some algebraic manipulation, this yields the following linear system of equations, which can be solved to evaluate $\widetilde{C}_{m0,\alpha}$, $\widetilde{C}_{m,N}$, and $\widetilde{C}_{m,A}$

$$\begin{bmatrix} \sum_{i=1}^{n}\sin^2(2\alpha_i) & \sum_{i=1}^{n}\left(\widetilde{C}_{L_i}\cos\alpha_i\sin(2\alpha_i)\right) & -\sum_{i=1}^{n}\left(\widetilde{C}_{L_i}\sin\alpha_i\sin(2\alpha_i)\right) \\ \sum_{i=1}^{n}\left(\widetilde{C}_{L_i}\cos\alpha_i\sin(2\alpha_i)\right) & \sum_{i=1}^{n}\left(\widetilde{C}_{L_i}{}^2\cos^2\alpha_i\right) & -\sum_{i=1}^{n}\left(\widetilde{C}_{L_i}{}^2\cos\alpha_i\sin\alpha_i\right) \\ \sum_{i=1}^{n}\left(\widetilde{C}_{L_i}\sin\alpha_i\sin(2\alpha_i)\right) & \sum_{i=1}^{n}\left(\widetilde{C}_{L_i}{}^2\cos\alpha_i\sin\alpha_i\right) & -\sum_{i=1}^{n}\left(\widetilde{C}_{L_i}{}^2\sin^2\alpha_i\right) \end{bmatrix} \begin{Bmatrix} \widetilde{C}_{m0,\alpha} \\ \widetilde{C}_{m,N} \\ \widetilde{C}_{m,A} \end{Bmatrix} = \begin{Bmatrix} \sum_{i=1}^{n}\left(\widetilde{C}_{m_{O_i}}\sin(2\alpha_i)\right) \\ \sum_{i=1}^{n}\left(\widetilde{C}_{m_{O_i}}\widetilde{C}_{L_i}\cos\alpha_i\right) \\ \sum_{i=1}^{n}\left(\widetilde{C}_{m_{O_i}}\widetilde{C}_{L_i}\sin\alpha_i\right) \end{Bmatrix} \tag{3.55}$$

For symmetric airfoils, Eq. (3.55) becomes singular. The reason for this singularity is at this time not fully understood, but could be related to the fact that $\widetilde{C}_{m0,\alpha}$, $\widetilde{C}_{m,N}$, and $\widetilde{C}_{m,A}$ are not linearly independent, as discussed in Section 3.2.1. From general airfoil theory, it can be shown that $\widetilde{C}_{m,A}=0$ for symmetric airfoils. However, there potentially exists an unknown number of solutions for $\widetilde{C}_{m0,\alpha}$, and $\widetilde{C}_{m,N}$ that satisfy Eq. (3.55). Therefore while $\widetilde{C}_{m,A}$ is known in the case of symmetric airfoils, the relation between $\widetilde{C}_{m0,\alpha}$, and $\widetilde{C}_{m,N}$ is not presently known and we conclude

$$\widetilde{C}_{m,A}=0,\quad \widetilde{C}_{m0,\alpha}=f\left(\widetilde{C}_{m,N}\right) \tag{3.56}$$

A method for uniquely evaluating these two coefficients for symmetric airfoils will be the topic of future research.

3.4 The Aerodynamic Center of Airfoils in Inviscid Flow

In general, the location of the aerodynamic center can be correctly predicted using Eqs. (1.12) and (1.13). Recall that this definition for the location of the aerodynamic center is a general definition, in that it does not include any linearizing or small-angle approximations. We shall now consider the location of the aerodynamic center of inviscid airfoils as predicted by the relations developed from classical thin airfoil theory, given in Eqs. (3.1) and (3.2), compared with the relations developed from general airfoil theory, given in Eqs. (3.25) and (3.41). First we consider only the case of inviscid flow, i.e., $\widetilde{C}_D = 0$. From Eqs. (1.3) and (1.4), this gives

$$\widetilde{C}_A = -\widetilde{C}_L \sin\alpha \tag{3.57}$$

$$\widetilde{C}_N = \widetilde{C}_L \cos\alpha \tag{3.58}$$

3.4.1 Thin Airfoil Theory with Trigonometric Nonlinearities

Predictions for the aerodynamic center from thin airfoil theory are traditionally obtained by applying aerodynamic and trigonometric linearizing approximations to Eqs. (1.12) and (1.13). This method was outlined previously, and results in an aerodynamic center location given in Eq. (1.7). After the discussion surrounding the general definition of the aerodynamic center given by Eqs. (1.12)-(1.14), one may be inclined to apply the linear aerodynamic equations from thin airfoil theory while retaining the geometric nonlinearities of Eqs. (3.57) and (3.58). Here we examine the results of such an approach. Using Eq. (3.1) in Eqs. (3.57) and (3.58), differentiating the result twice along with Eq. (3.2), and applying the resulting derivatives to Eqs. (1.12)–(1.14) gives

$$\frac{x_{ac}}{c} = \frac{(\alpha_{L0} - \alpha)\sin\alpha + 2\cos\alpha}{4(\alpha - \alpha_{L0})^2 + 8} \tag{3.59}$$

$$\frac{y_{ac}}{c} = \frac{(\alpha - \alpha_{L0})\cos\alpha + 2\sin\alpha}{4(\alpha - \alpha_{L0})^2 + 8} \tag{3.60}$$

$$\widetilde{C}_{m_{ac}} = \frac{-\widetilde{C}_{L,\alpha}(\alpha - \alpha_{L0})^3 + \widetilde{C}_{m_{c/4}}[(\alpha - \alpha_{L0})^2 + 2]}{4[(\alpha - \alpha_{L0})^2 + 2]} \tag{3.61}$$

Note that the aerodynamic center and associated pitching moment given by Eqs. (3.59)–(3.61) is a nonlinear function of angle of attack. We now compare this result to that from general airfoil theory.

3.4.2 General Airfoil Theory

The aerodynamic center of an arbitrary inviscid airfoil can be more accurately found by using the lift and pitching-moment relations from general airfoil theory. Using Eqs. (3.25) and (3.41) in Eqs. (3.57) and (3.58), differentiating twice, and applying the resulting derivatives to Eqs. (1.12)–(1.14) gives

$$\frac{x_{ac}}{c} = -2\frac{\widetilde{C}_{m0,\alpha}}{\widetilde{C}_{L0,\alpha}}\cos^2\alpha_{L0} - \widetilde{C}_{m,N} \tag{3.62}$$

$$\frac{y_{ac}}{c} = \frac{\widetilde{C}_{m0,\alpha}}{\widetilde{C}_{L0,\alpha}}\sin(2\alpha_{L0}) + \widetilde{C}_{m,A} \tag{3.63}$$

$$\widetilde{C}_{m_{ac}} = \widetilde{C}_{m0,\alpha}\sin(2\alpha_{L0}) \tag{3.64}$$

Notice that Eqs. (3.62)–(3.64) are independent of angle of attack. **Therefore, the location of the aerodynamic center for an arbitrary airfoil in inviscid flow is a single point, independent of angle of attack. This point does not in general lie at the airfoil quarter chord, but is a single point dependent on airfoil thickness and camber.** This solution was developed from general airfoil theory, which does not make any assumptions for small angles of attack, small camber, or small thickness. It is rather remarkable that when all geometric and aerodynamic nonlinearities are retained in the lift and pitching moment equations, along with those in the definition of the aerodynamic center, the relations for the aerodynamic center reduce to such a simple expression, independent of angle of attack, for inviscid flow.

Figure 7 shows the aerodynamic center for the NACA 8415 airfoil as predicted by the traditional thin airfoil theory given in Eq. (1.7), thin airfoil theory with trigonometric nonlinearities given in Eqs. (3.59) and (3.60), and the general airfoil theory given in Eqs. (3.62) and (3.63). Figure 8 shows the pitching moment about the aerodynamic center predicted by each theory as a function of angle of attack. Figures 7 and 8 also include results from second-order finite difference approximations obtained from inviscid numerical solutions for the NACA 8415 airfoil and Eqs. (1.12)–(1.14).

Equations (3.59)-(3.61) represent a mix of using linear aerodynamics from thin airfoil theory while retaining the trigonometric nonlinearities given in Eqs. (3.57) and (3.58). This produces non-physical results and should never be used to approximate the aerodynamic center and the associated pitching moment. Note that the aerodynamic center predicted by Eqs. (3.62) and (3.63) does not lie at the quarter-chord, but is a single

point 1.8% chord aft and 2.1% chord above the quarter-chord point. Equations (3.62)-(3.64) match the finite-difference computational results exactly.

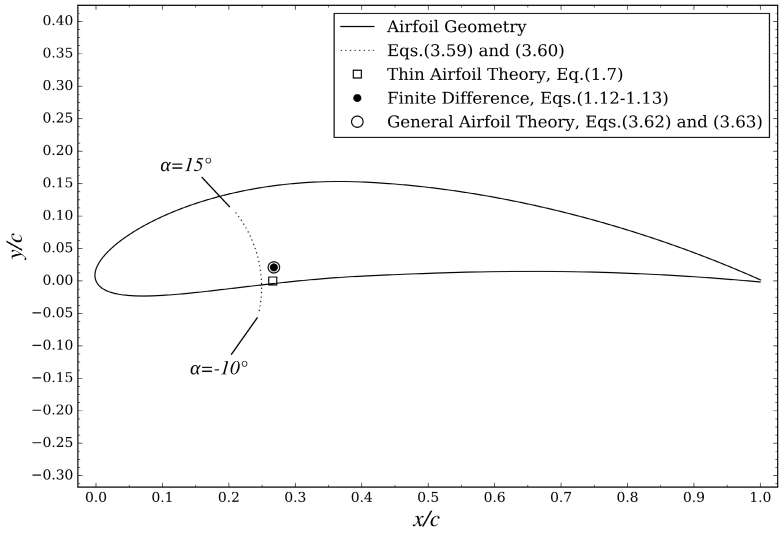

Figure 7. The location of the aerodynamic center for a NACA 8415 airfoil as predicted by thin airfoil theory, Eqs. (3.59)-(3.60), general airfoil theory, and finite differencing.

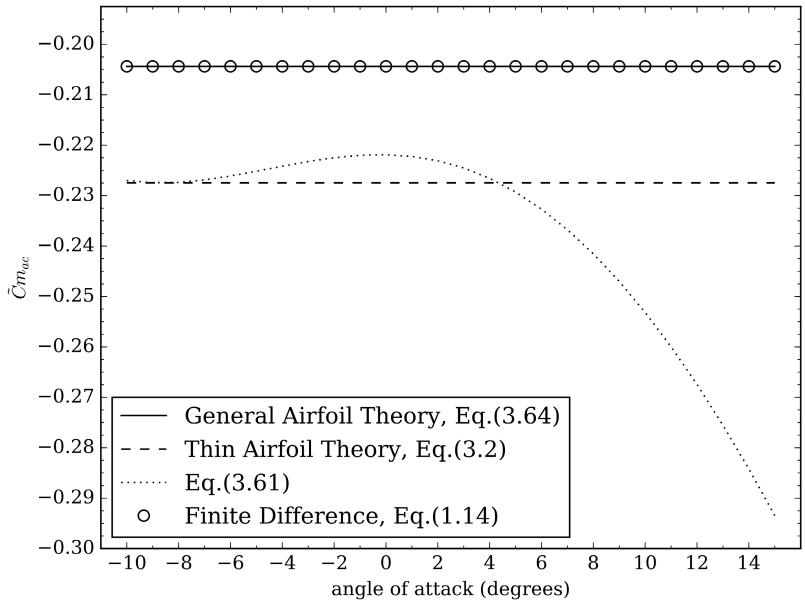

Figure 8. Pitching moment about the aerodynamic center as predicted by thin airfoil theory, Eq. (3.61), general airfoil theory, and finite differencing.

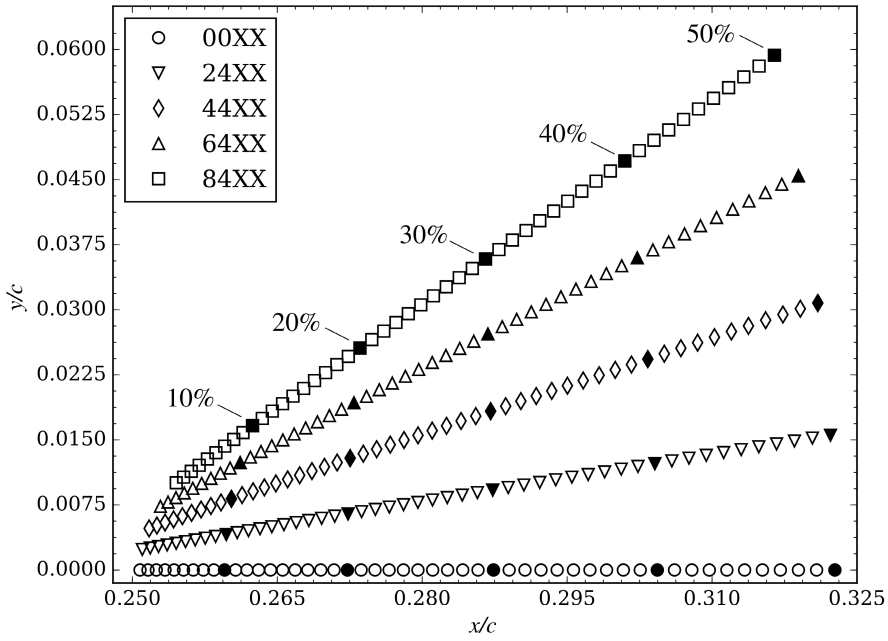

Figure 9. The aerodynamic center location as predicted from Eqs. (3.62**) and (**3.63**) for 250 NACA 4-digit airfoils as a function of camber and thickness. Filled markers represent airfoil thickness increments of 10%.**

Figure 9 shows the aerodynamic center as predicted from Eqs. (3.62) and (3.63) for 250 NACA 4-digit-series airfoils as a function of camber and thickness [Appendix D]. These results show that increasing thicknesses tends to shift the aerodynamic center aft, while camber tends to shift the aerodynamic center normal to the chord line. Notice that airfoils of 10% thickness can have up to 1% deviation in both axial and normal directions relative to the quarter-chord. Because the static margin is often on the order of 5% for a stable aircraft, the difference in these approximations for the location of the aerodynamic center can be somewhat significant. We have thus far considered characteristics of

airfoils only in inviscid flow. As will be shown, viscosity also significantly impacts the location of the aerodynamic center.

CHAPTER 4
THE AERODYNAMIC CENTER OF VISCOUS AIRFOILS

4.1 The Aerodynamic Center of Airfoils in Viscous Airflows

Up to this point, we have neglected the influence of viscosity on the aerodynamic forces and moments created by an airfoil. The largest effect of viscosity on airfoils at angles of attack below stall is the production of friction along the surface of the airfoil. Below stall, this skin friction generally does not significantly impact the lift but does produce drag and alters the pitching moment relative to the inviscid scenario. The section drag coefficient is traditionally related to the section lift coefficient using a quadratic equation. Here we use the traditional relation

$$\widetilde{C}_D = \widetilde{C}_{D_0} + \widetilde{C}_{D_0,L}\widetilde{C}_L + \widetilde{C}_{D_0,L^2}\widetilde{C}_L^2 \tag{4.1}$$

where $\widetilde{C}_{D_0}$, $\widetilde{C}_{D_0,L}$, and $\widetilde{C}_{D_0,L^2}$ are constant coefficients for a given airfoil drag polar. Note that the second term on the right-hand side is required to adequately model drag polars that do not have a minimum at zero lift. Such is the case for most non-symmetric airfoils.

Viscosity also affects the pitching moment produced by the airfoil. Recall that Eq. (3.41) was developed from airfoil theory based on conformal mapping, which is built on the assumption of an inviscid flow. This equation for the pitching moment can be extended to account for viscous effects by including the drag-component acting in the normal and axial directions,

$$\widetilde{C}_m = \widetilde{C}_{m0,\alpha}\sin(2\alpha) + \widetilde{C}_{m,N}\widetilde{C}_N + \widetilde{C}_{m,A}\widetilde{C}_A \tag{4.2}$$

or, in light of Eqs. (1.3) and (1.4),

$$\begin{aligned}\widetilde{C}_m &= \widetilde{C}_{m0,\alpha}\sin(2\alpha) + \widetilde{C}_{m,N}(\widetilde{C}_L\cos\alpha + \widetilde{C}_D\sin\alpha) \\ &\quad + \widetilde{C}_{m,A}(\widetilde{C}_D\cos\alpha - \widetilde{C}_L\sin\alpha)\end{aligned} \tag{4.3}$$

Differentiating Eq. (4.2) and applying the result to Eqs. (1.12) and (1.13) gives the exact solution for the location of the aerodynamic center including viscous effects

$$\frac{x_{ac}}{c} = -2\widetilde{C}_{m0,\alpha}\frac{2\sin(2\alpha)\widetilde{C}_{A,\alpha} + \cos(2\alpha)\widetilde{C}_{A,\alpha,\alpha}}{\widetilde{C}_{N,\alpha}\widetilde{C}_{A,\alpha,\alpha} - \widetilde{C}_{A,\alpha}\widetilde{C}_{N,\alpha,\alpha}} - \widetilde{C}_{m,N} \tag{4.4}$$

$$\frac{y_{ac}}{c} = -2\widetilde{C}_{m0,\alpha}\frac{2\sin(2\alpha)\widetilde{C}_{N,\alpha} + \cos(2\alpha)\widetilde{C}_{N,\alpha,\alpha}}{\widetilde{C}_{N,\alpha}\widetilde{C}_{A,\alpha,\alpha} - \widetilde{C}_{A,\alpha}\widetilde{C}_{N,\alpha,\alpha}} + \widetilde{C}_{m,A} \tag{4.5}$$

Applying Eqs. (4.2), (4.4), and (4.5) to Eq. (1.14) gives the associated pitching moment

$$\widetilde{C}_{m_{ac}} = \widetilde{C}_{m0,\alpha}\left[\sin(2\alpha) + 2\frac{2\sin(2\alpha)(\widetilde{C}_{N,\alpha}\widetilde{C}_A - \widetilde{C}_N\widetilde{C}_{A,\alpha}) + \cos(2\alpha)(\widetilde{C}_A\widetilde{C}_{N,\alpha,\alpha} - \widetilde{C}_N\widetilde{C}_{A,\alpha,\alpha})}{\widetilde{C}_{N,\alpha}\widetilde{C}_{A,\alpha,\alpha} - \widetilde{C}_{A,\alpha}\widetilde{C}_{N,\alpha,\alpha}}\right] \tag{4.6}$$

Equations. (4.4), (4.5), and (4.6) can be used to find the exact location of the aerodynamic center and the associated pitching moment for any airfoil including viscous effects.

In order to be able to compute solutions to Eqs. (4.4-4.6) we need expressions for the normal and axial forces and their respective first and second derivatives with respect

to angle of attack. These can be found analytically by using Eqs. (3.25) and (4.1) in Eqs. (1.3) and (1.4) and differentiating to give

$$\begin{aligned}\widetilde{C}_A &= \cos\alpha[\widetilde{C}_{D_0} + \widetilde{C}_{D_0,L}\widetilde{C}_{L0,\alpha}(\sin\alpha - \cos\alpha\tan\alpha_{L0}) \\ &\quad + \widetilde{C}_{D_0,L^2}\widetilde{C}_{L0,\alpha}{}^2(\sin\alpha - \cos\alpha\tan\alpha_{L0})^2] \\ &\quad - \widetilde{C}_{L0,\alpha}\sin\alpha(\sin\alpha - \cos\alpha\tan\alpha_{L0})\end{aligned} \tag{4.7}$$

$$\begin{aligned}\widetilde{C}_N &= \sin\alpha[\widetilde{C}_{D_0} + \widetilde{C}_{D_0,L}\widetilde{C}_{L0,\alpha}(\sin\alpha - \cos\alpha\tan\alpha_{L0}) \\ &\quad + \widetilde{C}_{D_0,L^2}\widetilde{C}_{L0,\alpha}{}^2(\sin\alpha - \cos\alpha\tan\alpha_{L0})^2] \\ &\quad + \widetilde{C}_{L0,\alpha}\cos\alpha(\sin\alpha - \cos\alpha\tan\alpha_{L0})\end{aligned} \tag{4.8}$$

$$\begin{aligned}\widetilde{C}_{A,\alpha} &= \cos\alpha[2\widetilde{C}_{D_0,L^2}(\cos\alpha + \sin\alpha\tan\alpha_{L0})(\sin\alpha - \cos\alpha\tan\alpha_{L0})\widetilde{C}_{L0,\alpha}{}^2 \\ &\quad + \widetilde{C}_{D_0,L}(\cos\alpha + \sin\alpha\tan\alpha_{L0})\widetilde{C}_{L0,\alpha}] \\ &\quad - \sin\alpha[\widetilde{C}_{D_0} + \widetilde{C}_{D_0,L}\widetilde{C}_{L0,\alpha}(\sin\alpha - \cos\alpha\tan\alpha_{L0}) \\ &\quad + \widetilde{C}_{D_0,L^2}\widetilde{C}_{L0,\alpha}{}^2(\sin\alpha - \cos\alpha\tan\alpha_{L0})^2] \\ &\quad - \widetilde{C}_{L0,\alpha}\cos\alpha(\sin\alpha - \cos\alpha\tan\alpha_{L0}) \\ &\quad - \widetilde{C}_{L0,\alpha}\sin\alpha(\cos\alpha + \sin\alpha\tan\alpha_{L0})\end{aligned} \tag{4.9}$$

$$\begin{aligned}\widetilde{C}_{N,\alpha} &= \sin\alpha[2\widetilde{C}_{D_0,L^2}(\cos\alpha + \sin\alpha\tan\alpha_{L0})(\sin\alpha - \cos\alpha\tan\alpha_{L0})\widetilde{C}_{L0,\alpha}{}^2 \\ &\quad + \widetilde{C}_{D_0,L}(\cos\alpha + \sin\alpha\tan\alpha_{L0})\widetilde{C}_{L0,\alpha}] \\ &\quad + \cos\alpha[\widetilde{C}_{D_0} + \widetilde{C}_{D_0,L}\widetilde{C}_{L0,\alpha}(\sin\alpha - \cos\alpha\tan\alpha_{L0}) \\ &\quad + \widetilde{C}_{D_0,L^2}\widetilde{C}_{L0,\alpha}{}^2(\sin\alpha - \cos\alpha\tan\alpha_{L0})^2] \\ &\quad + \widetilde{C}_{L0,\alpha}\cos\alpha(\cos\alpha + \sin\alpha\tan\alpha_{L0}) \\ &\quad - \widetilde{C}_{L0,\alpha}\sin\alpha(\sin\alpha - \cos\alpha\tan\alpha_{L0})\end{aligned} \tag{4.10}$$

$$
\begin{aligned}
\tilde{C}_{A,\alpha,\alpha} &= 2\tilde{C}_{L0,\alpha}\sin\alpha(\sin\alpha-\cos\alpha\tan\alpha_{L0})-2\tilde{C}_{L0,\alpha}\cos\alpha(\cos\alpha+\sin\alpha\tan\alpha_{L0})\\
&\quad-\cos\alpha[\tilde{C}_{D_0,L}\tilde{C}_{L0,\alpha}(\sin\alpha-\cos\alpha\tan\alpha_{L0})\\
&\quad-2\tilde{C}_{D_0,L^2}\tilde{C}_{L0,\alpha}{}^2(\cos\alpha+\sin\alpha\tan\alpha_{L0})^2\\
&\quad+2\tilde{C}_{D_0,L^2}\tilde{C}_{L0,\alpha}{}^2(\sin\alpha-\cos\alpha\tan\alpha_{L0})^2]\\
&\quad-\cos\alpha[\tilde{C}_{D_0}+\tilde{C}_{D_0,L}\tilde{C}_{L0,\alpha}(\sin\alpha-\cos\alpha\tan\alpha_{L0})\\
&\quad+\tilde{C}_{D_0,L^2}\tilde{C}_{L0,\alpha}{}^2(\sin\alpha-\cos\alpha\tan\alpha_{L0})^2]\\
&\quad-2\sin\alpha[2\tilde{C}_{D_0,L^2}\tilde{C}_{L0,\alpha}{}^2(\cos\alpha+\sin\alpha\tan\alpha_{L0})(\sin\alpha-\cos\alpha\tan\alpha_{L0})\tilde{C}_{L0,\alpha}{}^2\\
&\quad+\tilde{C}_{D_0,L}(\cos\alpha+\sin\alpha\tan\alpha_{L0})\tilde{C}_{L0,\alpha}]
\end{aligned}
\tag{4.11}
$$

$$
\begin{aligned}
\tilde{C}_{N,\alpha,\alpha} &= -2\tilde{C}_{L0,\alpha}\cos\alpha(\sin\alpha-\cos\alpha\tan\alpha_{L0})-2\tilde{C}_{L0,\alpha}\sin\alpha(\cos\alpha+\sin\alpha\tan\alpha_{L0})\\
&\quad-\sin\alpha[\tilde{C}_{D_0,L}\tilde{C}_{L0,\alpha}(\sin\alpha-\cos\alpha\tan\alpha_{L0})\\
&\quad-2\tilde{C}_{D_0,L^2}\tilde{C}_{L0,\alpha}{}^2(\cos\alpha+\sin\alpha\tan\alpha_{L0})^2\\
&\quad+2\tilde{C}_{D_0,L^2}\tilde{C}_{L0,\alpha}{}^2(\sin\alpha-\cos\alpha\tan\alpha_{L0})^2]\\
&\quad-\sin\alpha[\tilde{C}_{D_0}+\tilde{C}_{D_0,L}\tilde{C}_{L0,\alpha}(\sin\alpha-\cos\alpha\tan\alpha_{L0})\\
&\quad+\tilde{C}_{D_0,L^2}\tilde{C}_{L0,\alpha}{}^2(\sin\alpha-\cos\alpha\tan\alpha_{L0})^2]\\
&\quad+2\cos\alpha[2\tilde{C}_{D_0,L^2}\tilde{C}_{L0,\alpha}{}^2(\cos\alpha+\sin\alpha\tan\alpha_{L0})(\sin\alpha-\cos\alpha\tan\alpha_{L0})\tilde{C}_{L0,\alpha}{}^2\\
&\quad+\tilde{C}_{D_0,L}(\cos\alpha+\sin\alpha\tan\alpha_{L0})\tilde{C}_{L0,\alpha}]
\end{aligned}
\tag{4.12}
$$

Using Eqs. (4.7-4.12) in Eqs. (4.4), (4.5), and (4.6) yields solutions for the exact location of the aerodynamic center and the associated pitching moment including viscous effects for any airfoil. As can be seen from Eqs. (4.4) and (4.5), the x and y locations of the aerodynamic center are both functions of angle of attack. This differs from the inviscid solution given in Eqs. (3.62) and (3.63), which yield a single point independent of angle of attack.

These analytical expressions are quite cumbersome, and can be difficult to use in practical applications. However, they can be obtained symbolically using an analytical solver [Appendix C], which can be very useful if applied in a computational framework. The use of a third order approximation is much simpler, while remaining quite accurate as compared to the full higher-order analytical solutions.

4.2 Third Order Approximation

A third-order approximation for the exact location of the aerodynamic center and the associated pitching moment can be obtained using a series of higher order reductions. This is accomplished first by using small-angle-of-attack approximations

$$\begin{gathered}\sin\alpha \cong \alpha - \alpha^3/6, \quad \sin(2\alpha) \cong 2\alpha - 4\alpha^3/3, \quad \sin(3\alpha) \cong 3\alpha - 9\alpha^3/2, \\ \cos\alpha \cong 1 - \alpha^2/2, \quad \cos(2\alpha) \cong 1 - 2\alpha^2, \\ \cos(3\alpha) \cong 1 - 9\alpha^2/2, \quad \tan\alpha_{L0} \cong \alpha_{L0} + \alpha_{L0}^3/3\end{gathered} \tag{4.13}$$

in Eqs. (4.7)-(4.12) and applying the results to Eqs. (4.4)-(4.6). This yields an intermediate result for the now reduced location of the aerodynamic center and the associated pitching moment. Because the angle of attack, α, zero-lift angle of attack, α_{L0}, and drag are small compared to the section lift slope, $\widetilde{C}_{L0,\alpha}$, we apply the second reduction which is to neglect any terms that include fourth-order and higher combinations of α, α_{L0}, $\widetilde{C}_{D_0}$, $\widetilde{C}_{D_0,L}$, and $\widetilde{C}_{D_0,L^2}$. For airfoils at angles of attack below stall, values for these coefficients generally fall in the ranges $-0.2 < \alpha < 0.3$, $-0.1 < \alpha_{L0} < 0.1$,

$0.004 < \widetilde{C}_{D_0} < 0.010, -0.003 < \widetilde{C}_{D_0,L} < 0, 0.003 < \widetilde{C}_{D_0,L^2} < 0.015$. Therefore, we also apply the following simplifying approximations

$$\begin{gathered} \widetilde{C}_{D_0,L}\alpha_{L0} << 1, \quad \widetilde{C}_{D_0,L}\alpha << 1, \\ \widetilde{C}_{D_0}\widetilde{C}_{D_0,L^2} << 1, \quad \widetilde{C}_{D_0}^2 << 1, \quad \widetilde{C}_{D_0,L}^2 << 1 \end{gathered} \tag{4.14}$$

This process produces what will be referred to here as the third-order approximation for the aerodynamic center and associated pitching moment, and can be written as

$$\frac{x_{ac}}{c} = -2\frac{\widetilde{C}_{m0,\alpha}}{\widetilde{C}_{L0,\alpha}}\left[\frac{K_1[3(\alpha\alpha_{L0} - \alpha^2 - \alpha_{L0}^2/2) + 1] - K_2(1 + 3\alpha^2/2) - 1}{K_1(1 + 3\alpha_{L0}^2/2) + 3K_2(\alpha^2/2 - \alpha\alpha_{L0} - 2K_2/3 - 1) - \alpha_{L0}^2 - 1}\right] - \widetilde{C}_{m,N} \tag{4.15}$$

$$\frac{y_{ac}}{c} = -2\frac{\widetilde{C}_{m0,\alpha}}{\widetilde{C}_{L0,\alpha}}\left[\frac{K_1(3\alpha - 2\alpha_{L0}) + \widetilde{C}_{D_0,L} + 3\alpha K_2 + \alpha_{L0}(1 + \alpha_{L0}^2/3)}{K_1(1 + 3\alpha_{L0}^2/2) + 3K_2(\alpha^2/2 - \alpha\alpha_{L0} - 2K_2/3 - 1) - \alpha_{L0}^2 - 1}\right] + \widetilde{C}_{m,A} \tag{4.16}$$

$$\widetilde{C}_{m_{ac}} = 2\widetilde{C}_{m0,\alpha}\left[\frac{\alpha_{L0}(K_1 + K_2 - \alpha_{L0}^2/3 - 1) + 6\alpha K_2(K_1 + K_2)}{K_1(1 + 3\alpha_{L0}^2/2) + 3K_2(\alpha^2/2 - \alpha\alpha_{L0} - 2K_2/3 - 1) - \alpha_{L0}^2 - 1}\right] \tag{4.17}$$

where $$K_1 \equiv \widetilde{C}_{L0,\alpha}\widetilde{C}_{D_0,L^2}, \quad K_2 \equiv \widetilde{C}_{D_0}/(2\widetilde{C}_{L0,\alpha})$$

Notice that Eqs. (4.15-4.17) are of the same form of Eqs. (3.62-3.64), however, they remain functions of angle of attack and drag. This can further be seen by setting all drag term in Eqs. (4.15-4.17) to zero and applying the approximation $\alpha_{L0}{}^2 << 1$ to obtain

$$\frac{x_{ac}}{c} = -2\frac{\widetilde{C}_{m0,\alpha}}{\widetilde{C}_{L0,\alpha}{}^2} - \widetilde{C}_{m,N} \tag{4.18}$$

$$\frac{y_{ac}}{c} = \frac{\widetilde{C}_{m0,\alpha}}{\widetilde{C}_{L0,\alpha}}\left(2\alpha_{L0}\right) + \widetilde{C}_{m,A} \tag{4.19}$$

$$\widetilde{C}_{m_{ac}} = \widetilde{C}_{m0,\alpha}\left(2\alpha_{L0}\right) \tag{4.20}$$

Here we have recovered exactly the small angle approximation of Eqs. (3.62-3.64). This result at first glance seems somewhat remarkable; however, it is to be expected as the results obtained in Eqs. (4.18-4.20) include the small-angle-of-attack approximations given by Eq. (4.13) and upon removal of all remaining viscous drag terms should result in the small angle approximation of the inviscid solution obtained in Chapter 3. Solutions for Eqs. (4.15-4.17) were obtained symbolically using an analytical solver [Appendix C].

4.3 Sample Results

Equations (4.15)–(4.17) can be used as a rather accurate estimate for the aerodynamic center and associated pitching moment for any airfoil. Of course, the accuracy of any estimate for the aerodynamic center is also dependent on the accuracy to which the coefficients in Eqs. (3.25), (4.1), and (4.3) are known. These coefficients can be obtained from a set of data using the least-squares regression method outlined in

Section 4.4. For example, data for several NACA 4-digit airfoils were digitized from plots of lift, drag, and pitching moment published by Abbott and von Doenhoff [26]. These data were fit to Eqs. (3.25), (4.1), and (4.3) using the least-squares regression method outlined in Section 4.4. The resulting aerodynamic coefficients for these airfoils are shown in Table 4.

Table 4. Coefficients for several NACA airfoils as computed from the least-squares algorithm outlined in Section 4.4 using data from Abbott and von Doenhoff [26].

NACA	1408	1412	2412	2424	4415	4418	4424
α_{L0}	-0.01457	-0.02160	-0.04556	-0.03540	-0.07343	-0.06851	-0.06285
$\widetilde{C}_{L,\alpha}$	6.18977	6.02468	5.75810	5.18830	5.68654	5.71103	5.38038
$\widetilde{C}_{D_0}$	0.00515	0.00587	0.00640	0.00845	0.00751	0.00790	0.00879
$\widetilde{C}_{D_0,L}$	-0.00176	-0.00135	-0.00208	-0.00076	-0.00254	-0.00256	-0.00178
$\widetilde{C}_{D_0,L^2}$	0.00802	0.00537	0.00619	0.00636	0.00419	0.00401	0.00533
$\widetilde{C}_{m0,\alpha}$	0.86774	0.54239	0.49412	0.56386	0.64057	0.66330	0.68051
$\widetilde{C}_{m,A}$	-0.03221	-0.01838	-0.02634	0.02839	-0.02452	-0.02351	-0.00591
$\widetilde{C}_{m,N}$	-0.53493	-0.42972	-0.41442	-0.43311	-0.46852	-0.47075	-0.47971

Figure 10 shows the aerodynamic center location for each of these airfoils over the range $-15 < \alpha < 15$ as computed from the exact solution obtained from analytical derivatives applied to Eqs. (4.4) and (4.5), as well as the estimated aerodynamic center predicted by Eqs. (4.15) and (4.16). As can be seen from these results, Eqs. (4.15) and (4.16) quite accurately match the exact solutions for each of the airfoils considered. Note that for the airfoils shown in Fig. 10 at positive angles of attack, the aerodynamic center is positioned higher than at negative angles of attack. This vertical deviation can be as large as 2% of the chord. The aerodynamic center predicted by thin airfoil theory is the

quarter-chord location for all airfoils, and is also included in the plot for reference. Notice that the aerodynamic center predictions including viscous effects deviate from the quarter chord by as much as 3.5% in the axial direction and 4.5% in the normal direction as a percentage of chord.

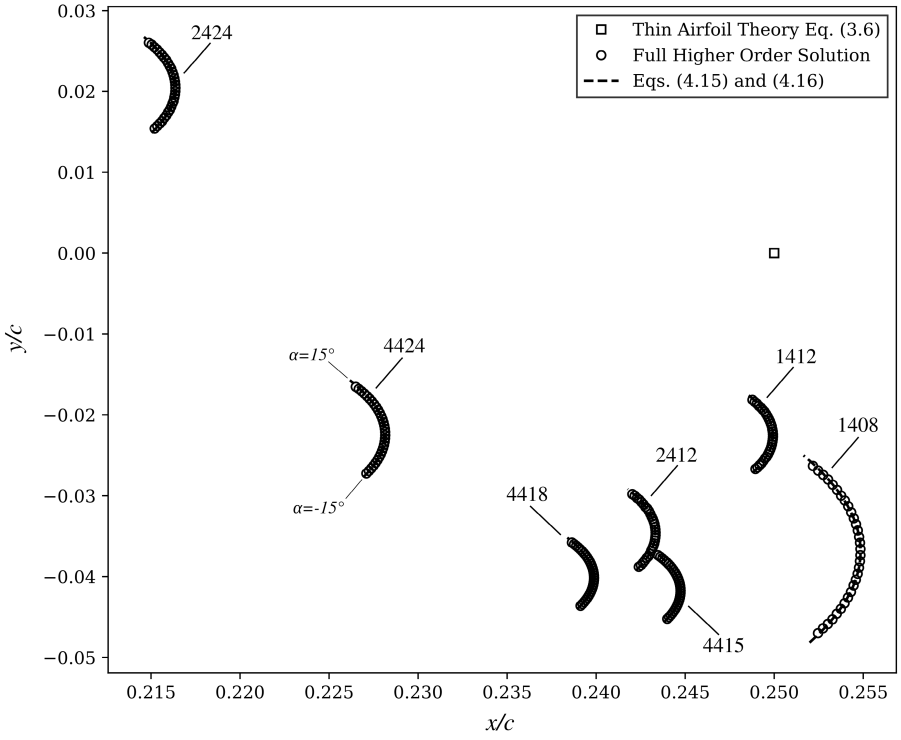

Figure 10. The aerodynamic center location as predicted by the full viscous higher order solution and the third order viscous approximation given by Eqs. (4.15) and (4.16) over a range of angles of attack below stall.

Table 5 gives results for the root-mean-square error between solutions for the location of the aerodynamic center and the associated pitching moment obtained using the full higher order relations and the third order approximation respectively for the selection of NACA 4-digit airfoils. This table also gives the root-mean-square error

between the $(x,y)_{ac}$ pairs using the full higher order relations and the third order approximation. It can be seen from this table that indeed the third order approximation is quite accurate when compared to the much more complicated and cumbersome higher order solution with the largest RMS error on the order of 1E-03.

Table 5. Root-mean-square error between the full higher order exact location of the aerodynamic center and the associated pitching moment, and the third order approximations given by Eqs. (4.15-4.17) respectively using data obtained from Abbott and Von Doenhoff [26]. Root-mean-square error between the high order and third order $(x,y)_{ac}$ pairs for a selection of NACA 4 digit airfoils. Percent deviation between the average high order $(x,y)_{ac}$ pair and the traditional quarter chord location of the aerodynamic center for a selection of NACA 4 digit airfoils.

	Root Mean Squared Error				% Deviation
Airfoil	x_{ac}/c	y_{ac}/c	$\widetilde{C}_{m_{ac}}$	$(x,y)_{ac}$	$c/4$
1408	2.02E-04	5.20E-04	1.04E-03	5.58E-04	3.68%
1412	7.51E-05	2.15E-04	4.21E-04	2.27E-04	2.24%
2412	9.18E-05	2.32E-04	4.43E-04	2.50E-04	3.50%
2424	9.30E-05	2.69E-04	4.59E-04	2.84E-04	4.00%
4415	1.02E-04	2.12E-04	3.99E-04	2.35E-04	4.16%
4418	9.81E-05	2.08E-04	3.90E-04	2.30E-04	4.10%
4424	1.14E-04	2.82E-04	5.07E-04	3.04E-04	3.12%

The rightmost column in Table 5 shows the deviation of the solution in percent chord for the location of the aerodynamic center as obtained from the full higher order relations compared to the quarter chord location predicted by thin airfoil theory. Notice that the percent deviation varies for the selection of NACA airfoils, with the majority between approximately 2-4%. **While the deviation of the aerodynamic center from the commonly used approximation of the quarter chord may seem insignificant for most**

airfoils, results have strong implications for the pitch stability of complete aircraft, which generally have a static margin on the order of 5%.

Results shown in Fig. 9 for the numerically obtained location of the aerodynamic center in inviscid flow show definite trends for the location of the aerodynamic center as a function of airfoil camber and thickness. It can be seen from Fig. 9 as camber increases the location of the aerodynamic center increases in the y direction. As thickness increases the aerodynamic center location shifts rearward of the quarter chord location. With the addition of viscous effects as shown in Fig. 10, it is difficult to exactly discern a trend as a function of camber and airfoil thickness. However, the addition of camber or thickness appear to move the location of the aerodynamic center forward and down below the quarter chord location predicted by thin airfoil theory. Given that the results in Fig. 10 were predicted using experimental viscous data, we can expect that correctly predicting the location of the aerodynamic center for any airfoil depends greatly on the method used and accuracy to which we can obtain data.

Viscous aerodynamic data can also be predicted numerical through the utilization of an integral boundary layer method such as is done in the MIT airfoil development code XFOIL [27]. This widely available tool is used for preliminary airfoil analysis and design. More detail on the methods employed within XFOIL can be found from a number of sources [28-30]. Numerical data for the same selection of NACA 4-digit airfoils as discussed above was independently obtained using XFOIL. These data were fit to Eqs. (3.25), (4.1), and (4.3) using the least-squares regression method outlined in Section 4.4. Figure 11 shows results for the aerodynamic center location for each of the airfoils over

the range $-15 < \alpha < 15$ as computed from the exact solution obtained from analytical derivatives applied to Eqs. (4.4) and (4.5), as well as the estimated aerodynamic center predicted by Eqs. (4.15) and (4.16). In both the case of the full higher order analytical solution and the third order approximation, the location of the aerodynamic center in general remains a function of angle of attack. As can be seen from these results, Eqs. (4.15) and (4.16) quite accurately match the exact solutions for each of the airfoils considered. Note that for the airfoils shown in Fig. 11 at positive angles of attack, the aerodynamic center is positioned higher than at negative angles of attack.

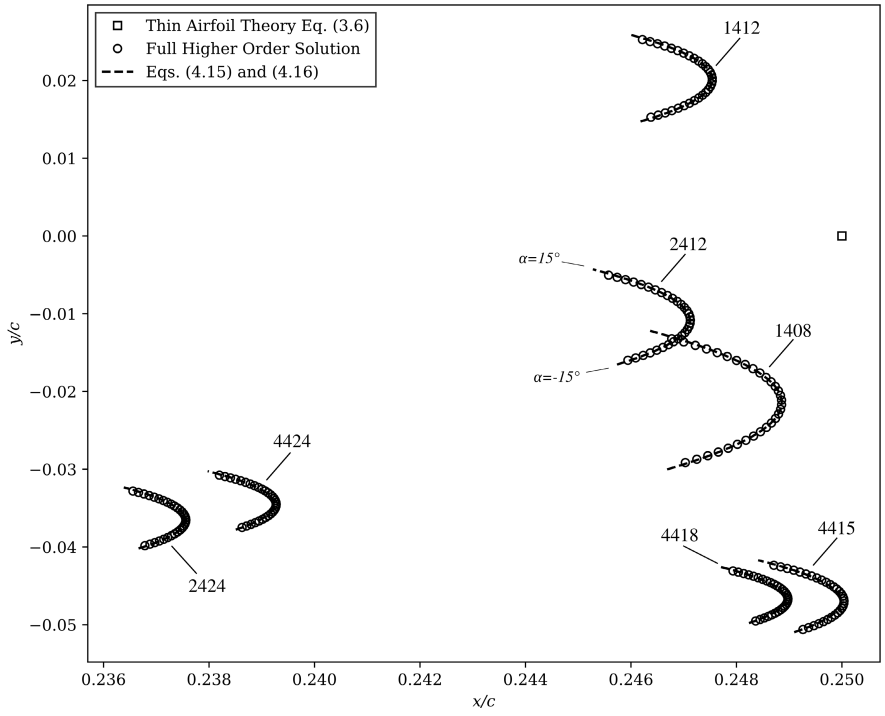

Figure 11. The aerodynamic center location as predicted by the full viscous higher order solution and the third order viscous approximation given by Eqs. (4.15) and (4.16) over a range of angle of attack below stall.

Table 6 shows results for the root-mean-square errors and percent deviations described for Table 5, however, using data obtained from XFOIL.

Table 6. Root-mean-square error between the full higher order exact location of the aerodynamic center and the associated pitching moment, and the second order approximations given by Eqs. (4.15-4.17) respectively using data obtained from XFOIL [27]. Root-mean-square error between the high order and third order $(x,y)_{ac}$ pairs for a selection of NACA 4 digit airfoils. Percent deviation between the average high order $(x,y)_{ac}$ pair and the traditional quarter chord location of the aerodynamic center for a selection of NACA 4 digit airfoils.

	Root Mean Squared Error				% Deviation
Airfoil	x_{ac}/c	y_{ac}/c	$\widetilde{C}_{m_{ac}}$	$(x,y)_{ac}$	$c/4$
1408	1.53E-04	4.01E-04	8.21E-04	4.29E-04	2.12%
1412	8.61E-05	2.50E-04	5.18E-04	2.65E-04	2.05%
2412	1.06E-04	2.79E-04	5.80E-04	2.99E-04	1.10%
2424	6.01E-05	1.77E-04	3.43E-04	1.87E-04	3.85%
4415	1.16E-04	2.24E-04	4.71E-04	2.52E-04	4.64%
4418	8.98E-05	1.73E-04	3.54E-04	1.95E-04	4.62%
4424	8.27E-05	1.79E-04	3.48E-04	1.97E-04	3.58%

Notice that the percent deviation across all of the airfoils examined varies between approximately 1-5%. As was stated before, **while the deviation of the aerodynamic center from the commonly used approximation of the quarter chord may seem insignificant for most airfoils, results have strong implications for the pitch stability of complete aircraft, which generally have a static margin on the order of 5%.**

As was the case in Fig. 10, it is difficult from Fig. 11 to determine exactly a definite trend to the location of the aerodynamic center as a function of airfoil camber and thickness. However, while the results in both Fig.10 and Fig. 11 follow the same general trend, it is apparent that their results are different. From this observation we

conclude that **the ability to correctly predict the location of the aerodynamic center for any airfoil using the full higher order analytical solution or the third order approximations depends greatly on the method used and accuracy to which we can obtain data.**

To understand how large the deviation of the aerodynamic center as a function of angle of attack can be in comparison to the airfoil geometry, results for the NACA 1408 airfoil are shown in Fig. 12. Predictions for the aerodynamic center from three methods are included. These are thin airfoil theory, the inviscid prediction from Eqs. (3.62) and (3.63) using data from the vortex panel method [Appendix B], and full viscous results from Eqs. (4.4) and (4.5) using data from Abbott and von Doenhoff [26]. Included is the estimate given in Eqs. (4.15) and (4.16), which overlap the exact solution from Eqs. (4.4) and (4.5). Note that while thin airfoil theory and the inviscid solution predict an aerodynamic center that is independent of angle of attack, the full viscous solution predicts that the aerodynamic center is a function of angle of attack. For this airfoil, experimental results show that the aerodynamic center falls below the geometry of the airfoil at angles of attack within normal operating conditions.

Figure 13 shows the pitching moment for the same airfoil as a function of angle of attack predicted from thin airfoil theory, the inviscid prediction from Eq. (3.64) using data from the vortex panel method [Appendix B], and full viscous results from Eq. (4.6) compared to the estimate given in Eq. (4.17) using data from Abbott and von Doenhoff [26]. In this case, thin airfoil theory matches the full viscous solution surprisingly well, partially due to the fact that viscosity tends to cancel thickness effects [31].

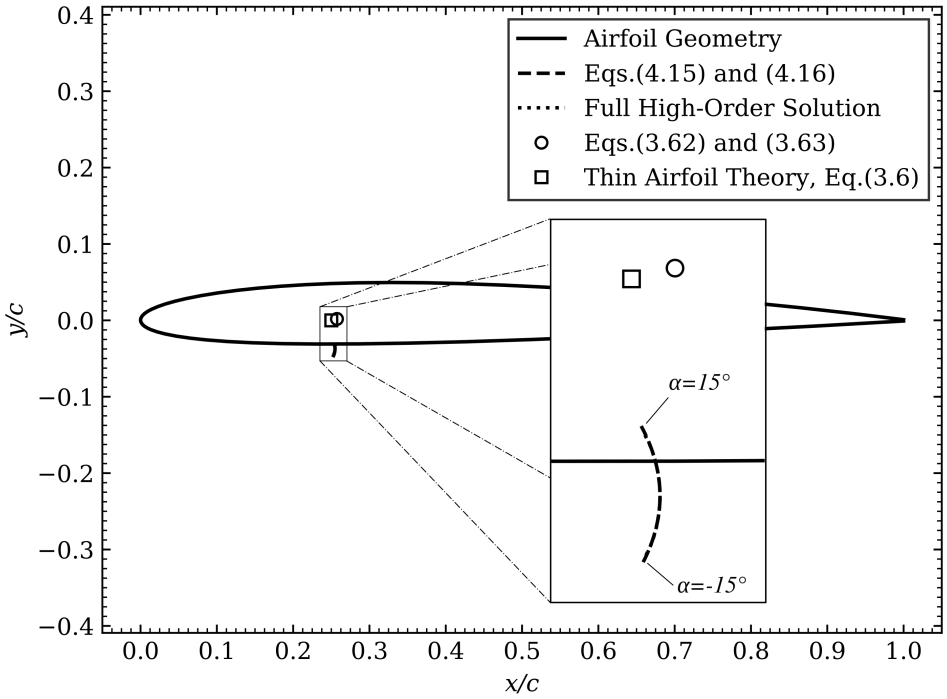

Figure 12. Aerodynamic center locations for the NACA 1408 airfoil as predicted by thin airfoil theory, inviscid computations, and experimental data.

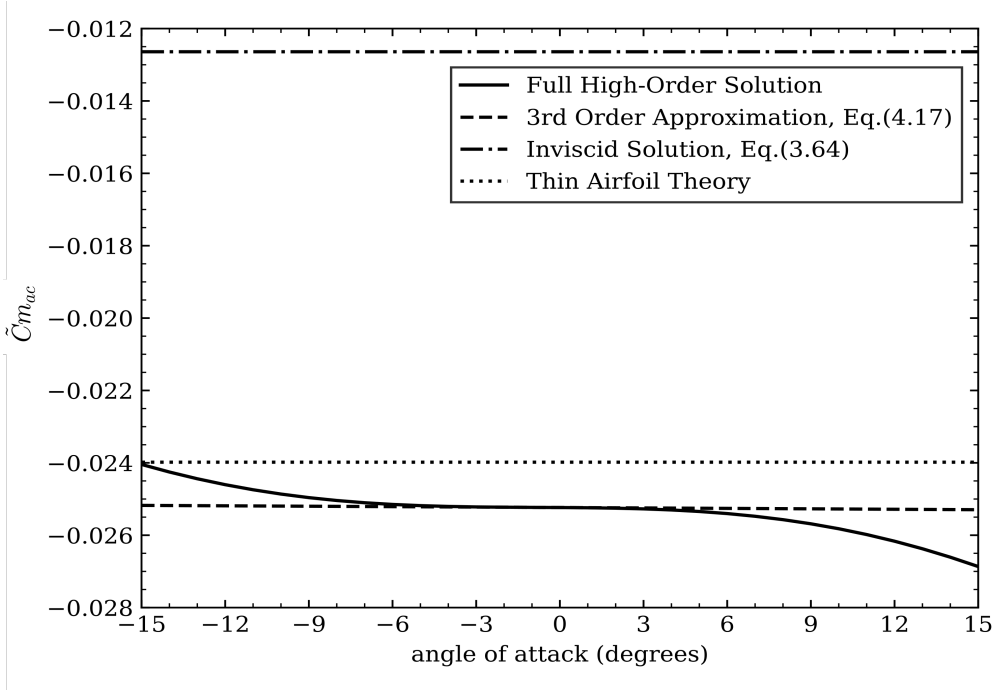

Figure 13. Pitching moment about the aerodynamic center of the NACA 1408 airfoil as predicted by thin airfoil theory, inviscid computations, and experimental data.

The process of finding values for the location of the aerodynamic center and the associated pitching moment from the full higher order solution, or the third order approximation given by Eqs. (4.15-4.17) can be done in general for any airfoil. This requires knowledge of the coefficients $\widetilde{C}_{L0,\alpha}$, α_{L0}, $\widetilde{C}_{m0,\alpha}$, $\widetilde{C}_{m,N}$, $\widetilde{C}_{m,A}$, $\widetilde{C}_{D_0}$, $\widetilde{C}_{D_0,L}$, and $\widetilde{C}_{D_0,L^2}$ to be used in Eqs. (3.25), (4.1), and (4.3). Values for these coefficients must be evaluated numerically. This can be done using the method of Least Squares Regression in a manner similar to that which was done in Section 3.3, however for airfoils in viscous flow.

4.4 Least Squares Regression Fit Coefficients – Viscous Flow

A vertical least squares regression method was used in Section 3.3 to develop inviscid fit equations for $\widetilde{C}_{L,\alpha}$, α_{L0}, and $\widetilde{C}_{m_{c/4}}$ to be used in the classical thin-airfoil relations for $\widetilde{C}_L$ and $\widetilde{C}_{m_O}$, given by Eqs. (3.1) and (3.2). These inviscid fit equations, given by Eqs. (3.50)-(3.52) can also be used for a thin-airfoil approximation of airfoils in viscous flow as Eqs. (3.1) and (3.2) are not functions of drag and therefore are not altered by the inclusion of viscous effects. Inviscid fit equations for $\widetilde{C}_{L0,\alpha}$, and α_{L0} used in the general airfoil theory relation for $\widetilde{C}_L$ (Eq. (3.25)) were also developed in Section 3.3. These general airfoil theory inviscid fit equations, given by Eqs. (3.54) and (3.53) can be used for airfoils in viscous flow as Eq. (3.25) is not a function of drag and therefore is not altered by the inclusion of viscous effects. However, the pitching moment fit coefficients $\widetilde{C}_{m0,\alpha}$, $\widetilde{C}_{m,N}$, and $\widetilde{C}_{m,A}$ given in Section 3.3 cannot be used for airfoils in viscous flow. Equation (3.55) provides solutions for these pitching moment coefficients and can only be applied to Eq. (3.41), which is the pitching moment of an airfoil in an inviscid flowfield, but does not include the effects of drag.

The pitching moment of an airfoil in a viscous flowfield including the effects of drag is defined by Eq. (4.3). Applying the least squares regression process to Eq. (4.3) yields the following linear system of equations, which can be solved to evaluate $\widetilde{C}_{m0,\alpha}$, $\widetilde{C}_{m,N}$, and $\widetilde{C}_{m,A}$

$$\begin{bmatrix} \sum_{i=1}^{n}\sin^2(2\alpha_i) & \sum_{i=1}^{n}\left(\sin(2\alpha_i)\widetilde{C}_{N_i}\right) & \sum_{i=1}^{n}\left(\sin(2\alpha_i)\widetilde{C}_{A_i}\right) \\ \sum_{i=1}^{n}\left(\sin(2\alpha_i)\widetilde{C}_{N_i}\right) & \sum_{i=1}^{n}\left(\widetilde{C}_{N_i}{}^2\right) & \sum_{i=1}^{n}\left(\widetilde{C}_{N_i}\widetilde{C}_{A_i}\right) \\ \sum_{i=1}^{n}\left(\sin(2\alpha_i)\widetilde{C}_{A_i}\right) & \sum_{i=1}^{n}\left(\widetilde{C}_{N_i}\widetilde{C}_{A_i}\right) & \sum_{i=1}^{n}\left(\widetilde{C}_{A_i}{}^2\right) \end{bmatrix} \begin{Bmatrix} \widetilde{C}_{m0,\alpha} \\ \widetilde{C}_{m,N} \\ \widetilde{C}_{m,A} \end{Bmatrix} = \begin{Bmatrix} \sum_{i=1}^{n}\left(\widetilde{C}_{m_{O_i}}\sin(2\alpha_i)\right) \\ \sum_{i=1}^{n}\left(\widetilde{C}_{m_{O_i}}\widetilde{C}_{N_i}\right) \\ \sum_{i=1}^{n}\left(\widetilde{C}_{m_{O_i}}\widetilde{C}_{A_i}\right) \end{Bmatrix} \tag{4.21}$$

where $\widetilde{C}_{Ai} = \widetilde{C}_{D_i}\cos(\alpha_i) - \widetilde{C}_{L_i}\sin(\alpha_i)$ and $\widetilde{C}_{Ni} = \widetilde{C}_{L_i}\cos(\alpha_i) + \widetilde{C}_{D_i}\sin(\alpha_i)$.

In order to evaluate Eq. (4.21), which includes the effects of drag, the three unknown coefficients from Eq. (4.1) must first be obtained from the least squares process. This yields the following linear system of equations, which can be solved to evaluate $\widetilde{C}_{D_0}$, $\widetilde{C}_{D_0,L}$, and $\widetilde{C}_{D_0,L^2}$.

$$\begin{bmatrix} n & \sum_{i=1}^{n}\widetilde{C}_{L_i} & \sum_{i=1}^{n}\widetilde{C}_{L_i}{}^2 \\ \sum_{i=1}^{n}\widetilde{C}_{L_i} & \sum_{i=1}^{n}\widetilde{C}_{L_i}{}^2 & \sum_{i=1}^{n}\widetilde{C}_{L_i}{}^3 \\ \sum_{i=1}^{n}\widetilde{C}_{L_i}{}^2 & \sum_{i=1}^{n}\widetilde{C}_{L_i}{}^3 & \sum_{i=1}^{n}\widetilde{C}_{L_i}{}^4 \end{bmatrix} \begin{Bmatrix} \widetilde{C}_{D_0} \\ \widetilde{C}_{D_0,L} \\ \widetilde{C}_{D_0,L^2} \end{Bmatrix} = \begin{Bmatrix} \sum_{i=1}^{n}\widetilde{C}_{D_0 i} \\ \sum_{i=1}^{n}\left(\widetilde{C}_{D_0 i}\widetilde{C}_{L_i}\right) \\ \sum_{i=1}^{n}\left(\widetilde{C}_{D_0 i}\widetilde{C}_{L_i}{}^2\right) \end{Bmatrix} \tag{4.22}$$

For the special case of a symmetric airfoil in viscous flow, several modifications to the least squares regression fit coefficient relations must be made. The thin airfoil

theory fit coefficient relations given by Eqs. (3.50)-(3.52) for $\widetilde{C}_{L,\alpha}$, α_{L0}, and $\widetilde{C}_{m_{c/4}}$ reduce to

$$\widetilde{C}_{m_{c/4}} = \alpha_{L0} = 0, \quad \widetilde{C}_{L,\alpha} = \frac{\sum_{i=1}^{n} (\widetilde{C}_{L_i} \alpha_i)}{\sum_{i=1}^{n} \alpha_i^{\,2}} \tag{4.23}$$

Similarly the general airfoil theory fit coefficient relations for $\widetilde{C}_{L0,\alpha}$, and α_{L0}, given by Eqs. (3.54) and (3.53), reduce to

$$\alpha_{L0} = 0, \quad \widetilde{C}_{L0,\alpha} = \frac{\sum_{i=1}^{n} (\widetilde{C}_{L_i} \sin \alpha_i)}{\sum_{i=1}^{n} \sin \alpha_i^{\,2}} \tag{4.24}$$

Additionally, the linear system of equations given by Eq. (4.22) for a symmetric airfoil reduces to

$$\widetilde{C}_{D_0,L} = 0, \quad \begin{bmatrix} n & \sum_{i=1}^{n} \widetilde{C}_{L_i}^{\,2} \\ \sum_{i=1}^{n} \widetilde{C}_{L_i}^{\,2} & \sum_{i=1}^{n} \widetilde{C}_{L_i}^{\,4} \end{bmatrix} \begin{Bmatrix} \widetilde{C}_{D_0} \\ \widetilde{C}_{D_0,L^2} \end{Bmatrix} = \begin{Bmatrix} \sum_{i=1}^{n} \widetilde{C}_{D_0 i} \\ \sum_{i=1}^{n} \left(\widetilde{C}_{D_0 i} \widetilde{C}_{L_i}^{\,2} \right) \end{Bmatrix} \tag{4.25}$$

As was the case for Eq. (3.55) in Section 3.3.2 for symmetric airfoils, the linear system of equations given by Eq. (4.21) becomes singular for symmetric airfoils. The reason for this singularity is at this time not fully understood, but could be related to the fact that $\widetilde{C}_{m0,\alpha}$, $\widetilde{C}_{m,N}$, and $\widetilde{C}_{m,A}$ are not linearly independent, as discussed in Section 3.2.1. From general airfoil theory, it can be shown that $\widetilde{C}_{m,A} = 0$ for symmetric airfoils. However, there

potentially exists an unknown number of solutions for $\widetilde{C}_{m0,\alpha}$, and $\widetilde{C}_{m,N}$ that satisfy Eq. (4.21). Therefore while $\widetilde{C}_{m,A}$ is known in the case of symmetric airfoils, the relation between $\widetilde{C}_{m0,\alpha}$, and $\widetilde{C}_{m,N}$ is not presently known and we conclude

$$\widetilde{C}_{m,A} = 0, \quad \widetilde{C}_{m0,\alpha} = f\left(\widetilde{C}_{m,N}\right) \tag{4.26}$$

A method for uniquely evaluating these two coefficients for symmetric airfoils will be the topic of future research.

Appendix A contains results for the thin airfoil theory and general airfoil theory least squares regression fit coefficients for a wide range of NACA 4, 5, and 6 digit airfoils in viscous flow. These coefficients can be used in order to evaluate the location of the aerodynamic center and the associated pitching moment from the full higher order analytical solution or the third order approximations given by Eqs. (4.15)-(4.17).

CHAPTER 5
CONCLUSION

Although thin airfoil theory predicts that the aerodynamic center of an airfoil lies at the quarter chord, it is widely acknowledged that this is, in general, not correct. Rather, the aerodynamic center lies at the quarter chord only in the limit as the airfoil thickness and camber both approach zero. Traditional linear methods of predicting the lift and pitching moment coefficients of airfoils as a function of angle of attack neglect trigonometric and aerodynamic nonlinearities associated with the aerodynamics of airfoils. Hence, traditional approximations do not accurately predict the location of the aerodynamic center, even below stall.

General nonlinear relations for the lift and pitching moment of arbitrary airfoils as a function of angle of attack have been developed here, which include the trigonometric and aerodynamic nonlinearities of airfoils with arbitrary thickness and camber at arbitrary angles of attack. These general relations are given in Eqs. (3.25) and (3.41). These have been shown to match airfoil data for arbitrary airfoils to much higher accuracy than the traditional lift and pitching-moment equations based on thin-airfoil theory, as demonstrated in Figs. 5 and 6. However, **the significance of general airfoil formulation is not that it more accurately fits experimental data or CFD simulations.** Indeed, the accuracy of the traditional equations based on thin airfoil theory is well within the accuracy of experimental or CFD results. **Rather the significance of the general airfoil formulation becomes apparent when second derivatives for lift or pitching moment**

as a function of angle of attack are needed, which is the case in the estimation of the location of the aerodynamic center.

Using the general airfoil theory formulation, it has been shown that the aerodynamic center of any arbitrary airfoil in inviscid flow is a single point, independent of angle of attack, given by Eqs. (3.62) and (3.63). The corresponding pitching moment about the aerodynamic center is given in Eq. (3.64). This matches results predicted by second order finite difference approximations from numerical vortex panel data to machine precision and differs from estimations based on thin airfoil theory, as shown in Fig. 7.

Estimates for the aerodynamic center based on thin airfoil theory also neglect any effects due to viscosity. **It has been shown that, once viscous effects are included, the aerodynamic center is no longer a single point, but is in general a function of angle of attack. The degree to which we can accurately calculate the location of the aerodynamic center depends greatly on the method used and accuracy to which we can obtain viscous aerodynamic data, whether experimentally or numerically.**

A database of least squares regression fit coefficients has been obtained for a wide range of NACA 4, 5, and 6 digit airfoils in viscous flow. These fit coefficients for both thin airfoil theory and general airfoil theory can be used in order to predict the location of the aerodynamic center and the associated pitching moment.

While the difference in the location of the aerodynamic center predicted using thin airfoil theory and general airfoil theory is typically only on the order of one to four percent, this becomes significant when predicting important aircraft static stability

parameters, such as the static margin, which is generally less than 10 percent of the mean chord.

REFERENCES

[1] Diehl, W. S., "The Mean Aerodynamic Chord and the Aerodynamic Center of a Tapered Wing," NACA TR-751, Jan. 1942.

[2] Mathews, C. W., and Kurbjun M. C., "An Analysis of the Factors Affecting the Loss in Lift and Shift in Aerodynamic Center Produced by the Distortion of a Swept Wing Under Aerodynamic Load," NACA TN-2901, Mar. 1953.

[3] Rodden, W. P., "Methods for Calculating the Subsonic Aerodynamic Center of Finite Wings," Journal of Aircraft, Vol. 40, No. 5, 2003, pp. 1003.

[4] Alford, J. E., and Lamar, J. E., "Aerodynamic-Center Considerations of Wings and Wing-Body Combinations," NASA-TN-D-3581, Oct. 1966.

[5] Munk, M. M., "General Theory of Thin Wing Sections," NACA TR-142, Jan. 1922.

[6] Birnbaum, W., "Die tragende Wirbelfläche als Hilfsmittel zur Behandlung des ebenen Problems der Tragflügeltheorie," Zeitschrift für Angewandte Mathematik und Mechanik, Vol. 3, No. 4, 1923, pp. 290–297.

[7] Glauert, H., "A Theory of Thin Aerofoils," Aeronautical Research Council, Reports and Memoranda 910, London,
Feb. 1924.

[8] Glauert, H., "Thin Aerofoils," The Elements of Aerofoil and Airscrew Theory, Cambridge Univ. Press, Cambridge, England, UK, 1926, pp. 87–93.

[9] Abbott, I. H., and von Doenhoff, A. E., "Theory of Thin Wing Sections," Theory of Wing Sections, McGraw–Hill,
New York, 1949, (republished by Dover, New York, 1959), pp. 64–79.

[10] Anderson, J. D., "Incompressible Flow over Airfoils," Fundamentals of Aerodynamics, McGraw–Hill, New York, 2011, pp. 357–361

[11] Thompson, M. J., "A Simple Method for Determining the Aerodynamic Center of an Airfoil," Journal of the Aeronautical Sciences, Vol. 5, No. 4, 1938, pp. 138-140.

[12] Phillips, W. F., Alley, N. R., and Niewoehner, R. J., "Effects of Nonlinearities on Subsonic Aerodynamic Center," Journal of Aircraft, Vol. 45, No. 4, July–Aug, 2008, pp. 1244–1255.

[13] Anderson, J. D., "Classical Thin Airfoil Theory," Fundamentals of Aerodynamics, 5th ed., McGraw–Hill, New York, 2011, pp. 338–357.

[14] Bertin, J. J., and Cummings, R. M., "Thin-Airfoil Theory," Aerodynamics for Engineers, 6th ed., Prentice–Hall, Upper Saddle River, NJ, 2014, pp. 298–317.

[15] Katz, J., and Plotkin, A., "Small-Disturbance Flow over Two-dimensional Airfoils," Low-Speed Aerodynamics, 2nd ed., Cambridge Univ. Press, Cambridge, England, U.K., 2001, pp. 94–121.

[16] Kuethe, A. M., and Chow, C. Y., "Aerodynamic Characteristics of Airfoils," Foundations of Aerodynamics: Bases of Aerodynamic Design, 5th ed., Wiley, New York, 1998, pp. 136–150.

[17] McCormick, B. W., "Thin Airfoil Theory," Aerodynamics, Aeronautics, and Flight Mechanics, 2nd ed., Wiley, New York, 1995, pp. 73–84.

[18] Phillips, W. F., "Incompressible Flow over Airfoils," Mechanics of Flight, 2nd ed., Wiley, Hoboken, NJ, 2010, pp. 26–39.

[19] Abbott, I. H., and Von Doenhoff, A. E., "Theory of Wing Sections of Finite Thickness," Theory of Wing Sections, Dover Publications, Inc., New York, 1959, pp. 46–63.

[20] Karamcheti, K., "Problem of the Airfoil," Principles of Ideal-Fluid Aerodynamics, Krieger, Malabar, Florida, 1980, pp. 466–491.

[21] Kutta, M. W., "Auftriebskrafte in Stromenenden Flussigkeiten," Illustrierte Aeronautische Mitteilungen, Vol. 6, No. 133, 1902.

[22] Joukowski, N. E., "Sur les Tourbillons Adjionts," Traraux de la Section Physique de la Societe Imperiale des Amis des Sciences Naturales, Vol. 13, No. 2, 1906.

[23] Blasius, H., “Funktionentheoretische Methoden in der Hydrodynamik,” Zeitschrift für Mathematik und Physik, Vol. 58, 1910, pp. 90-110.

[24] Hager, W. H., “Blasius: A life in research and education,” Experiments in Fluids, Vol. 34, 2003, pp. 566-571.

[25] Phillips, W. F., “Incompressible Flow over Airfoils,” Mechanics of Flight, 2nd ed., Wiley, Hoboken NJ, 2010, pp. 32–36.

[26]Abbott, I. H., and von Doenhoff, A. E., “Aerodynamic Characteristics of Wing Sections,” Theory of Wing Sections, McGraw–Hill, New York, 1949, (republished by Dover, New York, 1959), pp. 449-687.

[27] Drela, M., and Youngren, H., “XFOIL 6.9 User Primer,” User Guide in Plain Text, Nov. 30, 2001

[28] Drela, M., “XFOIL: An Analysis and Design System for Low Reynolds Number Airfoils,” Conference on Low Reynolds Number Airfoil Aerodynamics, University of Notre Dame, June 1989.

[29] Drela, M. and Giles, M.B., “Viscous-Inviscid Analysis of Transonic and Low Reynolds Number Airfoils,” AIAA Journal, Vol. 25, No. 10, October 1987, pp.1347–1355.

[30] Drela, M., “Integral Boundary Layer Formulation for Blunt Trailing Edges,” AIAA Paper AIAA-89-2166, August 1989.

[31] Phillips, W. F., “The Vortex Panel Method,” Mechanics of Flight, 2nd ed., Wiley, Hoboken NJ, 2010, pp. 32–39.

APPENDICES

APPENDIX A

Coefficients obtained from Experimental Data, Abbott and von Doenhoff [26]

NACA Airfoil	Re	Thin Airfoil Theory			General Airfoil Theory					Drag			α
		$C_{L,a}$	a_{L0}	$C_{mc/4}$	$C_{L0,a}$	a_{L0}	$C_{m0,\alpha}$	$C_{m,A}$	$C_{m,N}$	C_{D0}	$C_{D0,L}$	C_{D0,L^2}	
0006	3E+6	6.181421	0.000000	0.000000	6.189582	0.000000	-	0.000000	-	0.004605	0.000000	0.010322	-6 to 7º
	6E+6	6.100116	0.000000	0.000000	6.112849	0.000000	-	0.000000	-	0.004932	0.000000	0.006375	-7 to 9º
	9E+6	6.205852	0.000000	0.000000	6.216357	0.000000	-	0.000000	-	0.005218	0.000000	0.004296	-7 to 7º
0009	3E+6	6.089632	0.000000	0.000000	6.103080	0.000000	-	0.000000	-	0.005508	0.000000	0.005776	-8 to 8º
	6E+6	6.344274	0.000000	0.000000	6.357797	0.000000	-	0.000000	-	0.005672	0.000000	0.003633	-8 to 8º
	9E+6	6.289587	0.000000	0.000000	6.305649	0.000000	-	0.000000	-	0.005724	0.000000	0.002693	-8 to 8º
0012	3E+6	6.118259	0.000000	0.000000	6.149872	0.000000	-	0.000000	-	0.005790	0.000000	0.005896	-12 to 12º
	6E+6	6.183314	0.000000	0.000000	6.214021	0.000000	-	0.000000	-	0.005765	0.000000	0.004433	-11 to 12º
	9E+6	6.177693	0.000000	0.000000	6.206802	0.000000	-	0.000000	-	0.005741	0.000000	0.003659	-12 to 12º
1408	3E+6	6.168086	-0.014590	-0.023982	6.189772	-0.014568	0.867737	-0.032207	-0.534927	0.005151	-0.001759	0.008015	-8 to 10º
	6E+6	6.301070	-0.015595	-0.020854	6.314351	-0.015616	0.657319	0.016932	-0.457367	0.005628	-0.001324	0.004731	-8 to 10º
	9E+6	6.261541	-0.014387	-0.022490	6.276694	-0.014417	0.786238	0.006101	-0.499470	0.005452	-0.000871	0.003754	-9 to 10º
1410	3E+6	6.090839	-0.019132	-0.013013	6.111727	-0.019172	0.380982	-0.015116	-0.372816	0.005596	-0.001388	0.006575	-10 to 10º
	6E+6	6.170836	-0.015147	-0.016562	6.194926	-0.015158	0.613587	-0.010143	-0.446676	0.005586	-0.000938	0.004934	-11 to 12º
	9E+6	6.118072	-0.015833	-0.014208	6.138984	-0.015888	0.557532	-0.004581	-0.429428	0.005466	-0.001177	0.004469	-10 to 13º
1412	3E+6	6.001755	-0.021536	-0.021405	6.024677	-0.021601	0.542386	-0.018384	-0.429724	0.005874	-0.001349	0.005367	-10 to 11º
	6E+6	6.091784	-0.016802	-0.024162	6.119747	-0.016853	0.752251	0.011942	-0.493578	0.005647	-0.000234	0.003854	-10 to 12º
	9E+6	6.133597	-0.015878	-0.025978	6.155697	-0.015923	0.823418	0.001949	-0.518380	0.005612	-0.000413	0.003618	-10 to 10º
2408	3E+6	6.091846	-0.032610	-0.041816	6.110525	-0.032682	0.702485	-0.030144	-0.475019	0.005342	-0.001752	0.006456	-8 to 9º
	6E+6	6.073660	-0.030098	-0.047586	6.095314	-0.030130	0.849237	-0.017421	-0.525911	0.005410	-0.001553	0.004769	-8 to 10º
	9E+6	6.095589	-0.028866	-0.048982	6.117383	-0.028918	0.878380	-0.007438	-0.534153	0.005266	-0.001212	0.004401	-8 to 10º
2410	3E+6	6.221635	-0.034988	-0.045486	6.235686	-0.035010	0.696673	-0.012175	-0.471751	0.005809	-0.002028	0.006576	-9 to 12º
	6E+6	6.251356	-0.034312	-0.044758	6.265188	-0.034359	0.703542	-0.010119	-0.472714	0.005564	-0.001365	0.004977	-9 to 12º
	9E+6	6.239127	-0.034324	-0.045221	6.252557	-0.034349	0.704642	-0.014919	-0.475254	0.005516	-0.001074	0.004153	-8 to 12º

2412	3E+6	5.735879	-0.045493	-0.038841	5.758102	-0.045558	0.494124	-0.026337	-0.414420	0.006400	-0.002082	0.006188	-8 to 12º
	6E+6	5.726450	-0.042593	-0.039865	5.748630	-0.042669	0.503643	-0.002176	-0.419038	0.006127	-0.001044	0.004288	-8 to 10º
	9E+6	5.942871	-0.036513	-0.040618	5.965259	-0.036666	0.583567	0.010841	-0.439381	0.005789	-0.000889	0.004053	-8 to 10º
2415	3E+6	5.673667	-0.032895	-0.049724	5.688055	-0.032973	0.825610	-0.007745	-0.528454	0.006668	-0.001301	0.004762	-8 to 10º
	6E+6	5.776581	-0.030134	-0.047428	5.802051	-0.030312	0.824218	0.003879	-0.528124	0.005967	-0.000648	0.004677	-12 to 12º
	9E+6	6.060433	-0.028849	-0.047768	6.084060	-0.028982	0.893157	0.001861	-0.536979	0.006032	-0.000497	0.003724	-10 to 12º
2418	3E+6	5.690563	-0.041339	-0.040239	5.705331	-0.041378	0.535882	-0.002243	-0.426241	0.007403	-0.001636	0.004916	-8 to 8º
	6E+6	5.747011	-0.039935	-0.040612	5.773990	-0.039976	0.580398	-0.008685	-0.436021	0.006735	-0.000788	0.004581	-13 to 12º
	9E+6	5.853511	-0.037723	-0.038116	5.868849	-0.037785	0.607039	-0.004419	-0.445511	0.006768	-0.000695	0.003672	-10 to 12º
2421	3E+6	5.482827	-0.028982	-0.042323	5.498960	-0.028997	0.815568	-0.037512	-0.525707	0.007632	-0.000838	0.004986	-10 to 8º
	6E+6	5.713580	-0.030407	-0.040514	5.727586	-0.030463	0.726069	-0.021705	-0.489988	0.007334	-0.000569	0.003890	-8 to 8º
	9E+6	5.785282	-0.029825	-0.040106	5.800076	-0.029873	0.685713	0.009042	-0.477229	0.007079	-0.000464	0.003418	-8 to 8º
2424	3E+6	5.175580	-0.035389	-0.037437	5.188299	-0.035403	0.563858	0.028392	-0.433109	0.008448	-0.000758	0.006356	-8 to 8º
	6E+6	5.350890	-0.032789	-0.045521	5.373682	-0.032961	0.633593	-0.019616	-0.460110	0.007809	0.000012	0.004896	-12 to 10º
	9E+6	5.610325	-0.033106	-0.037235	5.626174	-0.033163	0.594102	0.022710	-0.440452	0.007935	-0.000054	0.004354	-10 to 10º
4412	3E+6	5.843108	-0.066762	-0.090013	5.859192	-0.066813	0.688557	-0.110713	-0.491349	0.006453	-0.003365	0.007242	-8 to 8º
	6E+6	6.057261	-0.067199	-0.089448	6.051318	-0.067214	0.702923	0.012215	-0.472179	0.006145	-0.002666	0.004725	-8 to 10º
	9E+6	6.012884	-0.067075	-0.092156	6.037428	-0.067063	0.713035	-0.009479	-0.483424	0.005847	-0.002491	0.004867	-9 to 10º
4415	3E+6	5.673553	-0.073398	-0.090258	5.686539	-0.073430	0.640571	-0.024522	-0.468523	0.007506	-0.002540	0.004190	-10 to 8º
	6E06	5.716730	-0.075196	-0.086808	5.720777	-0.075246	0.626418	-0.016697	-0.459590	0.006401	-0.002415	0.005108	-10 to 10º
	9E+6	5.796120	-0.071852	-0.090048	5.811326	-0.071862	0.662697	-0.004711	-0.470227	0.006122	-0.001896	0.004183	-10 to 10º
4418	3E+6	5.706191	-0.068478	-0.084508	5.711032	-0.068508	0.663301	-0.023506	-0.470753	0.007900	-0.002560	0.004011	-10 to 8º
	6E+6	5.718503	-0.064300	-0.083977	5.733114	-0.064363	0.693895	0.008571	-0.479265	0.007046	-0.002218	0.004647	-8 to 8º
	6E+6	5.798059	-0.064913	-0.082845	5.810737	-0.064985	0.682779	0.001780	-0.476071	0.006525	-0.001724	0.004529	-8 to 8º
4421	3E+6	5.534859	-0.065228	-0.078026	5.545927	-0.065266	0.667796	0.012813	-0.467814	0.008336	-0.001958	0.004871	-12 to 12º
	6E+6	5.693683	-0.065589	-0.077986	5.705878	-0.065621	0.629405	0.014778	-0.453952	0.007577	-0.001511	0.003834	-12 to 10º
	9E+6	5.852726	-0.065733	-0.081660	5.862931	-0.065732	0.631135	0.033698	-0.450134	0.007321	-0.001302	0.003362	-12 to 8º
4424	3E+6	5.375882	-0.062803	-0.076719	5.380375	-0.062847	0.680507	-0.005914	-0.479714	0.008792	-0.001781	0.005330	-10 to 8º
	6E+6	5.572906	-0.060265	-0.079361	5.578377	-0.060305	0.673568	0.030947	-0.470261	0.007901	-0.000985	0.004075	-12 to 8º
	9E+6	5.700749	-0.060103	-0.077360	5.706967	-0.060148	0.672613	0.042659	-0.469273	0.007456	-0.000936	0.003755	-10 to 8º
23012	3E+6	5.979710	-0.019216	-0.012753	6.000759	-0.019264	0.336826	0.015158	-0.358299	0.006988	-0.002303	0.005238	-10 to 12º
	6E+6	6.017477	-0.020185	-0.012110	6.052772	-0.020274	0.319013	0.014421	-0.350984	0.006204	-0.001394	0.004294	-12 to 12º
	9E+6	6.045419	-0.020622	-0.008444	6.075906	-0.020749	0.262420	0.000879	-0.336407	0.006018	-0.001191	0.003785	-10 to 14º

23015	3E+6	5.938874	-0.018845	-0.005843	5.957677	-0.018911	0.179111	0.019991	-0.296773	0.007177	-0.002109	0.005745	-10 to 12º
	6E+6	5.955494	-0.018042	-0.006619	5.989454	-0.018160	0.206994	0.023113	-0.310226	0.006277	-0.000981	0.004422	-10 to 12º
	9E+6	6.051603	-0.016673	-0.006509	6.081734	-0.016773	0.236275	0.030306	-0.318413	0.006209	-0.000690	0.003684	-10 to 14º
23018	3E+6	5.666324	-0.028672	-0.012240	5.686134	-0.028728	0.134011	0.021702	-0.284113	0.007502	-0.001445	0.004915	-13 to 10º
	6E+6	5.901569	-0.024154	-0.005806	5.922443	-0.024202	0.145350	0.017164	-0.288819	0.006939	-0.000901	0.003773	-11 to 12º
	9E+6	5.972945	-0.024113	-0.006768	6.001261	-0.024236	0.153323	0.017369	-0.294219	0.006868	-0.000667	0.003080	-11 to 12º
23021	3E+6	5.292591	-0.013700	-0.007753	5.307409	-0.013725	0.162467	0.043692	-0.290738	0.007698	-0.001933	0.006848	-12 to 10º
	6E+6	5.581320	-0.017372	-0.008857	5.602794	-0.017395	0.200770	0.036733	-0.302184	0.007136	-0.000854	0.005001	-12 to 12º
	9E+6	5.812017	-0.018011	-0.005844	5.832891	-0.018016	0.260178	0.023671	-0.321054	0.007064	-0.000776	0.003765	-10 to 13º
23024	3E+6	5.145307	-0.019800	0.003153	5.163103	-0.019864	0.060366	0.032572	-0.237427	0.008119	0.000464	0.006599	-8 to 10º
	6E+6	5.336206	-0.019260	-0.005488	5.351846	-0.019281	0.027999	0.031523	-0.233952	0.007721	0.000156	0.004959	-10 to 8º
	9E+6	5.600812	-0.021085	-0.001784	5.620946	-0.021129	0.052746	0.025534	-0.250493	0.007429	0.000219	0.003576	-10 to 10º
$6_3{}_2$-015	3E+6	6.610284	0.000000	0.000000	6.624243	0.000000	-	0.000000	-	0.005444	0.000000	0.005917	± 0 to 4.2º
										0.006812	0.000000	0.006056	± 4.2 to 10º
	6E+6	6.522596	0.000000	0.000000	6.544813	0.000000	-	0.000000	-	0.005117	0.000000	0.005335	± 0 to 3.8º
										0.006412	0.000000	0.004515	± 3.8 to 11º
	9E+6	6.591281	0.000000	0.000000	6.613621	0.000000	-	0.000000	-	0.004827	0.000000	0.009516	± 0 to 4.3º
										0.006123	0.000000	0.004327	± 4.3 to 12º
$6_4{}_1$-012	3E+6	6.432701	0.000000	0.000000	6.446674	0.000000	-	0.000000	-	0.004955	0.000000	0.006401	± 0 to 2.9º
										0.006733	0.000000	0.006217	± 2.9 to 11º
	6E+6	6.409336	0.000000	0.000000	6.423554	0.000000	-	0.000000	-	0.004461	0.000000	0.020149	± 0 to 3.0º
										0.006252	0.000000	0.004444	± 3.0 to 11º
	9E+6	6.386475	0.000000	0.000000	6.400883	0.000000	-	0.000000	-	0.004168	0.000000	0.026835	± 0 to 2.2º
										0.005457	0.000000	0.004516	± 2.2 to 11º

64_2-015	3E+6	6.284688	0.000000	0.000000	6.299905	0.000000	-	0.000000	-	0.005420	0.000000	0.003999	± 0 to 4.1°
										0.006465	0.000000	0.007108	± 4.1 to 10°
	6E+6	6.307967	0.000000	0.000000	6.322507	0.000000	-	0.000000	-	0.004557	0.000000	0.007069	± 0 to 3.1°
										0.005900	0.000000	0.005261	± 3.1 to 12°
	9E+6	6.351646	0.000000	0.000000	6.365895	0.000000	-	0.000000	-	0.004242	0.000000	0.014563	± 0 to 3.7°
										0.005982	0.000000	0.004563	± 3.7 to 12°
64_3-018	3E+6	6.088551	0.000000	0.000000	6.103873	0.000000	-	0.000000	-	0.005902	0.000000	0.001455	± 0 to 3.7°
										0.004802	0.000000	0.010974	± 3.7 to 10°
	6E+6	6.147039	0.000000	0.000000	6.162439	0.000000	-	0.000000	-	0.004929	0.000000	0.002372	± 0 to 3.7°
										0.005968	0.000000	0.005974	± 3.7 to 11°
	9E+6	6.357993	0.000000	0.000000	6.373660	0.000000	-	0.000000	-	0.004598	0.000000	0.003845	± 0 to 3.6°
										0.006077	0.000000	0.005080	± 3.6 to 12°
65_1-012	3E+6	6.240483	0.000000	0.000000	6.254937	0.000000	-	0.000000	-	0.003914	0.000000	0.007907	± 0 to 3.0°
										0.006444	0.000000	0.005926	± 3.0 to 10°
	6E+6	6.252728	0.000000	0.000000	6.266979	0.000000	-	0.000000	-	0.003771	0.000000	0.023150	± 0 to 2.5°
										0.005755	0.000000	0.005422	± 2.5 to 11°
	9E+6	6.264319	0.000000	0.000000	6.278622	0.000000	-	0.000000	-	0.003705	0.000000	0.014162	± 0 to 1.7°
										0.005495	0.000000	0.004594	± 1.7 to 11°
65_1-212	3E+6	6.198918	-0.014102	-0.038737	6.214146	-0.014118	1.335019	0.038239	-0.680002	0.006072	-0.001970	0.006479	-10 to -1.6°
										0.004664	-0.002224	0.009535	-1.6 to 3.8°
										0.010585	-0.010807	0.012718	3.8 to 10°
	6E+6	6.278492	-0.015401	-0.035940	6.293619	-0.015419	1.162492	0.002331	-0.628835	0.005999	-0.001015	0.005052	-10 to -1.1°
										0.004205	-0.005527	0.019424	-1.1 to 3.2°
										0.007369	-0.004373	0.006767	3.2 to 10°
	9E+6	6.286199	-0.013423	-0.038645	6.301603	-0.013440	1.349683	-0.015975	-0.688873	0.005747	-0.000762	0.004336	-10 to -1.4°
										0.005151	-0.015126	0.037611	-1.4 to 3.5°
										0.007075	-0.004410	0.006538	3.5 to 11°

65_2-015	3E+6	6.199212	0.000000	0.000000	6.213161	0.000000	-	0.000000	-	0.004937	0.000000	0.001957	± 0 to 3.6º
										0.006322	0.000000	0.007255	± 3.6 to 10º
	6E+6	6.290727	0.000000	0.000000	6.305509	0.000000	-	0.000000	-	0.004100	0.000000	0.003314	± 0 to 3.0º
										0.005826	0.000000	0.005518	± 3.0 to 11º
	9E+6	6.342150	0.000000	0.000000	6.355733	0.000000	-	0.000000	-	0.003948	0.000000	0.002935	± 0 to 2.6º
										0.005655	0.000000	0.004866	± 2.6 to 11º
66_1-012	3E+6	6.017035	0.000000	0.000000	6.030681	0.000000	-	0.000000	-	0.004033	0.000000	0.010373	± 0 to 2.7º
										0.006497	0.000000	0.007556	± 2.7 to 10º
	6E+6	6.131810	0.000000	0.000000	6.146134	0.000000	-	0.000000	-	0.003564	0.000000	0.012201	± 0 to 1.8º
										0.005791	0.000000	0.005753	± 1.8 to 10º
	9E+6	6.166211	0.000000	0.000000	6.173896	0.000000	-	0.000000	-	0.003164	0.000000	0.044701	± 0 to 1.6º
										0.005544	0.000000	0.005136	± 1.6 to 10º
66_2-015	3E+6	5.783112	0.000000	0.000000	5.791156	0.000000	-	0.000000	-	0.004582	0.000000	0.001936	± 0 to 3.3º
										0.007468	0.000000	0.008278	± 3.3 to 8º
	6E+6	6.001973	0.000000	0.000000	6.015151	0.000000	-	0.000000	-	0.003626	0.000000	0.010872	± 0 to 2.6º
										0.006057	0.000000	0.007059	± 2.6 to 9º
	9E+6	6.031154	0.000000	0.000000	6.044237	0.000000	-	0.000000	-	0.003362	0.000000	0.024016	± 0 to 2.2º
										0.006045	0.000000	0.005356	± 2.2 to 10º
66_3-018	3E+6	5.552828	0.000000	0.000000	5.565584	0.000000	-	0.000000	-	0.004781	0.000000	0.003304	± 0 to 4.4º
										0.003118	0.000000	0.024523	± 4.4 to 8º
	6E+6	5.917977	0.000000	0.000000	5.931538	0.000000	-	0.000000	-	0.003795	0.000000	0.005105	± 0 to 3.5º
										0.005225	0.000000	0.011594	± 3.5 to 8º
	9E+6	5.971148	0.000000	0.000000	5.984244	0.000000	-	0.000000	-	0.003099	0.000000	0.021320	± 0 to 4.1º
										0.006318	0.000000	0.004715	± 4.1 to 9º

APPENDIX B

VORTEX PANEL METHOD

The following program is a numerical vortex panel method designed to predict lift and pitching moment coefficients for any 4-digit NACA airfoil in inviscid flow. Additionally, the results for coefficient of lift are compared against those from thin airfoil theory.

```
------------------------------------------------------------------------
%%%%%%%%%%%%%%%%%%%%%%%%%%%%%%%% MAIN CODE %%%%%%%%%%%%%%%%%%%%%%%%%%%%
------------------------------------------------------------------------

%% Freestream Conditions
v00=1; % m/s, incoming freestream velocity
  prompt = 'Enter the desired free stream velocity [m/s] ';
v00 = input(prompt); % incoming freestream velocity

% Airfoil Properties
  prompt = 'Enter an even number of nodes you would like to use for the
4-Digit NACA airfoil  ';
N = input(prompt); % Total number of nodes to be used
  prompt = 'Enter the lowest angle of attack value (deg) to be examined
';
AOA_low = input(prompt);
  prompt = 'Enter the highest angle of attack value (deg) to be
examined ';
AOA_high = input(prompt);
  prompt = 'Do you want to use cosine clustering? (y) yes, (n) no ';
flag = input(prompt,'s');
  prompt = 'Do you want to close the airfoil trailing edge? (y/n) ';
tailFlag = input(prompt,'s'); % Total number of nodes to be used

AOA_Range = AOA_low:1:AOA_high;

% Series of user prompts for the specific NACA airfoil
prompt = 'What is the first digit of the 4-Digit NACA airfoil?  ';
m = input(prompt); % a1
m=m/100;
prompt = 'What is the second digit of the 4-Digit NACA airfoil?  ';
p = input(prompt); % a2
p=p/10;
prompt = 'What are the last two digits of the 4-Digit NACA airfoil?  ';
t = input(prompt); % a3
t=t/100;
prompt = 'Input the desired chord length ';
c = input(prompt); % % Total chord length

foilNameNum = [m*100,p*10,t*100];
a1 = num2str(foilNameNum(1,1));
a2 = num2str(foilNameNum(1,2));
```

```
a3 = num2str(foilNameNum(1,3));
foilNameStr = strcat(a1,a2,a3);

% Airfoil geometry generation
[ X,Y,xC,yC] = airFoilGeometry( N,c,p,m,t,foilNameStr, flag, tailFlag
);

% Thin Airfoil Theory
[ cl_thinAirfoil ] = thinAirfoilTheory( m,p,c,AOA_Range );

% Vortex Strength Distribution
[ gamma, V, L ] = vortexStrength( X,Y,xC,yC,AOA_Range,N,v00 );

% Calculated Coefficient of lift from vortex panels
[ cL, cMLE,] = aeroCoefficient( X,Y,c,L,v00,gamma,AOA_Range,N);

% Plots and Tables

figure(2) %Coefficient of Lift
p1 = plot(AOA_Range,cL,'-or'); % calculated CL
hold on
p2 = plot(AOA_Range,cl_thinAirfoil,'-.d'); %alpha in degrees plotted
against coefficient of lift for the thinairfoil theory
xlabel('Angle of Attack, Alpha')
ylabel('Coefficient of Lift, cL')
%title('Coefficient of Lift vs Angle of Attack')
legend([p1,p2],['cL NACA ' foilNameStr ' (calculated)'],'cL Thin
Airfoil Theory','Location','northwest')

figure(3) %Coefficient of Moment
p3 = plot(AOA_Range,cMLE,'-ob');
xlabel('Angle of Attack, Alpha')
ylabel('Coefficient of Moment leading edge, cM')
title('Coefficient of Moment vs Angle of Attack')
legend([p3],['cM (Leading Edge) NACA ' foilNameStr '
Calculated'],'Location','northeast')

--------------------------------------------------------------------------
%%%%%%%%%%%%%%%%%%%%%%%% SUPPORTING FUNCTIONS %%%%%%%%%%%%%%%%%%%%%%%%
--------------------------------------------------------------------------

function [ X,Y,xC,yC,x1pull,y1pull] = airFoilGeometry(
N,c,p,m,t,foilNameStr, flag, tailFlag )
%AIRFOILGEOMETRY Summary of this function goes here
%   Detailed explanation goes here

dtheta = pi/((N/2)-0.5); %designation of delta theta values

for i=1:N/2

    if flag == 'y'
        % Cosine Clustering for x values along the chord line
```

```
        x(i) = ( c*(0.5)*(1-cos(i*dtheta-0.5*dtheta)));
        distribution = '(cosine clustered)';
    elseif flag == 'n'
        x(i) = (2*c/N)*i;
        distribution = '(uniform distribution)';
    end

    %half thickness of the airfoil
    if tailFlag == 'y'
    %Yt(i) = (5*t*c*(0.2969*sqrt(x(i)/c)+(-0.1260)*(x(i)/c)+(-
0.3516)*(x(i)/c)^2+0.2843*(x(i)/c)^3+(-0.1036)*(x(i)/c)^4));
     Yt(i) = (5*t*c*(0.2969*sqrt(x(i)/c)+(-0.1260)*(x(i)/c)+(-
0.3523)*(x(i)/c)^2+0.2836*(x(i)/c)^3+(-0.1022)*(x(i)/c)^4));
    elseif tailFlag == 'n'
     Yt(i) = (5*t*c*(0.2969*sqrt(x(i)/c)+(-0.1260)*(x(i)/c)+(-
0.3516)*(x(i)/c)^2+0.2843*(x(i)/c)^3+(-0.1015)*(x(i)/c)^4));
    end

     if x(i) <= (p*c)
        dYc(i) = 2*m*(p-(x(i)/c))/(p^2);
     else
        dYc(i) = ((2*m)/(1-p)^2)*(p-(x(i)/c));
     end

    theta(i) = atan(dYc(i)); % angle distribution around the airfoil

    if  x(i) <= p*c
        Yc(i) = (m*(x(i)/p^2)*(2*p-(x(i)/c))); %mean chamber line
    else
        Yc(i) = (m*((c-x(i))/(1-p)^2)*(1+(x(i)/c)-2*p)); %mean chamber
line
    end

    %physical structure of the airfoil
    XL(i) = (x(i)+Yt(i)*sin(theta(i))); % x position along the lower
surface
    YL(i) = (Yc(i)-Yt(i)*cos(theta(i))); % y position along the lower
surface
    XU(i) = (x(i)-Yt(i)*sin(theta(i))); % x position along the upper
surface
    YU(i) = (Yc(i)+Yt(i)*cos(theta(i))); % y position along the upper
surface

    %Normal points along the panels, normalized by chord length
    xN(N/2+i) = XU(i)/c;
    yN(N/2+i) = YU(i)/c;
    xN(N/2+1-i) = XL(i)/c;
    yN(N/2+1-i) = YL(i)/c;

end

j=1;
for i=N/2:-1: 1
```

```
XLt(j) = XL(i);
YLt(j) = YL(i);

j=j+1;
end

X=[XLt,XU]/c; % x along the foil, normalized by chord length
Y=[YLt,YU]/c; % y along the foil, normalized by chord length

for i=1:N-1
    xC(i) = (X(i)+X(i+1))/2; %control points
    yC(i) = (Y(i)+Y(i+1))/2; %control points
end

figure(1);
plot(X,Y,'--b') % airfoil profile
hold on
plot(x/c,Yc/c,'k') % mean camber line
plot(xN,yN,'ok') % panel intersection points
plot(xC,yC,'*r') % mid-panel control points
xlabel('x')
ylabel('y')
title(['NACA ' foilNameStr ' Airfoil ' distribution])
legend('Airfoil Profile','Mean Camber Line','Panel Intersection
Point','Control Point')
axis equal

ch = get(gca,'children');
x1pull = get(ch(1),'xdata');
y1pull = get(ch(1),'ydata');
hold off

end


function [ clT ] = thinAirfoilTheory( m,p,c,AOA_Range )
%THINAIRFOILTHEORY Summary of this function goes here
%   Detailed explanation goes here

syms cT xT T

z1 = ((m*xT)/p^2) * (2*p-(xT/cT)); %eq for mean camber line
z2 = m*((cT-xT)/(1-p)^2)*(1+(xT/cT)-2*p); %eq for mean camber line

dZ1 = diff(z1,xT); %dz/dx
dZ2 = diff(z2,xT); %dz/dx

xT = (cT/2)*(1-cos(T));

dZ1 =  1/5 - ((cT/2)*(1-cos(T)))/(2*cT);
```

```
dZ2 = (cT/9 - ((cT/2)*(1-cos(T)))/9)/cT - ((cT/2)*(1-cos(T)))/(9*cT) -
1/45;

cT=1;
test1 = eval(dZ1);
test2 = eval(dZ2);

%dz/dt integrated between bounds given in wiki handout
part1 = eval( int(dZ1*(cos(T)-1),T,0,1.36944) ); %eq 4.61 Anderson
Aerodynamics
part2 = eval( int(dZ2*(cos(T)-1),T,1.36944,pi)); %eq 4.61 Anderson
Aerodynamics
alphaZero = (-1/pi) * part1 -(1/pi)* part2;  %eq 4.61 % Anderson
Aerodynamics


for i=1:length(AOA_Range)

    alphaT(i)=AOA_Range(i); %alpha values in degrees
    alpharT(i)= alphaT(i)*(pi/180); %alpha values in radians
    clT(i)=2*pi*(alpharT(i)-alphaZero); %coefficent of lift for each
values of alpha eq 4.60

end

end


function [ gamma, V, L ] = vortexStrength( X,Y,xC,yC,AOA_Range,N,v00 )
%VORTEXSTRENGTH Summary of this function goes here
%   Detailed explanation goes here

for j=1:N-1
L(j) = sqrt((X(j+1)-X(j))^2 + (Y(j+1)-Y(j))^2); %length of each panel
end

A=zeros(N);% set all elements to zero

for i=1:N-1

        for j=1:N-1

        xi  = (1/L(j)) * ((X(j+1)-X(j))*(xC(i)-X(j)) + (Y(j+1)-
Y(j))*(yC(i)-Y(j)));
        eta = (-(Y(j+1)-Y(j))*(xC(i)-X(j)) + (X(j+1)-X(j))*(yC(i)-
Y(j)))/L(j);

        phi = atan2(eta*L(j),eta^2+xi^2-xi*L(j));
        psi = (1/2)*log((xi^2+eta^2)/((xi-L(j))^2+eta^2));

        a11 = (X(j+1)-X(j));
```

```
        a12 = (-Y(j+1)+Y(j));
        a21 = (Y(j+1)-Y(j));
        a22 = (X(j+1)-X(j));

        b11 = ((L(j)-xi)*phi+eta*psi);
        b12 = (xi*phi-eta*psi);
        b21 = (eta*phi-(L(j)-xi)*psi-L(j));
        b22 = (-eta*phi-xi*psi+L(j));

        p11 = (1/(2 * pi * L(j)^2)) * (a11*b11 + a12*b21);
        p12 = (1/(2 * pi * L(j)^2)) * (a11*b12 + a12*b22);
        p21 = (1/(2 * pi * L(j)^2)) * (a21*b11 + a22*b21);
        p22 = (1/(2 * pi * L(j)^2)) * (a21*b12 + a22*b22);

        A(i,j) = A(i,j) + ((X(i+1)-X(i))/L(i))*p21 - ((Y(i+1)-
Y(i))/L(i))*p11;
        A(i,j+1) = A(i,j+1) + ((X(i+1)-X(i))/L(i))*p22 - ((Y(i+1)-
Y(i))/L(i))*p12;

        end

    % Application of the kutta condition
    A(N,1)=1;
    A(N,N)=1;
end

%%%%%%%%%%%%%%%%%%%%%%%%%%%%%%%%%%%%%%%%%%%%%%%%%%%%%%%%%%%%%%%%%%%%%%%%%%%%
%%%%
%Formation of the Right Hand Side

count=1;
for k = 1:1:length(AOA_Range)

        alphar=AOA_Range(1,k)*pi/180;

        for i=1:N-1
            B(i) = v00 * (((Y(i+1)-Y(i))*cos(alphar)-(X(i+1)-
X(i))*sin(alphar))/L(i)); %solution matrix
        end
         B(N)=0;
        if count ==1
            B = B';
        end

   gamma(:,count) = A\B; %solving for vortex panel strenght, gamma, at
each panel control point
   V(:,count)=abs(gamma(:,count));

    count=count+1;
end

end
```

```
function [ cL, cMLE] = aeroCoefficient( X,Y,c,L,v00,gamma,AOA_Range,N)
%AEROCOEFFICIENT Summary of this function goes here
%   Detailed explanation goes here


% lift coefficient

for j=1:length(AOA_Range);
sumL=0;
alphar=AOA_Range(j)*pi/180;

    for  i=1:N-1
           temp = (L(i)/c)*((gamma(i,j) + gamma(i+1,j))/v00);
           sumL = sumL + temp;
    end
    cL(j) = sumL;
end

% moment coefficient

for j=1:length(AOA_Range);
sumM=0;
alphar=AOA_Range(j)*pi/180;
    for  i=1:N-1
            arg1 =
((2*X(i)*gamma(i,j))+(X(i)*gamma(i+1,j))+(X(i+1)*gamma(i,j))+(2*X(i+1)*
gamma(i+1,j)))/(c*v00)*cos(alphar);
            arg2 =
(2*Y(i)*gamma(i,j)+(Y(i)*gamma(i+1,j))+(Y(i+1)*gamma(i,j))+(2*Y(i+1)*ga
mma(i+1,j)))/(c*v00)*sin(alphar);
            temp2 = (L(i)/c) * (arg1 + arg2);
            sumM = sumM + temp2;
    end
    cMLE(j) = -(1/3) * sumM;

end

end
```

APPENDIX C

The following program is a symbolic solver designed to analytically solve the full high order location of the aerodynamic center and the associated pitching moment in viscous flow using the general airfoil theory equations. This solver also solves for the second order approximation of the aerodynamic center and the associated pitching moment.

```
------------------------------------------------------------------------
%%%%%%%%%%%%%%%%%%%%%%%%%%%%%%%% MAIN CODE %%%%%%%%%%%%%%%%%%%%%%%%%%%%
------------------------------------------------------------------------

syms a alo cloa cmo cma CD0 CD0L CD0L2 CMLEa CMLEN CMLEA CMc4 K1 K2
syms cl(a)
syms CM(cl) CD(cl)

% prompt = ('Inviscid (i) or Viscous (v) ? ');
% flag = input(prompt,'s');
% prompt = ('Small angle approximation (s), General Airfoil Theory?
(g), Thin Airfoil w/o small angle (t) ');
% flagAngle = input(prompt,'s');
%
% prompt = ('Run Test? (y/n)');
% testFlag = input(prompt,'s');

flag = 'v'
flagAngle = 'g'
testFlag = 'y'

if flag == 'i' % inviscid flow

    if flagAngle == 's'
        cl(a) = cloa*(a-alo); % small angle approximation
        CA = -cl*a; % inviscid axial force coeff w/small angle approx
        CN = cl; % inviscid normal force coeff w/small angle approx
        %CM = cma*a+cmo; % traditional pitching moment equation
        CM = CMc4-cl/4;

    elseif flagAngle == 't'
        cl(a) = cloa*(a-alo); % small angle approximation
        CA = -cl*sin(a); % inviscid axial force coeff w/o small angle
approx
        CN = cl*cos(a); % inviscid normal force coeff w/o small angle
approx
        %CM = cma*a+cmo;
        CM = CMc4-cl/4; % traditional pitching moment equation

    elseif flagAngle == 'g'

        cl(a) = cloa*(sin(a)-tan(alo)*cos(a)); % non-small angle
approximation
```

```
        CA = -cl*sin(a); % inviscid axial force coefficient (Phillips
4.8.24)
        CN = cl*cos(a); % inviscid normal force coefficient (Phillips
4.8.25)
        CM = CMLEa*sin(2*a)+cl*CMLEN*cos(a)-cl*CMLEA*sin(a); % pitching
moment equation modified in paper
        %CM = CMLEa*sin(2*a)-cl*CMLEN*cos(a)+cl*CMLEA*tan(alo)*sin(a);
% joukowski pitching moment equation
    end

    cla(a)  = diff(cl,a);
    claa(a) = diff(cla,a);

    CAa     = diff(CA,a);
    CAaa    = diff(CAa,a);

    CNa     = diff(CN,a);
    CNaa    = diff(CNa,a);

    CMa     = diff(CM,a);
    CMaa    = diff(CMa,a);

elseif flag == 'v' % viscous flow



    if flagAngle == 's'
        cl(a) = cloa*(a-alo); % small angle approximation
        CD = CD0 + CD0L*cl + CD0L2*cl*cl; % parabolic drag model
        CA = -cl*a+CD; % viscous axial force coeff w/small angle approx
        CN = cl+CD*a; % viscous normal force coeff w/small angle approx
        %CM = cma*a+cmo; % traditional pitching moment equation
        CM = CMc4-cl/4; % traditional pitching moment equation

    elseif flagAngle == 't'
        cl(a) = cloa*(a-alo); % small angle approximation
        CD = CD0 + CD0L*cl + CD0L2*cl*cl; % parabolic drag model
        CA = -cl*sin(a)+CD*cos(a); % viscous axial force coeff w/o
small angle approx
        CN =  cl*cos(a)+CD*sin(a); % viscous normal force coeff w/o
small angle approx
        %CM = cma*a+cmo;
        CM = CMc4-cl/4; % traditional pitching moment equation

    elseif flagAngle == 'g'
        cl(a) = cloa*(sin(a)-tan(alo)*cos(a)); % non-small angle
approximation
        CD = CD0 + CD0L*cl + CD0L2*cl*cl; % parabolic drag model
        CA = -cl*sin(a) + CD*cos(a); % viscous axial force coefficient
(Phillips 4.8.24)
        CN =  cl*cos(a) + CD*sin(a); % viscous normal force coefficient
(Phillips 4.8.25)
```

```
        CM =
CMLEa*sin(2*a)+CMLEN*(cl*cos(a)+CD*sin(a))+CMLEA*(CD*cos(a)-cl*sin(a));
% (corrected) joukowski pitching moment equation
    end

    cla(a)  = diff(cl,a);
    claa(a) = diff(cla,a);
    %claa(a) = -cl(a)

    CAa     = diff(CA,a);
    CAaa    = diff(CAa,a);

    CNa     = diff(CN,a);
    CNaa    = diff(CNa,a);

    CMa     = diff(CM,a);
    CMaa    = diff(CMa,a);

end % inviscid vs viscous


disp('Non-Reduced standard-----------------------------------------------
-------')
disp(' ')

Xac = (CAa*CMaa-CMa*CAaa)/(CNa*CAaa-CAa*CNaa); % aerodynamic center
(Phillips 4.8.29)
XacO = Xac;
%
Yac = (CNa*CMaa-CMa*CNaa)/(CNa*CAaa-CAa*CNaa); % aerodynamic center
(Phillips 4.8.30)
YacO = Yac;
%
cmAC = CM + Xac*CN - Yac*CA; % moment coefficient (Phillips 4.8.31)
cmACO = cmAC;

% ????????????????????????????
% Xac = -2*CMLEa*((2*sin(2*a)*CAa+cos(2*a)*CAaa)/(CNa*CAaa-CAa*CNaa))-
CMLEN;
% Xac = simplify(Xac)
%
% Yac = -2*CMLEa*((2*sin(2*a)*CNa+cos(2*a)*CNaa)/(CNa*CAaa-
CAa*CNaa))+CMLEA;
% Yac = simplify(Yac)
%
% cmAC = CM + Xac*CN - Yac*CA; % moment coefficient (Phillips 4.8.31)
% cmAC = simplify(cmAC)



%disp('Non-Reduced pretty-------------------------------------------
---------')
```

```
%disp(' ')

% disp('Xac_original')
% pretty(Xac);
% disp('Yac_original')
% pretty(Yac);
% disp('cMAC_original')
% pretty(cmAC);

%% Full high order solution
if testFlag == 'y'
    cpass = 'k'; % color
    mpass = '.'; % marker
    [ xsave,ysave,cmsave ] = plotting( Xac,Yac,cmAC, cpass, mpass);
    dataSave(:,1) = xsave(:);
    dataSave(:,2) = ysave(:);
    dataSave(:,3) = cmsave(:);
end

%% Order Reduction
if flag == 'v'
   % EqOrderReduction(
CAa,CAaa,CNa,CNaa,CMa,CMaa,CN,CA,CM,a,alo,CD0,CD0L,CD0L2,cl, testFlag
)
   [CAa,CAaa,CNa,CNaa,CMa,CMaa,CN,CA,CM,a,alo,CD0,CD0L,CD0L2,cl, Xac,
Yac, cmAC,dataSave] = EqOrderReduction4(
CAa,CAaa,CNa,CNaa,CMa,CMaa,CN,CA,CM,a,alo,CD0,CD0L,CD0L2,cl,dataSave,
testFlag  );
end



disp('post reduction equations----------------------------------------
--')
% Xac = subs(Xac,cloa*CD0L2,K1);
% Xac = subs(Xac,CD0/(2*cloa),K2);
Xac  = simplify(Xac);
% Yac = subs(Yac,cloa*CD0L2,K1);
% Yac = subs(Yac,CD0/(2*cloa),K2);
Yac  = simplify(Yac);
% cmAC = subs(cmAC,cloa*CD0L2,K1);
% cmAC = subs(cmAC,CD0/(2*cloa),K2)
cmAC = simplify(cmAC);
% Xac
% Yac
% cmAC


[Xac,Yac,cmAC] = OrderReduction_Post( Xac,Yac,cmAC );
cpass = 'k'; % color
mpass = '*'; % marker
[ xsave,ysave,cmsave ] = plotting( Xac,Yac,cmAC, cpass, mpass );
dataSave(:,10) = xsave(:);
```

```
dataSave(:,11) = ysave(:);
dataSave(:,12) = cmsave(:);

% Check on final paper versions of 3rd order reduction
k1   = cloa*CD0L2 ;
k2   = CD0/(2*cloa);
xknum = k1*(3*(a*alo-a^2-alo^2/2)+1)-k2*(1+3*a^2/2)-1;
kden = k1*(1+3*alo^2/2)+3*k2*(a^2/2-a*alo-2*k2/3-1)-alo^2-1;

XacK = -2*CMLEa/cloa*(xknum/kden)-CMLEN;

yknum = k1*(3*a-2*alo)+CD0L+3*a*k2+alo*(1+alo^2/3);

YacK = -2*CMLEa/cloa*(yknum/kden)+CMLEA;

cmacknum = alo*(k1+k2-alo^2/3-1)+6*a*k2*(k1+k2);

cmACK = 2*CMLEa*(cmacknum/kden);

% final reduced equations after hand simplification
cpass = 'c'; % color
mpass = '^'; % marker
[ xsave,ysave,cmsave ] = plotting( XacK,YacK,cmACK, cpass, mpass );
dataSave(:,7) = xsave(:);
dataSave(:,8) = ysave(:);
dataSave(:,9) = cmsave(:);

% Comparison to Dr.Hunsaker code
xu    =  -3.0*cloa*CD0L2*a^2 + 3*cloa*CD0L2*a*alo -
3*cloa*CD0L2*alo^2/2 + cloa*CD0L2 + CD0L*alo - 1 - 3*CD0*a^2/(4*cloa) -
CD0/(2*cloa);
yu    = 3*cloa*CD0L2*a - 2*cloa*CD0L2*alo + CD0L + alo^3/3 + alo +
3*CD0*a/(2*cloa);
denom =  - 3*cloa*CD0L*CD0L2*a + 3*cloa*CD0L*CD0L2*alo +
3*cloa*CD0L2*alo^2/2 + cloa*CD0L2 + CD0*CD0L2 - CD0L^2 - alo^2 - 1 -
3*CD0*CD0L*a/(2*cloa) + 3*CD0*CD0L*alo/(2*cloa) + 3*CD0*a^2/(4*cloa) -
3*CD0*a*alo/(2*cloa) - 3*CD0/(2*cloa) - CD0^2/(2*cloa^2);

xu = xu*2*cloa;
yu = yu*2*cloa;
denom = denom*2*cloa*cloa;

XacTest  = -2*CMLEa* xu/denom - CMLEN;
YacTest  = -2*CMLEa* yu/denom + CMLEA;
%cmCATest =

%%%%%%%%%%%%%%%%%%%%%%%%%%%%%%%%%%%%%%%%%%%%%%%%%%%%%%%%%%%%%%%%%%%%%%%
%%%%

    % NACA 1408 data from Airfoil Appendix
    foilName = '1408';
    a     = 5*(pi/180);
```

```
    alo   = -0.0145678;
    cloa  = 6.1897717;
    CD0   = 0.0051515;
    CD0L  = -0.0017593;
    CD0L2 = 0.0080154;
    CMLEa = 0.8677365;
    CMLEA = -0.0322065;
    CMLEN = -0.5349267;

% Third Order + manual reduction Hunsaker code
format long
XacDk  = eval(subs(XacK));
YacDk  = eval(subs(YacK));
cmACDk = eval(subs(cmACK));

% Third Order Reduction Final of Pope code
format long
XacP  = eval(subs(Xac));
YacP  = eval(subs(Yac));
cmACP = eval(subs(cmAC));

format long
XacTest  = eval(subs(XacTest));
YacTest  = eval(subs(YacTest));
%cmACTest = eval(subs(cmACTest))


figure(2)
plot(dataSave(:,1),dataSave(:,2),'.-b',dataSave(:,7),dataSave(:,8),'.-
r')
xlabel('Xac')
ylabel('Yac')
title(['AC(alpha) for NACA ',foilName])
legend('Original','Reduced')
axis equal

figure(3)
plot((-15:1:15),dataSave(:,3),'.-b')
hold on
plot((-15:1:15),dataSave(:,6),'.-g')
plot((-15:1:15),dataSave(:,12),'.-k')
plot((-15:1:15),dataSave(:,9),'.-r')
xlabel('alpha')
ylabel('cmAC')
title(['cmAC(alpha) for NACA ',foilName])
legend('full','matlab','matlab R','paper')


XacP-XacTest
YacP-YacTest
XacP-XacDk
YacP-YacDk
```

```
------------------------------------------------------------------------
%%%%%%%%%%%%%%%%%%%%%%%% SUPPORTING FUNCTIONS %%%%%%%%%%%%%%%%%%%%%%%%
------------------------------------------------------------------------


function [ CAa,CAaa,CNa,CNaa,CMa,CMaa,CN,CA,CM,a,alo,CD0,CD0L,CD0L2,cl,
Xac, Yac, cmAC,dataSave] = EqOrderReduction4(
CAa,CAaa,CNa,CNaa,CMa,CMaa,CN,CA,CM,a,alo,CD0,CD0L,CD0L2,cl,dataSave,
testFlag  )
%EQORDERREDUCTION4

disp('RUN EQUATION REDUCTION FUNCTION ------------------------------')
disp(' ')


% Expand
%disp('Expanded Equations')
%disp(' ')
CA   = expand(CA);
CAa  = expand(CAa);
CAaa = expand(CAaa);
CN   = expand(CN);
CNa  = expand(CNa);
CNaa = expand(CNaa);
CM   = expand(CM);
CMa  = expand(CMa);
CMaa = expand(CMaa);


% Using Reduced Equations in Aerodynamic Center Equations (12,13)
disp('1st Reduction ------------------------------------------------
-')
disp(' ')

CA = subs(CA, sin(a),a-a^3/6);
CA = subs(CA, sin(2*a),2*a-4*a^3/3);
CA = subs(CA, sin(3*a),3*a-9*a^3/2);
CA = subs(CA, cos(a),1-a^2/2);
CA = subs(CA, cos(2*a),1-2*a^2);
CA = subs(CA, cos(3*a),1-9*a^2/2);
CA = subs(CA, tan(alo),alo+alo^3/3);

CAa = subs(CAa, sin(a),a-a^3/6);
CAa = subs(CAa, sin(2*a),2*a-4*a^3/3);
CAa = subs(CAa, sin(3*a),3*a-9*a^3/2);
CAa = subs(CAa, cos(a),1-a^2/2);
CAa = subs(CAa, cos(2*a),1-2*a^2);
CAa = subs(CAa, cos(3*a),1-9*a^2/2);
CAa = subs(CAa, tan(alo),alo+alo^3/3);

CAaa = subs(CAaa, sin(a),a-a^3/6);
```

```
CAaa = subs(CAaa, sin(2*a),2*a-4*a^3/3);
CAaa = subs(CAaa, sin(3*a),3*a-9*a^3/2);
CAaa = subs(CAaa, cos(a),1-a^2/2);
CAaa = subs(CAaa, cos(2*a),1-2*a^2);
CAaa = subs(CAaa, cos(3*a),1-9*a^2/2);
CAaa = subs(CAaa, tan(alo),alo+alo^3/3);

CN = subs(CN, sin(a),a-a^3/6);
CN = subs(CN, sin(2*a),2*a-4*a^3/3);
CN = subs(CN, sin(3*a),3*a-9*a^3/2);
CN = subs(CN, cos(a),1-a^2/2);
CN = subs(CN, cos(2*a),1-2*a^2);
CN = subs(CN, cos(3*a),1-9*a^2/2);
CN = subs(CN, tan(alo),alo+alo^3/3);

CNa = subs(CNa, sin(a),a-a^3/6);
CNa = subs(CNa, sin(2*a),2*a-4*a^3/3);
CNa = subs(CNa, sin(3*a),3*a-9*a^3/2);
CNa = subs(CNa, cos(a),1-a^2/2);
CNa = subs(CNa, cos(2*a),1-2*a^2);
CNa = subs(CNa, cos(3*a),1-9*a^2/2);
CNa = subs(CNa, tan(alo),alo+alo^3/3);

CNaa = subs(CNaa, sin(a),a-a^3/6);
CNaa = subs(CNaa, sin(2*a),2*a-4*a^3/3);
CNaa = subs(CNaa, sin(3*a),3*a-9*a^3/2);
CNaa = subs(CNaa, cos(a),1-a^2/2);
CNaa = subs(CNaa, cos(2*a),1-2*a^2);
CNaa = subs(CNaa, cos(3*a),1-9*a^2/2);
CNaa = subs(CNaa, tan(alo),alo+alo^3/3);

CM = subs(CM, sin(a),a-a^3/6);
CM = subs(CM, sin(2*a),2*a-4*a^3/3);
CM = subs(CM, sin(3*a),3*a-9*a^3/2);
CM = subs(CM, cos(a),1-a^2/2);
CM = subs(CM, cos(2*a),1-2*a^2);
CM = subs(CM, cos(3*a),1-9*a^2/2);
CM = subs(CM, tan(alo),alo+alo^3/3);

CMa = subs(CMa, sin(a),a-a^3/6);
CMa = subs(CMa, sin(2*a),2*a-4*a^3/3);
CMa = subs(CMa, sin(3*a),3*a-9*a^3/2);
CMa = subs(CMa, cos(a),1-a^2/2);
CMa = subs(CMa, cos(2*a),1-2*a^2);
CMa = subs(CMa, cos(3*a),1-9*a^2/2);
CMa = subs(CMa, tan(alo),alo+alo^3/3);

CMaa = subs(CMaa, sin(a),a-a^3/6);
CMaa = subs(CMaa, sin(2*a),2*a-4*a^3/3);
CMaa = subs(CMaa, sin(3*a),3*a-9*a^3/2);
CMaa = subs(CMaa, cos(a),1-a^2/2);
CMaa = subs(CMaa, cos(2*a),1-2*a^2);
CMaa = subs(CMaa, cos(3*a),1-9*a^2/2);
```

```
CMaa = subs(CMaa, tan(alo),alo+alo^3/3);

xDL = (CAa*CMaa);
xDR = (CMa*CAaa);
xNL = (CNa*CAaa);
xNR = (CAa*CNaa);

yDL = (CNa*CMaa);
yDR = (CMa*CNaa);
yNL = (CNa*CAaa);
yNR = (CAa*CNaa);

Xac = (xDL-xDR)/(xNL-xNR); % aerodynamic center (Phillips 4.8.29)
Yac = (yDL-yDR )/(yNL-yNR ); % aerodynamic center (Phillips 4.8.30)
cmAC = CM + Xac*CN - Yac*CA; % moment coefficient (Phillips 4.8.31)

cpass = 'g'; % color
mpass = '.'; % marker
plotting( Xac,Yac,cmAC, cpass, mpass );

disp('Second Reduction (alpha)----------------------------------------
----------')
disp(' ')

% Xac  = simplify(Xac);
% Yac  = simplify(Yac);
% cmAC = simplify(cmAC);
Xac  = expand(Xac);
Yac  = expand(Yac);
cmAC = expand(cmAC);


Xac = subs(Xac, a*a*a*a*a*a*a*a*a*a*a*a*a*a*a*a*a, 0); % 16a
Xac = subs(Xac, a*a*a*a*a*a*a*a*a*a*a*a*a*a*a*a, 0); % 15a
Xac = subs(Xac, a*a*a*a*a*a*a*a*a*a*a*a*a*a*a, 0); % 14a
Xac = subs(Xac, a*a*a*a*a*a*a*a*a*a*a*a*a*a, 0); % 13a
Xac = subs(Xac, a*a*a*a*a*a*a*a*a*a*a*a*a, 0); % 12a
Xac = subs(Xac, a*a*a*a*a*a*a*a*a*a*a*a, 0); % 11a
Xac = subs(Xac, a*a*a*a*a*a*a*a*a*a*a, 0); % 10a
Xac = subs(Xac, a*a*a*a*a*a*a*a*a*a, 0); % 9a
Xac = subs(Xac, a*a*a*a*a*a*a*a*a, 0); % 8a
Xac = subs(Xac, a*a*a*a*a*a*a*a, 0); % 7a
Xac = subs(Xac, a*a*a*a*a*a*a, 0); % 6a
Xac = subs(Xac, a*a*a*a*a*a, 0); % 5a
Xac = subs(Xac, a*a*a*a, 0); % 4a

Xac = subs(Xac, alo*alo*alo*alo*alo*alo*alo*alo*alo, 0); % 9alo
Xac = subs(Xac, alo*alo*alo*alo*alo*alo*alo*alo, 0); % 8alo
Xac = subs(Xac, alo*alo*alo*alo*alo*alo*alo, 0); % 7alo
Xac = subs(Xac, alo*alo*alo*alo*alo*alo, 0); % 6alo
Xac = subs(Xac, alo*alo*alo*alo*alo, 0); % 5alo
Xac = subs(Xac, alo*alo*alo*alo, 0); % 4alo
```

```
Yac = subs(Yac, a*a*a*a*a*a*a*a*a*a*a*a*a*a*a*a*a*a*a*a, 0); % 16a
Yac = subs(Yac, a*a*a*a*a*a*a*a*a*a*a*a*a*a*a*a*a*a*a, 0); % 15a
Yac = subs(Yac, a*a*a*a*a*a*a*a*a*a*a*a*a*a*a*a*a*a, 0); % 14a
Yac = subs(Yac, a*a*a*a*a*a*a*a*a*a*a*a*a*a*a*a*a, 0); % 13a
Yac = subs(Yac, a*a*a*a*a*a*a*a*a*a*a*a*a*a*a*a, 0); % 12a
Yac = subs(Yac, a*a*a*a*a*a*a*a*a*a*a*a*a*a*a, 0); % 11a
Yac = subs(Yac, a*a*a*a*a*a*a*a*a*a*a*a*a*a, 0); % 10a
Yac = subs(Yac, a*a*a*a*a*a*a*a*a*a*a*a*a, 0); % 9a
Yac = subs(Yac, a*a*a*a*a*a*a*a*a*a*a*a, 0); % 8a
Yac = subs(Yac, a*a*a*a*a*a*a*a*a*a*a, 0); % 7a
Yac = subs(Yac, a*a*a*a*a*a*a*a*a*a, 0); % 6a
Yac = subs(Yac, a*a*a*a*a*a*a*a*a, 0); % 5a
Yac = subs(Yac, a*a*a*a*a*a*a*a, 0); % 4a

Yac = subs(Yac, alo*alo*alo*alo*alo*alo*alo*alo*alo, 0); % 9alo
Yac = subs(Yac, alo*alo*alo*alo*alo*alo*alo*alo, 0); % 8alo
Yac = subs(Yac, alo*alo*alo*alo*alo*alo*alo, 0); % 7alo
Yac = subs(Yac, alo*alo*alo*alo*alo*alo, 0); % 6alo
Yac = subs(Yac, alo*alo*alo*alo*alo, 0); % 5alo
Yac = subs(Yac, alo*alo*alo*alo, 0); % 4alo

cmAC = subs(cmAC, a*a*a*a*a*a*a*a*a*a*a*a*a*a*a*a*a*a*a*a*a*a, 0); % 18a
cmAC = subs(cmAC, a*a*a*a*a*a*a*a*a*a*a*a*a*a*a*a*a*a*a*a*a, 0); % 17a
cmAC = subs(cmAC, a*a*a*a*a*a*a*a*a*a*a*a*a*a*a*a*a*a*a*a, 0); % 16a
cmAC = subs(cmAC, a*a*a*a*a*a*a*a*a*a*a*a*a*a*a*a*a*a*a, 0); % 15a
cmAC = subs(cmAC, a*a*a*a*a*a*a*a*a*a*a*a*a*a*a*a*a*a, 0); % 14a
cmAC = subs(cmAC, a*a*a*a*a*a*a*a*a*a*a*a*a*a*a*a*a, 0); % 13a
cmAC = subs(cmAC, a*a*a*a*a*a*a*a*a*a*a*a*a*a*a*a, 0); % 12a
cmAC = subs(cmAC, a*a*a*a*a*a*a*a*a*a*a*a*a*a*a, 0); % 11a
cmAC = subs(cmAC, a*a*a*a*a*a*a*a*a*a*a*a*a*a, 0); % 10a
cmAC = subs(cmAC, a*a*a*a*a*a*a*a*a*a*a*a*a, 0); % 9a
cmAC = subs(cmAC, a*a*a*a*a*a*a*a*a*a*a*a, 0); % 8a
cmAC = subs(cmAC, a*a*a*a*a*a*a*a*a*a*a, 0); % 7a
cmAC = subs(cmAC, a*a*a*a*a*a*a*a*a*a, 0); % 6a
cmAC = subs(cmAC, a*a*a*a*a*a*a*a*a, 0); % 5a
cmAC = subs(cmAC, a*a*a*a*a*a*a*a, 0); % 4a

cmAC = subs(cmAC, alo*alo*alo*alo*alo*alo*alo*alo*alo, 0); % 9alo
cmAC = subs(cmAC, alo*alo*alo*alo*alo*alo*alo*alo, 0); % 8alo
cmAC = subs(cmAC, alo*alo*alo*alo*alo*alo*alo, 0); % 7alo
cmAC = subs(cmAC, alo*alo*alo*alo*alo*alo, 0); % 6alo
cmAC = subs(cmAC, alo*alo*alo*alo*alo, 0); % 5alo
cmAC = subs(cmAC, alo*alo*alo*alo, 0); % 4alo

cpass = 'm'; % color
mpass = '.'; % marker
plotting( Xac,Yac,cmAC, cpass, mpass);

disp('3rd Reduction (alpha+alo)----------------------------------------
-----------')
disp(' ')
```

```
% Xac  = simplify(Xac);
% Yac  = simplify(Yac);
% cmAC = simplify(cmAC);

Xac  = subs(Xac, a*a*a*alo, 0);
Xac  = subs(Xac, a*a*alo*alo, 0);
Xac  = subs(Xac, a*alo*alo*alo, 0);

Yac  = subs(Yac, a*a*a*alo, 0);
Yac  = subs(Yac, a*a*alo*alo, 0);
Yac  = subs(Yac, a*alo*alo*alo, 0);

cmAC = subs(cmAC, a*a*a*alo, 0);
cmAC = subs(cmAC, a*a*alo*alo, 0);
cmAC = subs(cmAC, a*alo*alo*alo, 0);

cpass = 'r'; % color
mpass = '.'; % marker
plotting( Xac,Yac,cmAC, cpass, mpass);

disp('4th Reduction (drag combos)-----------------------------------
-------------')
disp(' ')

Xac  = expand(Xac);
Yac  = expand(Yac);
cmAC = expand(cmAC);
% Xac  = simplify(Xac);
% Yac  = simplify(Yac);
% cmAC = simplify(cmAC);

Xac = subs(Xac, CD0L*CD0L2*alo*alo, 0);
Xac = subs(Xac, CD0*CD0L2*alo*alo, 0);
Xac = subs(Xac, CD0L2*CD0L2*alo*alo, 0);
Xac = subs(Xac, CD0L*CD0L*alo*alo, 0);
%Xac = subs(Xac, CD0*CD0L2*alo, 0);
Xac = subs(Xac, CD0*CD0L2*alo*alo*alo, 0);
Xac = subs(Xac, CD0*CD0L*alo*alo*alo, 0);
Xac = subs(Xac, CD0L*alo*alo*alo, 0);
Xac = subs(Xac, CD0L*CD0L2*a*alo, 0);
Xac = subs(Xac, CD0*CD0L2*a*alo, 0);
Xac = subs(Xac, CD0*CD0L2*a*a*a, 0);
Xac = subs(Xac, CD0*CD0L2*a*a, 0);
Xac = subs(Xac, CD0*CD0L*a*a*a, 0);
Xac = subs(Xac, CD0*CD0L*a*a, 0);
Xac = subs(Xac, CD0L2*CD0L2*alo*alo, 0);
Xac = subs(Xac, CD0L2*CD0L2*a*a, 0);
Xac = subs(Xac, CD0L2*CD0L2*a*alo, 0);
Xac = subs(Xac, CD0*a*a*a, 0);
Xac = subs(Xac, CD0L*a*a*a, 0);
Xac = subs(Xac, CD0L2*a*a*a, 0);
Xac = subs(Xac, CD0L2*alo*alo*alo, 0);
Xac = subs(Xac, CD0L2*alo*alo*a, 0);
```

```
Xac = subs(Xac, CD0L2*alo*a*a, 0);


Yac = subs(Yac, CD0L*CD0L2*alo*alo, 0);
Yac = subs(Yac, CD0*CD0L2*alo*alo, 0);
Yac = subs(Yac, CD0L2*CD0L2*alo*alo, 0);
Yac = subs(Yac, CD0L*CD0L*alo*alo, 0);
%Yac = subs(Yac, CD0*CD0L2*alo, 0);
Yac = subs(Yac, CD0*CD0L2*alo*alo*alo, 0);
Yac = subs(Yac, CD0*CD0L*alo*alo*alo, 0);
Yac = subs(Yac, CD0L*alo*alo*alo, 0);
Yac = subs(Yac, CD0L*CD0L2*a*alo, 0);
Yac = subs(Yac, CD0*CD0L2*a*alo, 0);
Yac = subs(Yac, CD0*CD0L2*a*a*a, 0);
Yac = subs(Yac, CD0*CD0L2*a*a, 0);
Yac = subs(Yac, CD0*CD0L*a*a*a, 0);
Yac = subs(Yac, CD0*CD0L*a*a, 0);
Yac = subs(Yac, CD0L2*CD0L2*alo*alo, 0);
Yac = subs(Yac, CD0L2*CD0L2*a*a, 0);
Yac = subs(Yac, CD0L2*CD0L2*a*alo, 0);
Yac = subs(Yac, CD0*a*a*a, 0);
Yac = subs(Yac, CD0L*a*a*a, 0);
Yac = subs(Yac, CD0L2*a*a*a, 0);
Yac = subs(Yac, CD0L2*alo*alo*alo, 0);
Yac = subs(Yac, CD0L2*alo*alo*a, 0);
Yac = subs(Yac, CD0L2*alo*a*a, 0);


cmAC = subs(cmAC, CD0L*CD0L2*alo*alo, 0);
cmAC = subs(cmAC, CD0*CD0L2*alo*alo, 0);
cmAC = subs(cmAC, CD0L2*CD0L2*alo*alo, 0);
cmAC = subs(cmAC, CD0L*CD0L*alo*alo, 0);
cmAC = subs(cmAC, CD0*CD0L2*alo, 0);
cmAC = subs(cmAC, CD0*CD0L2*alo*alo*alo, 0);
cmAC = subs(cmAC, CD0*CD0L*alo*alo*alo, 0);
cmAC = subs(cmAC, CD0L*alo*alo*alo, 0);
cmAC = subs(cmAC, CD0L*CD0L2*a*alo, 0);
cmAC = subs(cmAC, CD0*CD0L2*a*alo, 0);
cmAC = subs(cmAC, CD0*CD0L2*a*a*a, 0);
cmAC = subs(cmAC, CD0*CD0L2*a*a, 0);
cmAC = subs(cmAC, CD0*CD0L*a*a*a, 0);
cmAC = subs(cmAC, CD0*CD0L*a*a, 0);
cmAC = subs(cmAC, CD0L2*CD0L2*alo*alo, 0);
cmAC = subs(cmAC, CD0L2*CD0L2*a*a, 0);
cmAC = subs(cmAC, CD0L2*CD0L2*a*alo, 0);
cmAC = subs(cmAC, CD0*a*a*a, 0);
cmAC = subs(cmAC, CD0L*a*a*a, 0);
cmAC = subs(cmAC, CD0L2*a*a*a, 0);
cmAC = subs(cmAC, CD0L2*alo*alo*alo, 0);
cmAC = subs(cmAC, CD0L2*alo*alo*a, 0);
cmAC = subs(cmAC, CD0L2*alo*a*a, 0);

cmAC = subs(cmAC, CD0*alo*alo*alo, 0);
```

```
cmAC = subs(cmAC, CD0*CD0L*alo*alo, 0);
cmAC = subs(cmAC, CD0*CD0L*a*alo, 0);
cmAC = subs(cmAC, CD0*CD0L*CD0L2*a, 0);
cmAC = subs(cmAC, CD0*CD0L*CD0L*a*alo, 0);
cmAC = subs(cmAC, CD0*CD0L*a*alo*alo, 0);
cmAC = subs(cmAC, CD0*a*alo*alo, 0);
cmAC = subs(cmAC, CD0*a*a*alo, 0);
cmAC = subs(cmAC, CD0*CD0*a*a, 0);
cmAC = subs(cmAC, CD0*CD0*a*alo, 0);
cmAC = subs(cmAC, CD0*CD0*CD0L*a, 0);
cmAC = subs(cmAC, CD0*CD0*CD0L*a*alo, 0);
cmAC = subs(cmAC, CD0*CD0*CD0L*alo, 0);
cmAC = subs(cmAC, CD0*CD0*CD0*a, 0);
cmAC = subs(cmAC, CD0*CD0*CD0*a*a, 0);
cmAC = subs(cmAC, CD0*CD0*a*a*alo, 0);
cmAC = subs(cmAC, CD0*CD0*CD0L2*a, 0);
cmAC = subs(cmAC, CD0*CD0*alo*alo*alo, 0);
cmAC = subs(cmAC, CD0L*a*a*alo, 0);
cmAC = subs(cmAC, CD0L*a*alo*alo, 0);
cmAC = subs(cmAC, CD0L*CD0L2*a*a, 0);
cmAC = subs(cmAC, CD0L*CD0L*a*a, 0);
cmAC = subs(cmAC, CD0L*CD0L*a*a*alo, 0);
cmAC = subs(cmAC, CD0L*CD0L*a*alo, 0);
cmAC = subs(cmAC, CD0L*CD0L*CD0*a, 0);
cmAC = subs(cmAC, CD0L*CD0L*CD0L2*a*a, 0);
cmAC = subs(cmAC, CD0L*CD0L*CD0L*a, 0);
cmAC = subs(cmAC, CD0L*CD0L*CD0L*alo, 0);
cmAC = subs(cmAC, CD0L*CD0L*CD0L*a*a, 0);
cmAC = subs(cmAC, CD0L*CD0L*CD0L*a*alo, 0);
cmAC = subs(cmAC, CD0L*CD0L*CD0L*a*a*alo, 0);

disp('%%%%%%%%%%%%%%%%%%%%%%%%%%%%%%%%%%%%%%%%%%%%%%%%%%%%%%%%%%%%%%%
%%%')

% Reduced model after equation reduction
cpass = 'c'; % color
mpass = '.'; % marker
[ xsave,ysave,cmsave ] = plotting( Xac,Yac,cmAC, cpass, mpass );
dataSave(:,4) = xsave(:);
dataSave(:,5) = ysave(:);
dataSave(:,6) = cmsave(:);

end
```

```
function [ xsave,ysave,cmsave ] = plotting( Xac,Yac,cmAC, cpass, mpass
)
%PLOTTING Summary of this function goes here
%   Detailed explanation goes here

    disp('test case-----------------------------------------------------
')


    j=1;
    for i = -15:1:15

%%%%%%%%%%%%%%%%%%%%%%%%%%%%%%%%%%%%%%%%%%%%%%%%%%%%
%     % NACA 0006 data from Airfoil Appendix
%     foilName = '0006';
%     a     = i*(pi/180);
%     alo   = 0;
%     cloa  = 6.18958236335962;
%     CD0   = 0.00460455864601409;
%     CD0L  = 0;
%     CD0L2 = 0.010321990400509;
%     CMLEa = 0;
%     CMLEA = 0;
%     CMLEN = -0.250178140301351;
%%%%%%%%%%%%%%%%%%%%%%%%%%%%%%%%%%%%%%%%%%%%%%%%%%%%
%%%%%%%%%%%%%%%%%%%%%%%%%%%%%%%%%%%%%%%%%%%%%%%%%%%%
%     % NACA 0012 data from Airfoil Appendix
%     foilName = '0012';
%     a     = i*(pi/180);
%     alo   = 0;
%     cloa  = 6.14987213746803;
%     CD0   = 0.00578980686984839;
%     CD0L  = 0;
%     CD0L2 = 0.00589558911360464;
%     CMLEa = 0;
%     CMLEA = 0;
%     CMLEN = -0.248792267683901;
%%%%%%%%%%%%%%%%%%%%%%%%%%%%%%%%%%%%%%%%%%%%%%%%%%%%
%%%%%%%%%%%%%%%%%%%%%%%%%%%%%%%%%%%%%%%%%%%%%%%%%%%%
    % NACA 1408 data from Airfoil Appendix
    foilName = '1408';
    a     = i*(pi/180);
    alo   = -0.0145678;
    cloa  = 6.1897717;
    CD0   = 0.0051515;
    CD0L  = -0.0017593;
    CD0L2 = 0.0080154;
    CMLEa = 0.8677365;
    CMLEA = -0.0322065;
    CMLEN = -0.5349267;
    %cmo   = 1;
    %cma   = 1;
    %Cmc4  = 1;
%%%%%%%%%%%%%%%%%%%%%%%%%%%%%%%%%%%%%%%%%%%%%%%%%%%%
%%%%%%%%%%%%%%%%%%%%%%%%%%%%%%%%%%%%%%%%%%%%%%%%%%%%
```

```
%     % NACA 1412 data from Airfoil Appendix
%     foilName = '1412';
%     a     = i*(pi/180);
%     alo   = -0.0216014394282236;
%     cloa  = 6.02467660173922;
%     CD0   = 0.00587402293302405;
%     CD0L  = -0.00134903274883071;
%     CD0L2 = 0.00536741319382652;
%     CMLEa = 0.542385993671305;
%     CMLEA = -0.0183836491952911;
%     CMLEN = -0.429724431443849;
%%%%%%%%%%%%%%%%%%%%%%%%%%%%%%%%%%%%%%%%%%%%%%%%%%%%%%
%%%%%%%%%%%%%%%%%%%%%%%%%%%%%%%%%%%%%%%%%%%%%%%%%%%%%%
%     % NACA 2410 data from Airfoil Appendix
%     foilName = '2410';
%     a     = i*(pi/180);
%     alo   = -0.0350101171310758;
%     cloa  = 6.23568559320461;
%     CD0   = 0.00580887637682987;
%     CD0L  = -0.00202820935139267;
%     CD0L2 = 0.00657649746862038;
%     CMLEa = 0.696673178623474;
%     CMLEA = -0.0121747099302256;
%     CMLEN = -0.471751212453014;
%%%%%%%%%%%%%%%%%%%%%%%%%%%%%%%%%%%%%%%%%%%%%%%%%%%%%%
%%%%%%%%%%%%%%%%%%%%%%%%%%%%%%%%%%%%%%%%%%%%%%%%%%%%%%
%     % NACA 2412 data from Airfoil Appendix
%     foilName = '2412';
%     a     = i*(pi/180);
%     alo   = -0.0455580244243206;
%     cloa  = 5.75810202691551;
%     CD0   = 0.00640032868295237;
%     CD0L  = -0.00208181252700775;
%     CD0L2 = 0.00618775485134525;
%     CMLEa = 0.494123897109009;
%     CMLEA = -0.0263366838973971;
%     CMLEN = -0.414419608257138;
%%%%%%%%%%%%%%%%%%%%%%%%%%%%%%%%%%%%%%%%%%%%%%%%%%%%%%
%%%%%%%%%%%%%%%%%%%%%%%%%%%%%%%%%%%%%%%%%%%%%%%%%%%%%%
%     % NACA 2424 data from Airfoil Appendix
%     foilName = '2424';
%     a     = i*(pi/180);
%     alo   = -0.0354033949938163;
%     cloa  = 5.18829911765801;
%     CD0   = 0.00844763624697131;
%     CD0L  = -0.00075778327782238;
%     CD0L2 = 0.00635556970934001;
%     CMLEa = 0.563857762725431;
%     CMLEA = 0.0283921893758112;
%     CMLEN = -0.433109250719577;
%%%%%%%%%%%%%%%%%%%%%%%%%%%%%%%%%%%%%%%%%%%%%%%%%%%%%%
%%%%%%%%%%%%%%%%%%%%%%%%%%%%%%%%%%%%%%%%%%%%%%%%%%%%%%
%     % NACA 4412 data from Airfoil Appendix
%     foilName = '4412';
```

```
%     a     = i*(pi/180);
%     alo   = -0.066813366237402;
%     cloa  = 5.85919194114081;
%     CD0   = 0.00645256725654991;
%     CD0L  = -0.00336480754312331;
%     CD0L2 = 0.00724157881965858;
%     CMLEa = 0.68855712967518;
%     CMLEA = -0.110712686814761;
%     CMLEN = -0.491349229675727;
%%%%%%%%%%%%%%%%%%%%%%%%%%%%%%%%%%%%%%%%%%%%%%%%
%%%%%%%%%%%%%%%%%%%%%%%%%%%%%%%%%%%%%%%%%%%%%%%%
%     % NACA 4415 data from Airfoil Appendix
%     foilName = '4415';
%     a     = i*(pi/180);
%     alo   = -0.0734303832901057;
%     cloa  = 5.68653896493843;
%     CD0   = 0.0075058042036877;
%     CD0L  = -0.00254026404822751;
%     CD0L2 = 0.00419036888285099;
%     CMLEa = 0.640570566841305;
%     CMLEA = -0.0245218565708409;
%     CMLEN = -0.468522511921671;
%%%%%%%%%%%%%%%%%%%%%%%%%%%%%%%%%%%%%%%%%%%%%%%%
%%%%%%%%%%%%%%%%%%%%%%%%%%%%%%%%%%%%%%%%%%%%%%%%
%     % NACA 4418 data from Airfoil Appendix
%     foilName = '4418';
%     a     = i*(pi/180);
%     alo   = -0.0685079303321731;
%     cloa  = 5.71103186575275;
%     CD0   = 0.00790011856241665;
%     CD0L  = -0.00256047509045299;
%     CD0L2 = 0.00401065120084031;
%     CMLEa = 0.663301464170368;
%     CMLEA = -0.0235063201303145;
%     CMLEN = -0.470752522108866;
%%%%%%%%%%%%%%%%%%%%%%%%%%%%%%%%%%%%%%%%%%%%%%%%
%%%%%%%%%%%%%%%%%%%%%%%%%%%%%%%%%%%%%%%%%%%%%%%%
%     % NACA 4424 data from Airfoil Appendix
%     foilName = '4424';
%     a     = i*(pi/180);
%     alo   = -0.0628467630852301;
%     cloa  = 5.38037549620744;
%     CD0   = 0.008792211847361;
%     CD0L  = -0.00178071313927388;
%     CD0L2 = 0.0053300138585352;
%     CMLEa = 0.680507117895762;
%     CMLEA = -0.00591426748485269;
%     CMLEN = -0.479713535634107;
%%%%%%%%%%%%%%%%%%%%%%%%%%%%%%%%%%%%%%%%%%%%%%%%
%%%%%%%%%%%%%%%%%%%%%%%%%%%%%%%%%%%%%%%%%%%%%%%%
%     % NACA 2412Dustin compressible data from Airfoil Appendix
%     foilName = '2412';
%     a     = i*(pi/180);
%     alo   = -0.035876678458286425;
```

```
%     cloa  = 11.392192346341583;
%     CD0   = 0.02056918358643251;
%     CD0L  = -0.026492229858322114;
%     CD0L2 = 0.11743008498986997;
%     CMLEa = 0.7257122234947719;
%     CMLEA = -1.2715452269152567;
%     CMLEN = -0.5147128651813082;
%%%%%%%%%%%%%%%%%%%%%%%%%%%%%%%%%%%%%%%%%%%%%%%%%%%%

%%%%%%%%%%%%%%%%%%% X FOIL %%%%%%%%%%%%%%%%%%%%

%%%%%%%%%%%%%%%%%%%%%%%%%%%%%%%%%%%%%%%%%%%%%%%%%%%%
%     % XNACA 0006 data from Airfoil Appendix
%     foilName = '0006';
%     a     = i*(pi/180);
%     alo   = 0;
%     cloa  = 6.24725277916935;
%     CD0   = 0.00317816842440291;
%     CD0L  = 0;
%     CD0L2 = 0.0127851315547638;
%     CMLEa = 0;
%     CMLEA = 0;
%     CMLEN = -0.24556228409321;
%%%%%%%%%%%%%%%%%%%%%%%%%%%%%%%%%%%%%%%%%%%%%%%%%%%%
%%%%%%%%%%%%%%%%%%%%%%%%%%%%%%%%%%%%%%%%%%%%%%%%%%%%
%     % xNACA 0012 data from Airfoil Appendix
%     foilName = '0012';
%     a     = i*(pi/180);
%     alo   = 0;
%     cloa  = 6.4126395802572;
%     CD0   = 0.00520318347755638;
%     CD0L  = 0;
%     CD0L2 = 0.00493201029734306;
%     CMLEa = 0;
%     CMLEA = 0;
%     CMLEN = -0.249436912071791;
%%%%%%%%%%%%%%%%%%%%%%%%%%%%%%%%%%%%%%%%%%%%%%%%%%%%
%%%%%%%%%%%%%%%%%%%%%%%%%%%%%%%%%%%%%%%%%%%%%%%%%%%%
%     % xNACA 1408 data from Airfoil Appendix
%     foilName = '1408';
%     a     = i*(pi/180);
%     alo   = -0.0180652358272032;
%     cloa  = 6.32226645998854;
%     CD0   = 0.00461237846328006;
%     CD0L  = -0.00136642750620477;
%     CD0L2 = 0.00717274422939727;
%     CMLEa = 0.750138280491661;
%     CMLEA = -0.0166962861688784;
%     CMLEN = -0.485906892418554;
%%%%%%%%%%%%%%%%%%%%%%%%%%%%%%%%%%%%%%%%%%%%%%%%%%%%
%%%%%%%%%%%%%%%%%%%%%%%%%%%%%%%%%%%%%%%%%%%%%%%%%%%%
%     % xNACA 1412 data from Airfoil Appendix
%     foilName = '1412';
%     a     = i*(pi/180);
```

```
%     alo   = -0.0178982511770066;
%     cloa  = 6.36814143933405;
%     CD0   = 0.00521938900679535;
%     CD0L  = -0.000876001965110274;
%     CD0L2 = 0.00505246982460321;
%     CMLEa = 0.673506992898865;
%     CMLEA = 0.0241548514697989;
%     CMLEN = -0.458825322979267;
%%%%%%%%%%%%%%%%%%%%%%%%%%%%%%%%%%%%%%%%%%%%%%%
%%%%%%%%%%%%%%%%%%%%%%%%%%%%%%%%%%%%%%%%%%%%%%%
%     % xNACA 2412 data from Airfoil Appendix
%     foilName = '2412';
%     a     = i*(pi/180);
%     alo   = -0.0373895121688584;
%     cloa  = 6.3253620978506;
%     CD0   = 0.00532949246530466;
%     CD0L  = -0.00182506208560641;
%     CD0L2 = 0.00522268362548347;
%     CMLEa = 0.714522309708262;
%     CMLEA = -0.00184803325645788;
%     CMLEN = -0.472541777595804;
%%%%%%%%%%%%%%%%%%%%%%%%%%%%%%%%%%%%%%%%%%%%%%%
%%%%%%%%%%%%%%%%%%%%%%%%%%%%%%%%%%%%%%%%%%%%%%
%     % xNACA 2424 data from Airfoil Appendix
%     foilName = '2424';
%     a     = i*(pi/180);
%     alo   = -0.0356187169129064;
%     cloa  = 6.02088351998069;
%     CD0   = 0.00726457301719901;
%     CD0L  = -0.00118756576598667;
%     CD0L2 = 0.00340876822456072;
%     CMLEa = 0.699560535536618;
%     CMLEA = -0.0279009300010138;
%     CMLEN = -0.46936193044925;
%%%%%%%%%%%%%%%%%%%%%%%%%%%%%%%%%%%%%%%%%%%%%%%
%%%%%%%%%%%%%%%%%%%%%%%%%%%%%%%%%%%%%%%%%%%%%%
%     % xNACA 4415 data from Airfoil Appendix
%     foilName = '4415';
%     a     = i*(pi/180);
%     alo   = -0.0738471950476704;
%     cloa  = 6.31439243010206;
%     CD0   = 0.00648995198238606;
%     CD0L  = -0.00310050333854929;
%     CD0L2 = 0.00400685412224384;
%     CMLEa = 0.707460219355764;
%     CMLEA = -0.0295899801763886;
%     CMLEN = -0.472658242541987;
%%%%%%%%%%%%%%%%%%%%%%%%%%%%%%%%%%%%%%%%%%%%%%%
%%%%%%%%%%%%%%%%%%%%%%%%%%%%%%%%%%%%%%%%%%%%%%
%     % xNACA 4418 data from Airfoil Appendix
%     foilName = '4418';
%     a     = i*(pi/180);
%     alo   = -0.0734820440836776;
%     cloa  = 6.29539227696611;
```

```
%     CD0   = 0.00703366550835054;
%     CD0L  = -0.00259656735970565;
%     CD0L2 = 0.0031449907696781;
%     CMLEa = 0.699822363875463;
%     CMLEA = -0.029676210380603;
%     CMLEN = -0.469847771314208;
%%%%%%%%%%%%%%%%%%%%%%%%%%%%%%%%%%%%%%%%%%%%%%%%%%%%
%%%%%%%%%%%%%%%%%%%%%%%%%%%%%%%%%%%%%%%%%%%%%%%%%%%%
%     % xNACA 4424 data from Airfoil Appendix
%     foilName = '4424';
%     a     = i*(pi/180);
%     alo   = -0.0709059112140821;
%     cloa  = 5.9874308077726;
%     CD0   = 0.00786583384450818;
%     CD0L  = -0.00205551523231613;
%     CD0L2 = 0.00336950600880986;
%     CMLEa = 0.678651851542374;
%     CMLEA = -0.0178801645616264;
%     CMLEN = -0.464528574908379;
%%%%%%%%%%%%%%%%%%%%%%%%%%%%%%%%%%%%%%%%%%%%%%%%%%%%

%%%%%%%%%%% SYMMETRIC ISSUE TEST %%%%%%%%%%%%%%

%%%%%%%%%%%%%%%%%%%%%%%%%%%%%%%%%%%%%%%%%%%%%%%%%%%%
%     % NACA 0012S data from Airfoil Appendix
%     foilName = '0012';
%     a     = i*(pi/180);
%     alo   = 0;
%     cloa  = 6.14987213746803;
%     CD0   = 0.00578980686984839;
%     CD0L  = 0;
%     CD0L2 = 0.00589558911360464;
%     CMLEa = 0;
%     CMLEA = 0;
%     CMLEN = -0.248792267683901;
%%%%%%%%%%%%%%%%%%%%%%%%%%%%%%%%%%%%%%%%%%%%%%%%%%%%


    % substitute symbolic variables for double numbers into symbolic
    % expressions and evaluate to decimals
    XacT  = eval(subs(Xac));
    YacT = eval(subs(Yac));
    cmACT = eval(subs(cmAC));

    xsave(j) = XacT;
    ysave(j) = YacT;
    cmsave(j) = cmACT;

    j=j+1;

    end

    figure(1)
```

```
    plot(xsave,ysave,'color',cpass,'marker',mpass)
    xlabel('Xac')
    ylabel('Yac')
    title(['AC(alpha) for NACA ',foilName])
    axis equal
    hold on
    legend('Original','1st Reduction', '2nd Reduction', '3rd
Reduction','4th Reduction','5th Reduction')

end


function [Xac,Yac,cmAC] = OrderReduction_Post( Xac,Yac,cmAC )

syms a alo cloa CD0 CD0L CD0L2 CMLEa CMLEN CMLEA

Xac  = expand(Xac);
Yac  = expand(Yac);
cmAC = expand(cmAC);

%%%%%%%%%%%%%%%%%%%%%%%%%%%%%%%%%%%%%%%%%%%%%%%%%%%%%%%%%%%%%%%%%%%%%%%%%%%%
%%%%

Xac = subs(Xac, a*a*a*a*a*a*a*a*a*a*a*a*a*a*a*a*a, 0); % 16a
Xac = subs(Xac, a*a*a*a*a*a*a*a*a*a*a*a*a*a*a*a, 0); % 15a
Xac = subs(Xac, a*a*a*a*a*a*a*a*a*a*a*a*a*a*a, 0); % 14a
Xac = subs(Xac, a*a*a*a*a*a*a*a*a*a*a*a*a*a, 0); % 13a
Xac = subs(Xac, a*a*a*a*a*a*a*a*a*a*a*a*a, 0); % 12a
Xac = subs(Xac, a*a*a*a*a*a*a*a*a*a*a*a, 0); % 11a
Xac = subs(Xac, a*a*a*a*a*a*a*a*a*a*a, 0); % 10a
Xac = subs(Xac, a*a*a*a*a*a*a*a*a*a, 0); % 9a
Xac = subs(Xac, a*a*a*a*a*a*a*a*a, 0); % 8a
Xac = subs(Xac, a*a*a*a*a*a*a*a, 0); % 7a
Xac = subs(Xac, a*a*a*a*a*a*a, 0); % 6a
Xac = subs(Xac, a*a*a*a*a*a, 0); % 5a
Xac = subs(Xac, a*a*a*a*a, 0); % 4a

Xac = subs(Xac, alo*alo*alo*alo*alo*alo*alo*alo*alo*alo, 0); % 9alo
Xac = subs(Xac, alo*alo*alo*alo*alo*alo*alo*alo*alo, 0); % 8alo
Xac = subs(Xac, alo*alo*alo*alo*alo*alo*alo*alo, 0); % 7alo
Xac = subs(Xac, alo*alo*alo*alo*alo*alo*alo, 0); % 6alo
Xac = subs(Xac, alo*alo*alo*alo*alo*alo, 0); % 5alo
Xac = subs(Xac, alo*alo*alo*alo*alo, 0); % 4alo

Yac = subs(Yac, a*a*a*a*a*a*a*a*a*a*a*a*a*a*a*a*a, 0); % 16a
Yac = subs(Yac, a*a*a*a*a*a*a*a*a*a*a*a*a*a*a*a, 0); % 15a
Yac = subs(Yac, a*a*a*a*a*a*a*a*a*a*a*a*a*a*a, 0); % 14a
Yac = subs(Yac, a*a*a*a*a*a*a*a*a*a*a*a*a*a, 0); % 13a
Yac = subs(Yac, a*a*a*a*a*a*a*a*a*a*a*a*a, 0); % 12a
Yac = subs(Yac, a*a*a*a*a*a*a*a*a*a*a*a, 0); % 11a
Yac = subs(Yac, a*a*a*a*a*a*a*a*a*a*a, 0); % 10a
Yac = subs(Yac, a*a*a*a*a*a*a*a*a*a, 0); % 9a
```

```
Yac = subs(Yac, a*a*a*a*a*a*a*a, 0); % 8a
Yac = subs(Yac, a*a*a*a*a*a*a, 0); % 7a
Yac = subs(Yac, a*a*a*a*a*a, 0); % 6a
Yac = subs(Yac, a*a*a*a*a, 0); % 5a
Yac = subs(Yac, a*a*a*a, 0); % 4a

Yac = subs(Yac, alo*alo*alo*alo*alo*alo*alo*alo*alo, 0); % 9alo
Yac = subs(Yac, alo*alo*alo*alo*alo*alo*alo*alo, 0); % 8alo
Yac = subs(Yac, alo*alo*alo*alo*alo*alo*alo, 0); % 7alo
Yac = subs(Yac, alo*alo*alo*alo*alo*alo, 0); % 6alo
Yac = subs(Yac, alo*alo*alo*alo*alo, 0); % 5alo
Yac = subs(Yac, alo*alo*alo*alo, 0); % 4alo

cmAC = subs(cmAC, a*a*a*a*a*a*a*a*a*a*a*a*a*a*a*a*a*a, 0); % 18a
cmAC = subs(cmAC, a*a*a*a*a*a*a*a*a*a*a*a*a*a*a*a*a, 0); % 17a
cmAC = subs(cmAC, a*a*a*a*a*a*a*a*a*a*a*a*a*a*a*a, 0); % 16a
cmAC = subs(cmAC, a*a*a*a*a*a*a*a*a*a*a*a*a*a*a, 0); % 15a
cmAC = subs(cmAC, a*a*a*a*a*a*a*a*a*a*a*a*a*a, 0); % 14a
cmAC = subs(cmAC, a*a*a*a*a*a*a*a*a*a*a*a*a, 0); % 13a
cmAC = subs(cmAC, a*a*a*a*a*a*a*a*a*a*a*a, 0); % 12a
cmAC = subs(cmAC, a*a*a*a*a*a*a*a*a*a*a, 0); % 11a
cmAC = subs(cmAC, a*a*a*a*a*a*a*a*a*a, 0); % 10a
cmAC = subs(cmAC, a*a*a*a*a*a*a*a*a, 0); % 9a
cmAC = subs(cmAC, a*a*a*a*a*a*a*a, 0); % 8a
cmAC = subs(cmAC, a*a*a*a*a*a*a, 0); % 7a
cmAC = subs(cmAC, a*a*a*a*a*a, 0); % 6a
cmAC = subs(cmAC, a*a*a*a*a, 0); % 5a
cmAC = subs(cmAC, a*a*a*a, 0); % 4a

cmAC = subs(cmAC, alo*alo*alo*alo*alo*alo*alo*alo*alo, 0); % 9alo
cmAC = subs(cmAC, alo*alo*alo*alo*alo*alo*alo*alo, 0); % 8alo
cmAC = subs(cmAC, alo*alo*alo*alo*alo*alo*alo, 0); % 7alo
cmAC = subs(cmAC, alo*alo*alo*alo*alo*alo, 0); % 6alo
cmAC = subs(cmAC, alo*alo*alo*alo*alo, 0); % 5alo
cmAC = subs(cmAC, alo*alo*alo*alo, 0); % 4alo

%%%%%%%%%%%%%%%%%%%%%%%%%%%%%%%%%%%%%%%%%%%%%%%%%%%%%%%%%%%%%%%%%%%%%%%%
%%%%

Xac  = expand(Xac);
Yac  = expand(Yac);
cmAC = expand(cmAC);

Xac  = subs(Xac, a*a*a*alo, 0);
Xac  = subs(Xac, a*a*alo*alo, 0);
Xac  = subs(Xac, a*alo*alo*alo, 0);

Yac  = subs(Yac, a*a*a*alo, 0);
Yac  = subs(Yac, a*a*alo*alo, 0);
Yac  = subs(Yac, a*alo*alo*alo, 0);

cmAC = subs(cmAC, a*a*a*alo, 0);
cmAC = subs(cmAC, a*a*alo*alo, 0);
```

```
cmAC = subs(cmAC, a*alo*alo*alo, 0);

%%%%%%%%%%%%%%%%%%%%%%%%%%%%%%%%%%%%%%%%%%%%%%%%%%%%%%%%%%%%%%%%%%%%%%%%%%%%%%%
%%%%

Xac  = expand(Xac);
Yac  = expand(Yac);
cmAC = expand(cmAC);

Xac = subs(Xac, CD0L*CD0L2*alo*alo, 0);
Xac = subs(Xac, CD0*CD0L2*alo*alo, 0);
Xac = subs(Xac, CD0L2*CD0L2*alo*alo, 0);
Xac = subs(Xac, CD0L*CD0L*alo*alo, 0);
Xac = subs(Xac, CD0*CD0L2*alo*alo*alo, 0);
Xac = subs(Xac, CD0*CD0L*alo*alo*alo, 0);
Xac = subs(Xac, CD0L*alo*alo*alo, 0);
Xac = subs(Xac, CD0L*CD0L2*a*alo, 0);
Xac = subs(Xac, CD0*CD0L2*a*alo, 0);
Xac = subs(Xac, CD0*CD0L2*a*a*a, 0);
Xac = subs(Xac, CD0*CD0L2*a*a, 0);
Xac = subs(Xac, CD0*CD0L*a*a*a, 0);
Xac = subs(Xac, CD0*CD0L*a*a, 0);
Xac = subs(Xac, CD0L2*CD0L2*alo*alo, 0);
Xac = subs(Xac, CD0L2*CD0L2*a*a, 0);
Xac = subs(Xac, CD0L2*CD0L2*a*alo, 0);
Xac = subs(Xac, CD0*a*a*a, 0);
Xac = subs(Xac, CD0L*a*a*a, 0);
Xac = subs(Xac, CD0L2*a*a*a, 0);
Xac = subs(Xac, CD0L2*alo*alo*alo, 0);
Xac = subs(Xac, CD0L2*alo*alo*a, 0);
Xac = subs(Xac, CD0L2*alo*a*a, 0);

Yac = subs(Yac, CD0L*CD0L2*alo*alo, 0);
Yac = subs(Yac, CD0*CD0L2*alo*alo, 0);
Yac = subs(Yac, CD0L2*CD0L2*alo*alo, 0);
Yac = subs(Yac, CD0L*CD0L*alo*alo, 0);
Yac = subs(Yac, CD0*CD0L2*alo*alo*alo, 0);
Yac = subs(Yac, CD0*CD0L*alo*alo*alo, 0);
Yac = subs(Yac, CD0L*alo*alo*alo, 0);
Yac = subs(Yac, CD0L*CD0L2*a*alo, 0);
Yac = subs(Yac, CD0*CD0L2*a*alo, 0);
Yac = subs(Yac, CD0*CD0L2*a*a*a, 0);
Yac = subs(Yac, CD0*CD0L2*a*a, 0);
Yac = subs(Yac, CD0*CD0L*a*a*a, 0);
Yac = subs(Yac, CD0*CD0L*a*a, 0);
Yac = subs(Yac, CD0L2*CD0L2*alo*alo, 0);
Yac = subs(Yac, CD0L2*CD0L2*a*a, 0);
Yac = subs(Yac, CD0L2*CD0L2*a*alo, 0);
Yac = subs(Yac, CD0*a*a*a, 0);
Yac = subs(Yac, CD0L*a*a*a, 0);
Yac = subs(Yac, CD0L2*a*a*a, 0);
Yac = subs(Yac, CD0L2*alo*alo*alo, 0);
Yac = subs(Yac, CD0L2*alo*alo*a, 0);
```

```
Yac = subs(Yac, CD0L2*alo*a*a, 0);

cmAC = subs(cmAC, CD0L*CD0L2*alo*alo, 0);
cmAC = subs(cmAC, CD0*CD0L2*alo*alo, 0);
cmAC = subs(cmAC, CD0L2*CD0L2*alo*alo, 0);
cmAC = subs(cmAC, CD0L*CD0L*alo*alo, 0);
cmAC = subs(cmAC, CD0*CD0L2*alo, 0);
cmAC = subs(cmAC, CD0*CD0L2*alo*alo*alo, 0);
cmAC = subs(cmAC, CD0*CD0L*alo*alo*alo, 0);
cmAC = subs(cmAC, CD0L*alo*alo*alo, 0);
cmAC = subs(cmAC, CD0L*CD0L2*a*alo, 0);
cmAC = subs(cmAC, CD0*CD0L2*a*alo, 0);
cmAC = subs(cmAC, CD0*CD0L2*a*a*a, 0);
cmAC = subs(cmAC, CD0*CD0L2*a*a, 0);
cmAC = subs(cmAC, CD0*CD0L*a*a*a, 0);
cmAC = subs(cmAC, CD0*CD0L*a*a, 0);
cmAC = subs(cmAC, CD0L2*CD0L2*alo*alo, 0);
cmAC = subs(cmAC, CD0L2*CD0L2*a*a, 0);
cmAC = subs(cmAC, CD0L2*CD0L2*a*alo, 0);
cmAC = subs(cmAC, CD0*a*a*a, 0);
cmAC = subs(cmAC, CD0L*a*a*a, 0);
cmAC = subs(cmAC, CD0L2*a*a*a, 0);
cmAC = subs(cmAC, CD0L2*alo*alo*alo, 0);
cmAC = subs(cmAC, CD0L2*alo*alo*a, 0);
cmAC = subs(cmAC, CD0L2*alo*a*a, 0);

cmAC = subs(cmAC, CD0*alo*alo*alo, 0);
cmAC = subs(cmAC, CD0*CD0L*alo*alo, 0);
cmAC = subs(cmAC, CD0*CD0L*a*alo, 0);
cmAC = subs(cmAC, CD0*CD0L*CD0L2*a, 0);
cmAC = subs(cmAC, CD0*CD0L*CD0L*a*alo, 0);
cmAC = subs(cmAC, CD0*CD0L*a*alo*alo, 0);
cmAC = subs(cmAC, CD0*a*alo*alo, 0);
cmAC = subs(cmAC, CD0*a*a*alo, 0);
cmAC = subs(cmAC, CD0*CD0*a*a, 0);
cmAC = subs(cmAC, CD0*CD0*a*alo, 0);
cmAC = subs(cmAC, CD0*CD0*CD0L*a, 0);
cmAC = subs(cmAC, CD0*CD0*CD0L*a*alo, 0);
cmAC = subs(cmAC, CD0*CD0*CD0L*alo, 0);
cmAC = subs(cmAC, CD0*CD0*CD0*a, 0);
cmAC = subs(cmAC, CD0*CD0*CD0*a*a, 0);
cmAC = subs(cmAC, CD0*CD0*a*a*alo, 0);
cmAC = subs(cmAC, CD0*CD0*CD0L2*a, 0);
cmAC = subs(cmAC, CD0*CD0*alo*alo*alo, 0);
cmAC = subs(cmAC, CD0L*a*a*alo, 0);
cmAC = subs(cmAC, CD0L*a*alo*alo, 0);
cmAC = subs(cmAC, CD0L*CD0L2*a*a, 0);
cmAC = subs(cmAC, CD0L*CD0L*a*a, 0);
cmAC = subs(cmAC, CD0L*CD0L*a*a*alo, 0);
cmAC = subs(cmAC, CD0L*CD0L*a*alo, 0);
cmAC = subs(cmAC, CD0L*CD0L*CD0*a, 0);
cmAC = subs(cmAC, CD0L*CD0L*CD0L2*a*a, 0);
cmAC = subs(cmAC, CD0L*CD0L*CD0L*a, 0);
cmAC = subs(cmAC, CD0L*CD0L*CD0L*alo, 0);
```

```
cmAC = subs(cmAC, CD0L*CD0L*CD0L*a*a, 0);
cmAC = subs(cmAC, CD0L*CD0L*CD0L*a*alo, 0);
cmAC = subs(cmAC, CD0L*CD0L*CD0L*a*a*alo, 0);

%%%%%%%%%%%%%%%%%%%%%%%%%%%%%%%%%%%%%%%%%%%%%%%%%%%%%%%%%%%%%%%%%%%%%%%%%%%%%%%
%%%%

end
```

APPENDIX D

The following program was used to calculate the location of the aerodynamic center for 250 NACA 4-digit airfoils as a function of airfoil camber and thickness in inviscid flow. This program uses the numerical vortex panel method from Appendix B.

```
--------------------------------------------------------------------------
%%%%%%%%%%%%%%%%%%%%%%%%%%%%%%%% MAIN CODE %%%%%%%%%%%%%%%%%%%%%%%%%%%%
--------------------------------------------------------------------------

% The purpose of this script is to sweep through a range of NACA 4-
digit airfoils and solve for coefficient of lift and moment over a
range of angles of attack using the vortex panel method. After
collecting the RMS error is computed to compare the VPM data results
against the traditional and alternative line fitting equations both
using a least squares regression technique.

% suffix "hunsaker" refers to relations developed from general airfoil
% theory and conformal mapping techniques

% suffix "traditional" refers to relations developed from thin airfoil
% theory

% suffix "traditional mod" refers to relations developed from thin
airfoiltheory, however, removes the small angle approximations

msweep = [0:2:8];      % first digit [2:2:8]
psweep = [0];          % second digit [4]
tsweep = [1:1:50];     % last two digits

c            = 1;      % chord length
v00          = 1;      % free stream velocity
N            = 400;    % number of panels to be used (even)
tailFlag     = 'y';    % close the trailing edge? (y/n)
AOA_low      = -5;    % low angle of attack (degrees)
AOA_high     = 5;     % high angle of attack (degrees)
A0Aincrement = 5;      % increment of the angles of attack
flag         = 'y';    % use cosine clustering? (y/n)

k =1;
for i=1:length(msweep) % first digit loop
    for j=1:1:length(tsweep) % last two digit loop

% import raw data
[ cLVortex, cMVortex, AOARangeVortex, cl_thinAirfoil] =
vortexPanelMethodFunction(v00,N,tailFlag,AOA_low,AOA_high,flag,msweep(i
),psweep(1),tsweep(j),c,A0Aincrement);

% filename = 'joukowskiAirfoilData.csv';
% data = csvread(filename,2,0);
CAvortex = -cLVortex.*sind(AOARangeVortex);
```

```
CNvortex = cLVortex.*cosd(AOARangeVortex);
data = vertcat(AOARangeVortex,CNvortex,CAvortex,cMVortex,cLVortex)';

datasweep(:,:,k) = data; % records vortex panel method data for each
airfoil

k = k+1;
    end % last 2 digit loops

    psweep = [4];
end % first digit loop

disp('Data Collection Complete')

%% Coefficient Solver
disp('running solver...')

limit = (k-1);
col1  = linspace(1,50,50);
col2  = linspace(51,100,50);
col3  = linspace(101,150,50);
col4  = linspace(151,200,50);
col5  = linspace(201,250,50);
guide = [col1;col2;col3;col4;col5]';

for k=1:limit

    alpha    = datasweep(:,1,k);
    alphaRad = alpha*(pi/180);
    CL       = datasweep(:,5,k);
    Cm       = datasweep(:,4,k);

% CL Coefficient Solver Traditional
alphaL0SolvedTRAD(k)    = (sum(CL)*sum(alphaRad.*alphaRad)-
sum(alphaRad)*sum(CL.*alphaRad))/(sum(CL)*sum(alphaRad)-
length(alphaRad)*sum(CL.*alphaRad));
CLalphaSolvedTRAD(k)    = sum(CL)/(sum(alphaRad)-
length(alphaRad)*alphaL0SolvedTRAD(k));

% CL Coefficient Solver Hunsaker
alphaL0Solved(k)  =
atan((sum(CL.*cos(alphaRad))*sum(sin(alphaRad).*sin(alphaRad))-
sum(CL.*sin(alphaRad))*sum(sin(alphaRad).*cos(alphaRad)))/(sum(sin(alph
aRad).*cos(alphaRad))*sum(CL.*cos(alphaRad))-
sum(CL.*sin(alphaRad))*sum(cos(alphaRad).*cos(alphaRad))));
CLalphaSolved(k)  =
sum(CL.*cos(alphaRad))/(sum(sin(alphaRad).*cos(alphaRad))-
tan(alphaL0Solved(k))*sum(cos(alphaRad).*cos(alphaRad)));

% CM Coefficient Solver Hunsaker
if k>50
```

```
A = [sum(sin(2*alphaRad).*sin(2*alphaRad)),
sum(CL.*cos(alphaRad).*sin(2*alphaRad)),  sum(-
CL.*sin(alphaRad).*sin(2*alphaRad));

sum(sin(2*alphaRad).*CL.*cos(alphaRad)),sum(CL.*CL.*cos(alphaRad).*cos(
alphaRad)),sum(-CL.*CL.*sin(alphaRad).*cos(alphaRad));

sum(sin(2*alphaRad).*CL.*sin(alphaRad)),sum(CL.*CL.*cos(alphaRad).*sin(
alphaRad)),sum(-CL.*CL.*sin(alphaRad).*sin(alphaRad)); ];

B =  [sum(Cm.*sin(2*alphaRad));
      sum(Cm.*CL.*cos(alphaRad));
      sum(Cm.*CL.*sin(alphaRad))];

  CMCoeffSolved = A^(-1)*B;
  CmLEAlpha(k)     = CMCoeffSolved(1);
  CmLENormal(k)    = CMCoeffSolved(2);
  CmLEAxial(k)     = CMCoeffSolved(3);

else

  CmLEAlpha(k)     = 0;
  CmLENormal(k)    =
sum(Cm.*CL.*cos(alphaRad))/sum(CL.*CL.*cos(alphaRad).*cos(alphaRad));
  CmLEAxial(k)     = 0;

end

% CM Coefficient Solver Traditional
 cmC4(k) = sum(Cm+CL./4)/length(alphaRad);

 for i=1:length(alphaRad)
    CL_Hunsaker(i) = CLalphaSolved(k)*(sin(alphaRad(i))-
tan(alphaL0Solved(k))*cos(alphaRad(i)));
    CL_Traditional(i) = CLalphaSolvedTRAD(k)*(alphaRad(i)-
alphaL0SolvedTRAD(k));

    Cm_Hunsaker(i) = CmLEAlpha(k)*sin(2*alphaRad(i)) +
CmLENormal(k)*CL_Hunsaker(i)*cos(alphaRad(i)) -
CmLEAxial(k)*CL_Hunsaker(i)*sin(alphaRad(i));
    Cm0_Traditional(i) = cmC4(k)-CL(i)/4;

 end

 % save data for the NACA 8415 case
 if k == 215
    cL8415Hunsaker    = CL_Hunsaker;
    cL8415Traditional = CL_Traditional;

    cm8415Hunsaker    = Cm_Hunsaker;
    cm8415Traditional = Cm0_Traditional;
 end
```

```
    % Calculate RMS Error values for each airfoil configuration
    CL_RMSE_Hunsaker(k)    = RMSE( CL, CL_Hunsaker, length(CL));
    CM_RMSE_Traditional(k) = RMSE( Cm, Cm0_Traditional, length(Cm));

    CL_RMSE_Traditional(k) = RMSE( CL, CL_Traditional, length(CL));
    CM_RMSE_Hunsaker(k)    = RMSE( Cm, Cm_Hunsaker, length(Cm));


    % Calculate aerodynamic center location for each airfoil
configuration
    XAC_hunsaker(k) = -
2*CmLEAlpha(k)/CLalphaSolved(k)*cos(alphaL0Solved(k))^2-CmLENormal(k);
    YAC_hunsaker(k) =
CmLEAlpha(k)/CLalphaSolved(k)*sin(2*alphaL0Solved(k))+CmLEAxial(k);


end

%% Plotting
disp('Plotting...')

figure(1) %%%%%%%%%%%%%%%%%%%%%%%%%%%%%%%%%%%%%%%%%%%%%%%%%%%%
p11 = semilogy(tsweep,CL_RMSE_Traditional(  1:50 ),'-r');
hold on
      semilogy(tsweep,CL_RMSE_Traditional( 51:100),'-r')
      semilogy(tsweep,CL_RMSE_Traditional(101:150),'-r')
      semilogy(tsweep,CL_RMSE_Traditional(151:200),'-r')
      semilogy(tsweep,CL_RMSE_Traditional(201:250),'-r')

p12 = semilogy(tsweep,CL_RMSE_Hunsaker(1:50),'-b');
semilogy(tsweep,CL_RMSE_Hunsaker( 51:100),'-b')
semilogy(tsweep,CL_RMSE_Hunsaker(101:150),'-b')
semilogy(tsweep,CL_RMSE_Hunsaker(151:200),'-b')
semilogy(tsweep,CL_RMSE_Hunsaker(201:250),'-b')
hold off
set(gca,'FontName','Times New Roman','FontSize',10)
xlabel('airfoil thickness','Fontname','Times New Roman')
ylabel('RMS Error','Fontname','Times New Roman')
title('CL')
legend([p11,p12],'traditional','hunsaker','location','southeast')

figure(2) %%%%%%%%%%%%%%%%%%%%%%%%%%%%%%%%%%%%%%%%%%%%%%%%%%%%
p21 = semilogy(tsweep,CM_RMSE_Traditional(  1:50),'-r');
hold on
      semilogy(tsweep,CM_RMSE_Traditional( 51:100),'-r')
      semilogy(tsweep,CM_RMSE_Traditional(101:150),'-r')
      semilogy(tsweep,CM_RMSE_Traditional(151:200),'-r')
      semilogy(tsweep,CM_RMSE_Traditional(201:250),'-r')

p22 = semilogy(tsweep,CM_RMSE_Hunsaker(  1:50 ),'-b');
      semilogy(tsweep,CM_RMSE_Hunsaker( 51:100),'-b')
```

```
      semilogy(tsweep,CM_RMSE_Hunsaker(101:150),'-b')
      semilogy(tsweep,CM_RMSE_Hunsaker(151:200),'-b')
      semilogy(tsweep,CM_RMSE_Hunsaker(201:250),'-b')

set(gca,'FontName','Times New Roman','FontSize',10)
xlabel('airfoil thickness','Fontname','Times New Roman')
ylabel('RMS Error','Fontname','Times New Roman')
title('CM','Fontname','Times New Roman')
legend([p21,p22],'Thin Airfoil Theory','General Airfoil
Theory','location','southeast')
hold off

figure(3) %%%%%%%%%%%%%%%%%%%%%%%%%%%%%%%%%%%%%%%%%%%%%%%%%%%%%%%%
semilogy(tsweep,CL_RMSE_Traditional(  1:50),'-');
hold on
semilogy(tsweep,CL_RMSE_Traditional( 51:100),'-')
semilogy(tsweep,CL_RMSE_Traditional(101:150),'-')
semilogy(tsweep,CL_RMSE_Traditional(151:200),'-')
semilogy(tsweep,CL_RMSE_Traditional(201:250),'-')
set(gca,'FontName','Times New Roman','FontSize',10)
xlabel('airfoil thickness','Fontname','Times New Roman')
ylabel('RMS Error','Fontname','Times New Roman')
title('CL Thin Airfoil Theory','Fontname','Times New Roman')
legend('00XX','24XX','44XX','64XX','84XX')
hold off

figure(4) %%%%%%%%%%%%%%%%%%%%%%%%%%%%%%%%%%%%%%%%%%%%%%%%%%%%%%%%
semilogy(tsweep,CL_RMSE_Hunsaker(  1:50),'-')
hold on
semilogy(tsweep,CL_RMSE_Hunsaker( 51:100),'-')
semilogy(tsweep,CL_RMSE_Hunsaker(101:150),'-')
semilogy(tsweep,CL_RMSE_Hunsaker(151:200),'-')
semilogy(tsweep,CL_RMSE_Hunsaker(201:250),'-')
set(gca,'FontName','Times New Roman','FontSize',10)
xlabel('airfoil thickness','Fontname','Times New Roman')
ylabel('RMS Error','Fontname','Times New Roman')
title('CL General Airfoil Theory','Fontname','Times New Roman')
legend('00XX','24XX','44XX','64XX','84XX')
hold off

figure(5) %%%%%%%%%%%%%%%%%%%%%%%%%%%%%%%%%%%%%%%%%%%%%%%%%%%%%%%%
semilogy(tsweep,CM_RMSE_Traditional(  1:50),'-');
hold on
semilogy(tsweep,CM_RMSE_Traditional( 51:100),'-')
semilogy(tsweep,CM_RMSE_Traditional(101:150),'-')
semilogy(tsweep,CM_RMSE_Traditional(151:200),'-')
semilogy(tsweep,CM_RMSE_Traditional(201:250),'-')
set(gca,'FontName','Times New Roman','FontSize',10)
xlabel('airfoil thickness','Fontname','Times New Roman')
ylabel('RMS Error','Fontname','Times New Roman')
title('CM Thin Airfoil Theory','Fontname','Times New Roman')
legend('00XX','24XX','44XX','64XX','84XX')
hold off
```

```
figure(6) %%%%%%%%%%%%%%%%%%%%%%%%%%%%%%%%%%%%%%%%%%%%%%%%%%%%%%%%
semilogy(tsweep,CM_RMSE_Hunsaker(  1:50),'-')
hold on
semilogy(tsweep,CM_RMSE_Hunsaker( 51:100),'-')
semilogy(tsweep,CM_RMSE_Hunsaker(101:150),'-')
semilogy(tsweep,CM_RMSE_Hunsaker(151:200),'-')
semilogy(tsweep,CM_RMSE_Hunsaker(201:250),'-')
set(gca,'FontName','Times New Roman','FontSize',10)
xlabel('airfoil thickness','Fontname','Times New Roman')
ylabel('RMS Error','Fontname','Times New Roman')
title('CM General Airfoil Theory','Fontname','Times New Roman')
legend('00XX','24XX','44XX','64XX','84XX')
hold off

figure(7) %%%%%%%%%%%%%%%%%%%%%%%%%%%%%%%%%%%%%%%%%%%%%%%%%%%%%%%%
cL8415Vortex = datasweep(:,5,215);
plot(alpha ,cL8415Vortex,'^k')
hold on
plot(alpha ,cL8415Traditional,'or')
plot(alpha ,cL8415Hunsaker,'sb')
xlabel('angle of attack (degrees)','Fontname','Times New Roman')
ylabel('Coefficient of Lift','Fontname','Times New Roman')
title('NACA 8415','Fontname','Times New Roman')
legend('Vortex Panel Method','Thin Airfoil Theory','General Airfoil
Theory','location','southeast')
hold off

figure(8) %%%%%%%%%%%%%%%%%%%%%%%%%%%%%%%%%%%%%%%%%%%%%%%%%%%%%%%%
cm8415Vortex = datasweep(:,4,215);
plot(alpha ,cm8415Vortex,'^k')
hold on
plot(alpha ,cm8415Traditional,'or')
plot(alpha ,cm8415Hunsaker,'sb')
xlabel('angle of attack (degrees)','Fontname','Times New Roman')
ylabel('Pitching Moment Coefficient','Fontname','Times New Roman')
title('NACA 8415','Fontname','Times New Roman')
legend('Vortex Panel Code','Thin Airfoil Theory','General Airfoil
Theory','location','northeast')
hold off

figure(9)
plot(XAC_hunsaker(1:50),YAC_hunsaker(1:50),'bo')
hold on
plot(XAC_hunsaker(51:100),YAC_hunsaker(51:100),'r+')
plot(XAC_hunsaker(101:150),YAC_hunsaker(101:150),'k^')
plot(XAC_hunsaker(151:200),YAC_hunsaker(151:200),'ms')
plot(XAC_hunsaker(151:200),YAC_hunsaker(201:250),'g>')
xlabel('x Position')
ylabel('y Position')
legend('00XX','24XX','44XX','64XX','84XX','location','northwest')

hold off
```

```
% General airfoil theory for NACA 8415
format long
datasweep(:,:,62)
alphaL0Solved(62)
CLalphaSolved(62)
CmLEAlpha(62)
CmLENormal(62)
CmLEAxial(62)

%%
for i=1:length(XAC_hunsaker)
extract(:,i) = datasweep(:,5,i);
end

--------------------------------------------------------------------------
%%%%%%%%%%%%%%%%%%%%%%%% SUPPORTING FUNCTIONS %%%%%%%%%%%%%%%%%%%%%%%%
--------------------------------------------------------------------------

function [ RMSE ] = RMSE( A, B, bound)
%RMSE Summary of this function goes here
%   Detailed explanation goes here
sum = 0;
for i=1:bound
diffsq(i) = (A(i) - B(i))^2;
sum = sum + diffsq(i);
end
RMSE = sqrt(sum/bound);

end
```